CHALMERS
UNIVERSITY OF TECHNOLOGY

PHD THESIS

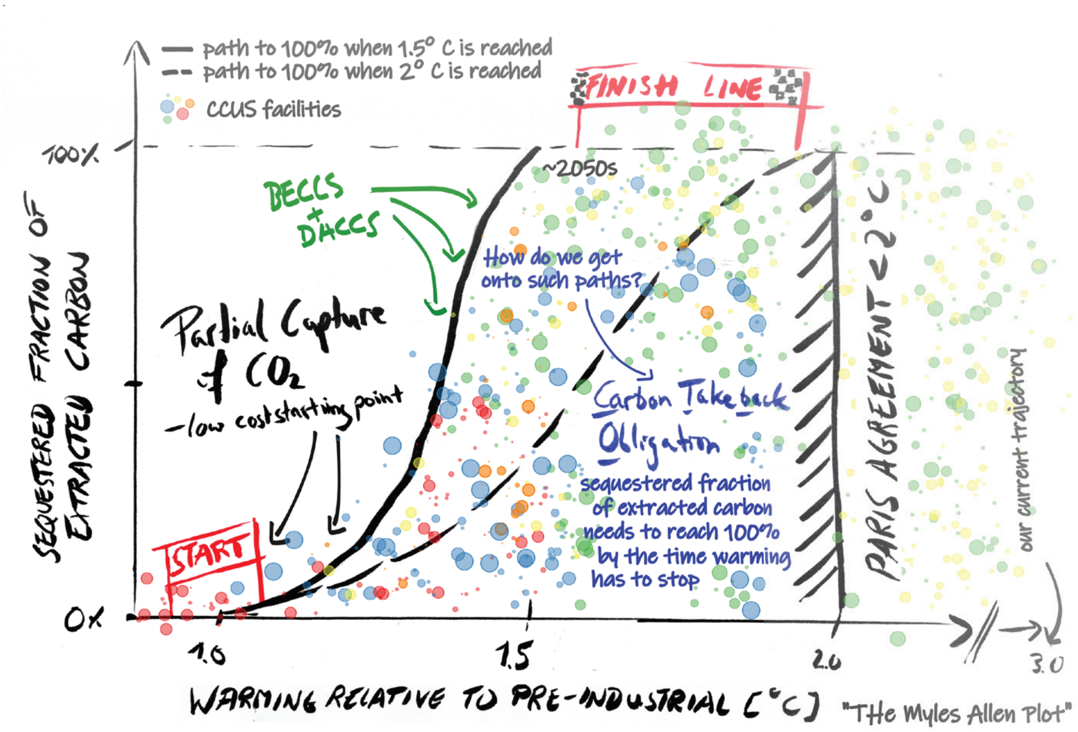

Partial CO_2 capture to facilitate cost-efficient deployment of carbon capture and storage in process industries

- Deliberations on process design, heat integration, and carbon allocation

MAXIMILIAN BIERMANN

DEPARTMENT OF SPACE, EARTH AND ENVIRONMENT
CHALMERS UNIVERSITY OF TECHNOLOGY
Gothenburg, Sweden 2022
www.chalmers.se

THESIS FOR THE DEGREE OF DOCTOR OF PHILOSOPHY

Partial CO_2 capture to facilitate cost-efficient deployment of carbon capture and storage in process industries

- Deliberations on process design, heat integration, and carbon allocation

MAXIMILIAN BIERMANN

Department of Space, Earth and Environment

CHALMERS UNIVERSITY OF TECHNOLOGY

Gothenburg, Sweden 2022

Partial CO_2 capture to facilitate cost-efficient deployment of carbon capture and storage in process industries
-Deliberations on process design, heat integration, and carbon allocation

Maximilian Biermann
ISBN 978-91-7905-704-6

Doktorsavhandlingar vid Chalmers tekniska högskola
Ny serie nr 5170
ISSN 0346-718X

Department of Space, Earth and Environment
Chalmers University of Technology
SE-412 96 Gothenburg
Sweden
Telephone + 46 (0)31-772 1000

Cover:
"The Myles Allen Plot" – artwork about partial CO_2 capture as low-cost opportunity to get on a path of CCS deployment also consistent with a carbon takeback obligation (CTBO) policy. Inspired by a keynote speech given by Prof. Myles Allen at TCCS-10, and the related work by Jenkins et al. (2021). See Section 7 for further reading on CTBO on p.56. and Section 2.1 about the CCUS facilities (colored bubbles) on p.9.

Printed by Chalmers Reproservice
Gothenburg, Sweden 2022

Partial CO_2 capture to facilitate cost-efficient deployment of carbon capture and storage in process industries

MAXIMILIAN BIERMANN
Division of Energy Technology
Department of Earth, Space and Environment
Chalmers University of Technology

Abstract

Climate change requires that all energy-related sectors reduce drastically their greenhouse gas (GHG) emissions, at a global rate of 1–2 $GtCO_2$ per year, starting now. Process industries, such as the iron and steel, cement, petrochemical, and oil-refining industries, are inherently carbon-intensive, and carbon capture and storage (CCS) is one of the few options available to achieve the required deep reductions in carbon dioxide (CO_2) emissions. Despite being technologically mature, CCS has so far not been implemented at the required rates. This is due *inter alia* to the low value created by CCS for process industries, which is attributed to uncertainties related to carbon pricing and the considerable investments required for CO_2 capture installations.

This thesis explores the concept of partial carbon capture as an opportunity for the process industry, as part of its transition, to operate in a net-zero emissions framework by the middle of this century. Partial capture is governed by market and site conditions, and aims to capture a designated share of the CO_2 emissions from an industrial site, thereby lowering the absolute and specific costs (in€/tCO_2) for CO_2 capture, as compared to a conventional full-capture system.

The thesis elaborates the relevant technical, economic, and policy-related aspects related to facilitating the near-term implementation of carbon capture at industrial sites. These aspects include: 1) the energy- and cost-effective design of solvent-based processes for partial capture, which can lead to capture cost savings of up to 10% for gases with a high CO_2 content (>17 vol.$\%_{wet}$); 2) the efficient use of residual heat and existing capacities on-site to power partial capture, which in case studies of an oil refinery and an integrated steel mill, are shown to confer cost savings along the entire CCS chain of 17%–24%; 3) the incorporation of site realities, such as temporal variations in heat availability, into techno-economic assessments; 4) the adaption of policies that address the allocation of carbon emissions reductions to low-carbon products, so that investments in mitigation technologies are incentivized with respect to the ambition level; and 5), the recognition of the rather narrow window of opportunity for partial capture with regard to the lifetime of the existing infrastructure, alternative production and (co-)mitigation technologies, as well as the regional energy and CO_2 transport and storage systems.

As the title image indicates, the share of carbon extracted from the earth that is sequestered needs to reach 100% by mid-century, in order to limit global warming in line with the targets of the Paris Agreement (i.e., 1.5°C or well below 2°C). Thus, partial capture is only a short-term solution for kick-starting CCS, and it will eventually have to lead to full capture, alternatively full mitigation (e.g., via carbon-free production), or be combined with renewable feedstocks if used in the longer term. Therefore, it is timely for the process industry to apply partial capture and, thereby, ramp up widespread adoption of CCS, so to build up the infrastructure for direct removal of carbon from the atmosphere, which will be required on the gigatonne scale in the second half of the 21st Century.

Keywords: Partial CO_2 capture; process industry; amine absorption; heat recovery; CCS; techno-economic assessment; carbon allocation

List of publications

This thesis is based on the following papers, which are referred to in the thesis by their Roman numerals.

I. Biermann, M.; Normann, F.; Johnsson, F.; Skagestad, R. *Partial Carbon Capture by Absorption Cycle for Reduced Specific Capture Cost*. *Ind. Eng. Chem. Res.* **2018** https://doi.org/10.1021/acs.iecr.8b02074

II. Biermann, M., Normann, F., Johnsson, F., R Hoballah, K Onarheim (2022). *Capture of CO_2 from steam reformer flue gases using monoethanolamine - pilot plant validation and process design for partial capture,* Submitted for Publication, **2022**

III. Sundqvist, M.; Biermann, M.; Normann, F.; Larsson, M.; Nilsson, L. *Evaluation of Low and High Level Integration Options for Carbon Capture at an Integrated Iron and Steel Mill*. Int. J. Greenh. Gas Control **2018**. https://doi.org/10.1016/j.ijggc.2018.07.008

IV. Biermann, M.; Ali, H.; Sundqvist, M.; Larsson, M.; Normann, F.; Johnsson, F. Excess-*Heat Driven Carbon Capture at an Integrated Steel Mill – Considerations for Capture Cost Optimization*. *Submitted for Publication*. **2019**. https://doi.org/10.1016/j.ijggc.2019.102833

V. Biermann, M., Langner, C., Roussanaly, S., Normann, F., & Harvey, S. *The role of energy supply in abatement cost curves for CO_2 capture from process industry – a case study of a Swedish refinery*. *Appl. Energy* **2022**. https://doi.org/10.1016/j.apenergy.2022.119273

VI. Biermann, M., Montañés, R. M., Normann, F., and Johnsson, F. *Carbon Allocation in Multi-Product Steel Mills That Co-process Biogenic and Fossil Feedstocks and Adopt Carbon Capture Utilization and Storage Technologies*. Front. Chem. Eng. **2020** https://doi.org/10.3389/fceng.2020.596279

Authors' contributions

Maximilian Biermann is the principal author of **Papers I** and **II and IV–VI**. As second author, he has contributed to **Paper III** with modeling and evaluation of the CO_2 absorption process, writing, discussions and editing. Prof. Fredrik Normann has contributed with the conceptualization, discussions and editing to all six papers. Prof. Filip Johnsson has contributed with discussions and editing to **Papers I–IV** and **VI**. Dr. Rayane Hoballah and Kristin Onarheim have both contributed to **Paper II** with discussions and editing. Maria Sundqvist is the principal author of **Paper III** and has contributed to **Paper IV** with modeling and discussions, mainly regarding the performance of the steel mill. Leif Nilsson has contributed with discussions to **Paper III**. Dr. Hassan Ali has contributed to **Paper IV** with the techno-economic assessment and discussion of the steam generation cost. Ragnhild Skagestad has performed the underlying cost calculations for **Papers I** and **IV**. Dr. Mikael Larsson has contributed with discussions and editing to **Papers III** and **IV**. Christian Langner has contributed to **Paper V** with modeling (optimization), writing, discussions and editing. Simon Roussanaly has contributed to **Paper V** with the cost function regression, cost methodology, discussions and editing. Prof. Simon Harvey has contributed with discussions and editing to

Paper V. Dr. Rubén Mocholí Montañés has contributed to **Paper VI** with discussions and editing.

Two publications co-authored by Maximilian Biermann are appended as supplementary material, as their topic of partial capture and temporal variations is discussed in Section 6.2.

A. Martinez Castilla, G.; Biermann, M.; Montañés, R. M.; Normann, F.; Johnsson, F. *Integrating Carbon Capture into an Industrial Combined-Heat-and-Power Plant: Performance with Hourly and Seasonal Load Changes*. Int. J. Greenh. Gas Control **2019** https://doi.org/10.1016/j.ijggc.2019.01.015

B. Eliasson, Å., Fahrman, E., Biermann, M., Normann, F., & Harvey, S. *Efficient Heat Integration of Industrial CO_2 Capture and District Heating Supply.* Submitted for Publication.**2022** https://doi.org/10.1016/j.ijggc.2022.103689

Other publications by the author related to the topic of the thesis are listed below. These have not been included in the thesis because they are either outside the scope of the thesis or overlap with the appended papers.

Conference papers:

Biermann et al. *Partial capture from refineries through utilization of existing site energy systems*', GHGT-15, **2021**, https://doi.org/10.2139/ssrn.3820101

Eliasson et al. *Integration of Industrial CO_2 Capture with Industrial District Heating Networks: A Refinery Case Study,* TCCS-11, **2021**, https://research.chalmers.se/publication/526225

Garðarsdóttir et al., *'Preem CCS– A Pioneering Swedish-Norwegian Collaboration Showcasing the Full CCS Chain',* GHGT-15 Abu Dhabi, **2021**, http://dx.doi.org/10.2139/ssrn.3820698

Reyes-Lúa et al., *Potential Impact of the Preem-CCS Project*, TCCS-11, **2021**, https://research.chalmers.se/publication/526227

Martinez Castilla et al., *Operation of Carbon-Capture Integrated into Industrial Combined-Heat-and-Power Plants – Dependency on Hourly to Seasonal Changes*, GHGT-14, **2019**, http://dx.doi.org/10.2139/ssrn.3365889

Sundqvist et al. *Cost Efficient Partial CO_2 Capture at an Integrated Iron and Steel Mill,* GHGT-14, **2019**, http://dx.doi.org/10.2139/ssrn.3365609

Biermann et al. *Evaluation of Steel Mills as Carbon Sinks*. International Conference on Negative Emissions, Gothenburg, **2018**, https://research.chalmers.se/publication/504017

Project reports:

Biermann et al., *Preem CCS - Synthesis of main project findings and insights*, **2022**, https://research.chalmers.se/publication/528685

Normann et al., *CO2stCap - Reducing the Cost of Carbon Capture in Process Industry*, **2019**, https://research.chalmers.se/publication/512527

Acknowledgments

I am truly grateful for all that I have experienced on my PhD journey. The entire endeavor would have been less-fruitful or even not possible without all the support that I received from so many people, all of whom I wish to thank.

First and foremost, I would like to thank my supervisors Prof. Fredrik Normann and Prof. Filip Johnsson. Filip, your inputs, your eye for the bigger picture, and your knack for comprehensible wording have proven invaluable. Your dedication to reading your PhD students' texts, often at short-notice and despite having a packed schedule, is remarkable. Fredrik, I am deeply grateful for your guidance, our numerous discussions, and your skills with structuring texts and reducing matters to the essential, all of which are truly inspiring and have proven most helpful on many occasions. Not least, thank you for giving me the opportunity to do both my Master's and my PhD thesis under your excellent supervision.

I am indebted to all of my co-authors and the partners in the research projects in which I have been involved. To Prof. Simon Harvey – thank you for all the inspiration, guidance, feedback, and our shared business trips to Norway as part of the Preem CCS project. Thank you Christian for your help with the optimization model. Thank you Åsa, Elin, and Guillermo for the excellent work in your Master's theses, which you were able to turn into valuable journal articles. Rubén, thank you for our discussions, your support in supervising the Master's thesis projects, your insights into process dynamics, as well as your encouragement to tackle the experimental side of things. To the engaged people at SINTEF Energy Research, Aker Carbon Capture, and Preem AB: thank you for your insights, your help with data and cost management, and the technical discussions that we had in Preem CCS. The participants in the Torero project, especially Wim van Stricht, I thank for the inputs on carbon allocation. Not least, to the partners in the CO_2stCap project, my thanks for the many learnings I could draw from this first research project in which I was engaged. Especially, to the people at SINTEF Industry (formerly Tel-Tek), the University of South-Eastern Norway, and Swerim AB: my thanks for sharing your knowledge of cost engineering, heat collection networks, and iron and steelmaking, respectively. To Assoc. Prof. Vincent Collins, thank you for your assistance with the English language, which has been very helpful and highly appreciated.

To Stefanía, to whom I am much obliged for introducing me to the world of amine absorption and CCS – your helpfulness and dedication have set a good example for me and others. Thank you!

To all my present and former colleagues at the Division of Energy Technology, I am ever so grateful to you for creating a welcoming and supportive work environment. To the members of the thermodynamics teaching team, the Särö-group, and the former combustion and separation technology group: I cherish all the discussions, exchange of ideas, learnings, and fun that we experienced together. Special thanks to Marie and Katarina (the A-team), for making sure that us PhD students do not get lost in the paperwork. To my present and former office mates - Anna, Sébastien, and Aaron – I am eternally grateful to you for lending an ear and for making the long office hours more enjoyable.

Finally, my warmest thanks to my friends and my beloved family – foremost my parents Albert and Brigitte, and my sister Maresa - for all your love, support and encouragement no matter how far we are apart. To Nora and Henry, I feel humbled, proud, and filled with joy seeing you grow up – thank you for helping me to recognize the important things in life and for always raising my spirits with your laughter. To my partner Jenny, words are not enough to express how grateful I am for your love and all the support throughout these PhD years – I wouldn't have even started this journey if it wasn't for you!

Maximilian Biermann, Steninge, 6th August 2022

Notes

This work has been financially supported by the Swedish Energy Agency and the project partners of CO_2stCap (P40445-1) and Preem CCS (P47607-1). In addition, financial support was provided by the partners in TORERO (ID: 745810) and the European Union’s Horizon 2020 Programme (H2020-EU.3.3.3. – Alternative fuels and mobile energy sources).

The colors used in this thesis are from https://colorbrewer2.org/ by Prof. Cynthia A. Brewer, Department of Geography, Pennsylvania State University, USA.

For the extraction of data from the literature, the WebPlotDigitizer V4.5 by Ankit Rohatgi was used. https://automeris.io/WebPlotDigitizer/citation.html

List of abbreviations

ACCs	Abatement Cost Curves
AMP	2-Amino-2-Methyl-1-Propanol
BAT	Best-Available Technology
BECCS	Bio-Energy CCS
BF	Blast Furnace
BFG	Blast Furnace Gas
CBAM	Carbon Border Adjustment Mechanism
CAPEX	CAPital EXpenditure
CCfD	Carbon Contracts for Difference
CCS	Carbon Capture and Storage
CCU	Carbon Capture and Utilization
CCUS	Carbon Capture Utilization and Storage
CDA	Carbon Direct Avoidance
CDQ	Coke Dry Quenching
CHP	Combined Heat and Power
CTBO	Carbon Take-Back Obligation
DACCS	Direct Air Carbon Capture and Storage
DH	District Heating
DRI	Direct Reduced Iron
DSG	Dry Slag Granulation
EAF	Electric Arc Furnace
EDF	Enhanced Detailed Factor
ECC	Energy supply Cost Curve
EPC	Engineering, Procurement, and Construction
EOR	Enhanced Oil (and gas) Recovery
ETS	Emissions Trading System
EUA	European Union Allowance
EW	Electro-Winning
FGHR	Flue Gas Heat Recovery

GHG	Greenhouse Gas
GCCSI	Global CCS Institute (CCS advocacy)
IAM	Integrated Assessment Models
IEA	International Energy Agency
IES	Industrial Energy System
IPCC	Intergovernmental Panel on Climate Change
LCFS	Low-Carbon Fuel Standard
MEA	Monoethanolamine
MILP	Mixed-Integer Linear Programming
MSR	Market Stability Reserve
Mtpa	Million Tonnes Per Annum
NG	Natural Gas
OPEX	OPerational EXpenditure
PZ	Piperazine
RGGI	Regional Greenhouse Gas Initiative
SRD	Specific Reboiler Duty
SRP/ODP	Separation Rate Path/Off-Design Path
SSP	Split Stream Path
TCR	Total Capital Requirement
TDC	Total Direct Cost
TDCPC	Total Direct Cost with Process Contingency
TEA	Techno-Economic Assessment
TPC	Total Plant Cost
TRL	Technology Readiness Level
WtE	Waste-to-Energy

Table of contents

1 Introduction

Climate change is one of the major global environmental challenges of the 21st Century. As part of the Paris Agreement, the world's nations have agreed to limit the global temperature rise to well below 2°C above the pre-industrial level [1]. In their 2018 Special Report, the Intergovernmental Panel on Climate Change (IPCC) motivated that humanity should further limit the global temperature rise to 1.5°C [2], so as to minimize the impacts of climate change, including the loss of human life. Climate modeling shows that global CO_2 levels have to be net-zero in the early 2050s in all pathways that limit warming to 1.5°C [3]. The recent rise in public awareness in the wake of the Special Report on 1.5°C by the IPCC has led to a dramatic increase in net-zero pledges, which are often announced for Year 2050 or earlier (India and China are later) on national, subnational and corporate levels, although <20% of these meet the minimum procedural standards laid out by the UN Race to Zero campaign [4]. Nonetheless, emissions have to start falling significantly now and consistently throughout the 2020s, in the order of 1–2 $GtCO_2$ per year, so as to restrict global warming to levels in the range of 1.5°C to well below 2°C [2], [5] and, thus, the urgency linked to large-scale mitigation. Fortunately, the energy sector is showing an enormous potential to mitigate emissions via renewable wind and solar power at cost levels that are much lower than previous expectations [6] and that are at or below the costs for power generation from fossil fuels [3]. The industrial sector is, however, not 'on-track' and requires attention [6]. In Year 2020, the direct CO_2 emissions from industry accounted for ~26% of the global CO_2 emissions (8.7 $GtCO_2$), with the main contributing sectors being: iron and steel (30%), cement industry (29%), (petro-)chemicals (13%), aluminum (3%), and pulp and paper (2%) [7]. These so-called 'hard-to-abate' sectors, in which carbon is inherent to the manufacturing process, will require transformative changes beyond energy and material efficiency measures, such as the adoption of new production technologies and/or carbon capture and storage (CCS) [8], [9].

The industrial facilities are typically large point sources of CO_2 with relatively high CO_2 concentrations in their off-gases (compared to power plant flue gases), which lowers the specific energy requirements for carbon capture [10]. In addition, they often have significant amounts of residual (excess) heat available. These are good prerequisites for a cost-effective implementation of CCS, which therefore can play a significant role in decarbonizing industry and addressing the need for large-scale and timely mitigation. Carbon capture entails the separation of CO_2 from a CO_2-rich gas, which is compressed for transport by ship or pipeline to (preferably) off-shore geologic storage sites, such as saline aquifers or depleted oil fields. CCS is: 1) capable of reducing emissions at-scale, and is expected to mitigate a considerable share of the cumulative emissions [11]. It represents, therefore, a crucial technology in most emission pathways that are consistent with the targets for limiting global warming to 1.5°C [2] and 2°C [12]; and 2) concerning the abovementioned timeline for climate mitigation, CCS is readily available at commercial scale when using amine absorption processes for capture and storage in saline formations [13], and is, therefore, implementable today. However, cross-sector deployment of CCS has yet not started [12]. This is due to a number of reasons [14], such as low public awareness of CCS [15], low social acceptance in the past (concerning CCS from coal power and onshore storage, e.g., in Germany), and perhaps most importantly, climate policies that have so far failed to establish market conditions that allow value creation from CCS.

In light of the urgently required emissions mitigation actions, the present thesis addresses the challenge of initiating large-scale, near-term mitigation in the process industry. More specifically, the work evaluates partial carbon capture as a means to reduce the capture cost, and thereby lower the hurdles for CCS deployment. Partial capture is here defined as a CCS concept, in which only a fraction of the accessible CO_2 is separated from a CO_2-rich gas. It was originally proposed for coal and gas-fired power plants to meet emission performance standards [16]–[18], to handle flexibility depending on the merit order of power utilities in the electricity system (based on marginal cost) [19], and to reduce cost [20], [21]. The magnitude of this fraction is determined by a range of factors, such as the characteristics of the source of CO_2 (concentration and flow) and energy supply (heat recovery potential, local energy system) at the site, as well as economic and policy-related conditions. Partial capture comes with a reduced absolute energy penalty and reduced *absolute* capital expenditures, which decrease the investment risks [16], [18], as compared to CCS with a so-called *full capture* approach. Full capture represents almost-maximized separation rates (e.g., 90%) of CO_2 from CO_2-rich gases, so as to minimize the *specific* capital expenditures per tCO_2-captured through economy of scale. To be clear, partial capture aims to reduce the *total specific* cost, i.e., capital and operating expenditures, as compared to full capture. Overall, partial capture is evaluated as a low-cost, near-term mitigation option to initiate the decarbonization of the process industry, which needs to be completed by mid-century in line with the Paris Agreement.

1.1 Aims and scope

The overarching aim of this thesis is to delineate a timely and efficient transition of carbon-intensive industries to their operation within a carbon-constrained ("net-zero"), sustainable society in line with the goals of the Paris Agreement. The focus is on partial CO_2 capture as the catalyst for such a transition and for the ramping up of CCS activities that will help to achieve the necessary reductions in global emissions. The specific aims are to identify relevant technical, economic, and policy-related aspects that facilitate the near-term implementation of carbon capture at industrial sites. To perform this assessment, the thesis contributes to necessary method development by:

i. Extending the application of process models to include design options for partial capture of CO_2; and

ii. Incorporating site-related realities, such as (temporally varying) heat availability, into techno-economic assessments (TEA) in order to, for example, enhance the representativeness of site-level abatement cost curves.

With the application of these developed and already existing methods in the field, the thesis intends to:

i. Contribute to the cost-effective design of amine absorption cycles for partial capture of CO_2 from large industrial gas flows with high CO_2 concentrations;
ii. Define the relationships between cost, energy consumption, and carbon capture rates in process industry, so as to identify cost-effective partial capture scenarios (*inter alia,* via site-level abatement cost curves) using the examples of integrated steel mills and refineries;
iii. Highlight the ramifications of CCS from a product perspective, and discuss the role of flexibility in the carbon allocation of mitigated CO_2 emissions to industrial products;
iv. Assess the role of heat supply for CO_2 capture in process industry, and the impacts of heat recovery on the capture cost and the full-chain cost of CCS; and
v. Construct an overall perspective on partial capture in synergy with and in the transition to other mitigation options or full capture over time for relevant industrial sectors.

1.2 Outline of the thesis

This thesis comprises a summary essay and six main papers (plus two supplementary papers). The eight chapters of the essay describe and contextualize the key findings of the papers. Chapter 2 gives the background to the work by reviewing CCS development and mitigation options for process industry. Chapter 3 gives an overview of the applied methods. The key outcomes of the work are presented in Chapters 4–6: Chapter 4 describes the concept of partial capture and its motivation; Chapter 5 highlights the impacts of partial capture and carbon allocation principles on the products' costs and their emissions intensities; and Chapter 6 demonstrates the application of partial capture via techno-economic assessments with the focus on process design, management of variations in heat supply, and the utilization of abatement cost curves. Chapter 7 discusses partial capture as a near-term mitigation option and valuable strategy for process industry in their transition to net-zero emissions. Chapter 8 concludes the essay.

The focuses of the appended papers are briefly described below. The linkages between the papers are illustrated in Figure 1-1.

In **Paper I,** two design paths for partial capture are described, modeled, and evaluated based on their energy demands and capture costs in relation to the amount of CO_2 separated from a CO_2-rich gas, i.e., assuming high concentrations of CO_2 of around 20 vol.%, which are typical for process industries, such as pulp and paper, cement, petroleum refining, and iron and steel. This paper focuses on the design of amine absorption cycles with regard to scale, CO_2 concentration, and the CO_2 separation rate in the absorber.

Paper II reports the experimental findings of pilot-scale CO_2 capture from the flue gases of a steam reformer using monoethanolamine (MEA) and verifies the energy performance results from **Paper I** for partial capture (via lower separation rates). The energy performance is further examined as a function of the basic column design using numerical modeling.

Paper III assesses the amount of available heat as the yearly average in a reference integrated steel mill for the purpose of powering partial CO_2 capture from either the blast furnace gas or combined heat and power (CHP) plant flue gases. The paper emphasizes the different levels of integration of CCS within the steel mill and compares the levels of CO_2 capture that are achievable, using the designs from **Paper I,** from these two CO_2 sources depending upon the amount of retrieved heat.

Paper IV extends the technical assessment made in **Paper III** to include a third CO_2 source and to include the economic dimension as a criterion of performance. Full capture from all three major CO_2 sources is compared to the best-performing partial capture scenarios. In addition, the paper sets the full-chain cost for partial capture, including transport and storage, into a relation with carbon price projections, to assess the conditions for near-term implementation of partial capture in the steel industry.

Paper V develops a methodology for the identification, classification, and evaluation of heat sources at industrial sites, which also includes observed temporal variations in available heat. Based on a multi-period optimization of a mix of heat sources, the cost of heat supply to the CO_2 capture unit is determined as a function of the site-level capture rate and is incorporated into the site-level abatement cost to identify partial capture scenarios in a case study of an oil refinery.

Paper VI focuses on the product perspective and the valorization of mitigation efforts by investigating the impact of carbon allocation, i.e., the allocation of renewable content and avoided CO_2 emissions, to the industrial products cogenerated from units that co-process fossil and biogenic carbon and apply CCUS technologies. Ultimately, the flexibility of carbon allocation that policymakers may give (or not) to companies is discussed using the example of a blast furnace into which biochar is injected with subsequent CO_2 capture (for storage) from the blast furnace gas and downstream fermentation of blast furnace gas into ethanol. The qualification of the ethanol as a biofuel is discussed in relation to the flexibility of the carbon allocation.

Supplementary **Papers A** and **B** are shown in Figure 1-1. **Paper A** describes the dynamic behavior of an amine absorption cycle designed for partial capture in response to temporal variations in heat (and gas) supply on an hourly to seasonal scale. **Paper B** assesses the techno-economics of CO_2 capture with seasonally varying heat load in the context of district heating (DH) from industrial sources or waste-to-energy plants.

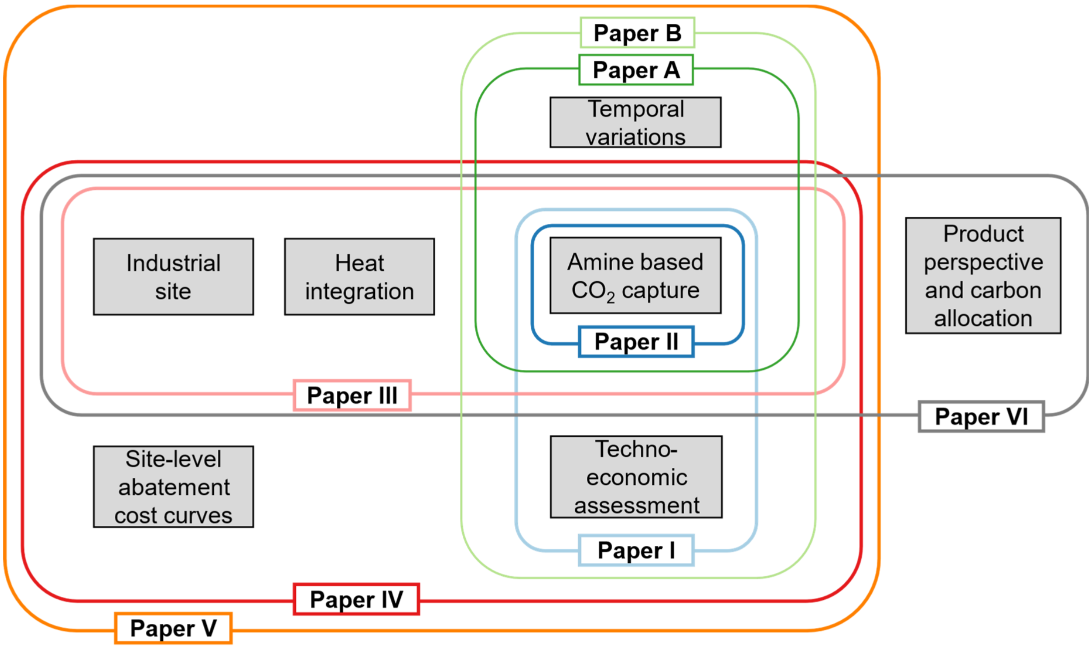

Figure 1-1: Overview of the topics covered and the linkages between the papers appended to this thesis.

2 Background

2.1 Development of CCS –a shift in trends?

CO_2 has been captured since the 1970s, mainly from natural gas (NG) processing and the chemical industry, to be utilized (carbon capture and utilization, CCU) in enhanced oil recovery (EOR) activities based in the US. During the 2000s, the carbon capture utilization and storage (CCUS) technology increasingly attracted interest as a mitigation technology for coal- and gas-fired power plants. For various reasons, including the lack of political will, policy support, and financial incentives (enhanced by the global financial crisis in Years 2007/2008) CCUS did not take off in the power sector. Moreover, local social acceptance issues prevented onshore CO_2 storage projects in the Netherlands and Germany [22]. In the 2010s, governmental support facilitated full-scale CO_2 capture from the coal power plants Boundary Dam (CA) and Petra Nova (US), mostly for the purpose of EOR. Currently, only about 40 Mtpa of CO_2 are being stored globally.

The past 2–3 years have seen a sharp increase in the numbers of planned and announced CCUS projects – the first increase since Year 2011 [22] – with a potential storage volume of ~220 Mtpa by Year 2030. Figure 2-1 shows the development of this CCUS project pipeline[*] and carbon prices. Possible reasons for the recent increase of interest in CCUS include: 1) raised public awareness of climate change catalyzed, for example, by the school strikes for climate ("Greta effect"), the release of the IPCC special report on 1.5°C which found broad coverage, and the increase in magnitude of extreme weather events (e.g., the wildfires in California and Australia); 2) increased political will, e.g., communicated net-zero climate targets by governments and corporations; which has led to 3) a higher level of ambition, for example the *Fit for 55* package of the European Commission, implemented policy measures, e.g., the US *Inflation Reduction Act* that revises the federal "45Q" tax credit for CCUS, and regulation, e.g., the provisional adoption of the CCS amendment to the London Protocol to allow cross-border ship transport of CO_2; and 4) increased financial incentives through revised emissions (cap and) trading systems (ETS), for instance, the incorporation of CCUS into the low-carbon fuel standard (LCFS) in California and the establishment of the market stability reserve (MSR) in the EU ETS, and via public funding, as exhibited through the EU Innovation Fund [23] or the support granted by the Government of Norway.

Figure 2-2 illustrates the development of the historic and announced CCUS facilities by sector and type, including the purpose (utilization vs. storage) and source (fossil, biogenic, or air) of CO_2. If the announced facilities become realized, this would imply the following shifts in trends: 1) dedicated storage (indicated in blue) of CO_2 is projected to dominate EOR and other CCU; 2) most of the potentially stored volume would originate from industrial sectors, such as chemicals/fertilizers, hydrogen, ethanol and cement, although the power sector is projected to

---

[*] CCUS facilities that are operated, under construction, planned or are announced in a given year.

be the largest single sector; and 3) the increase in CCUS facilities projected to predominate in the US and EU.

Still, even if all the projected facilities are realized, the volumes fall short of the ~1,600 Mtpa of sequestered CO_2 in Year 2030 required by the Net-Zero-by-2050 scenario of the IEA [24]. Public awareness of CCUS is still low [25], and policy measures that could trigger widespread implementation and create predictable, long-term financial incentives, such as carbon contracts for difference (CCfDs) that close a possible gap to the ETS price or the carbon border adjustment mechanisms (CBAM) that protect against carbon leakage and create markets on a level playing field [9], are not yet implemented.

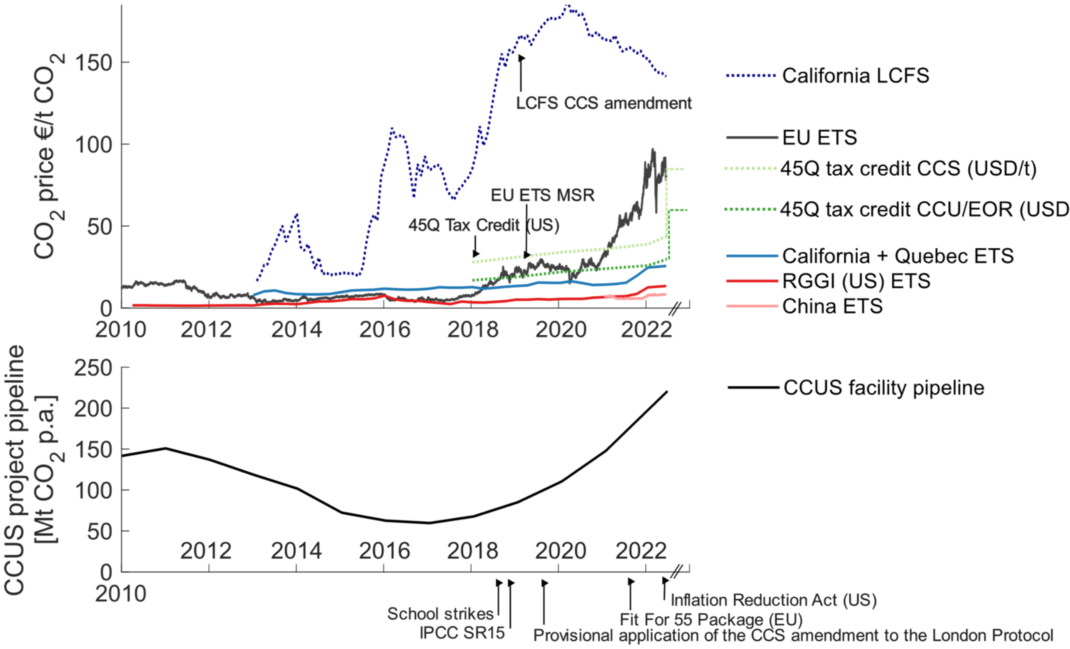

Figure 2-1: The development of carbon prices (cap and trade) is adopted from [26] **and the CCUS pipeline is derived from** [27][28][29]**, i.e., facilities that have been operated, constructed, planned and announced in a given year. The arrows indicate policy changes to cap and trade systems and regulations and events that influence public awareness of the climate crisis. Notations: 45Q, a US federal tax credit of up to 60 \$/tCO_2 and 85 \$/tCO_2 for CCU/EOR and CCS, respectively** [30]**; EU ETS, the EU Emissions Trading System, which incorporated the market stability reserve (MSR) in Year 2019; LCFS, low-carbon fuel standard in California (which included CCS in Year 2019); RGGI , regional GHG initiative of north-eastern US states; IPCC SR15, the Special Report on 1.5°C was released by the IPCC in the autumn of 2018; IMO, International Maritime Organization, which is responsible for the London Protocol that incorporated a CCS amendment in Year 2009 (that can be provisionally applied from Year 2019), enabling cross-border ship transportation of $CO_2$for the purpose of geologic storage.**

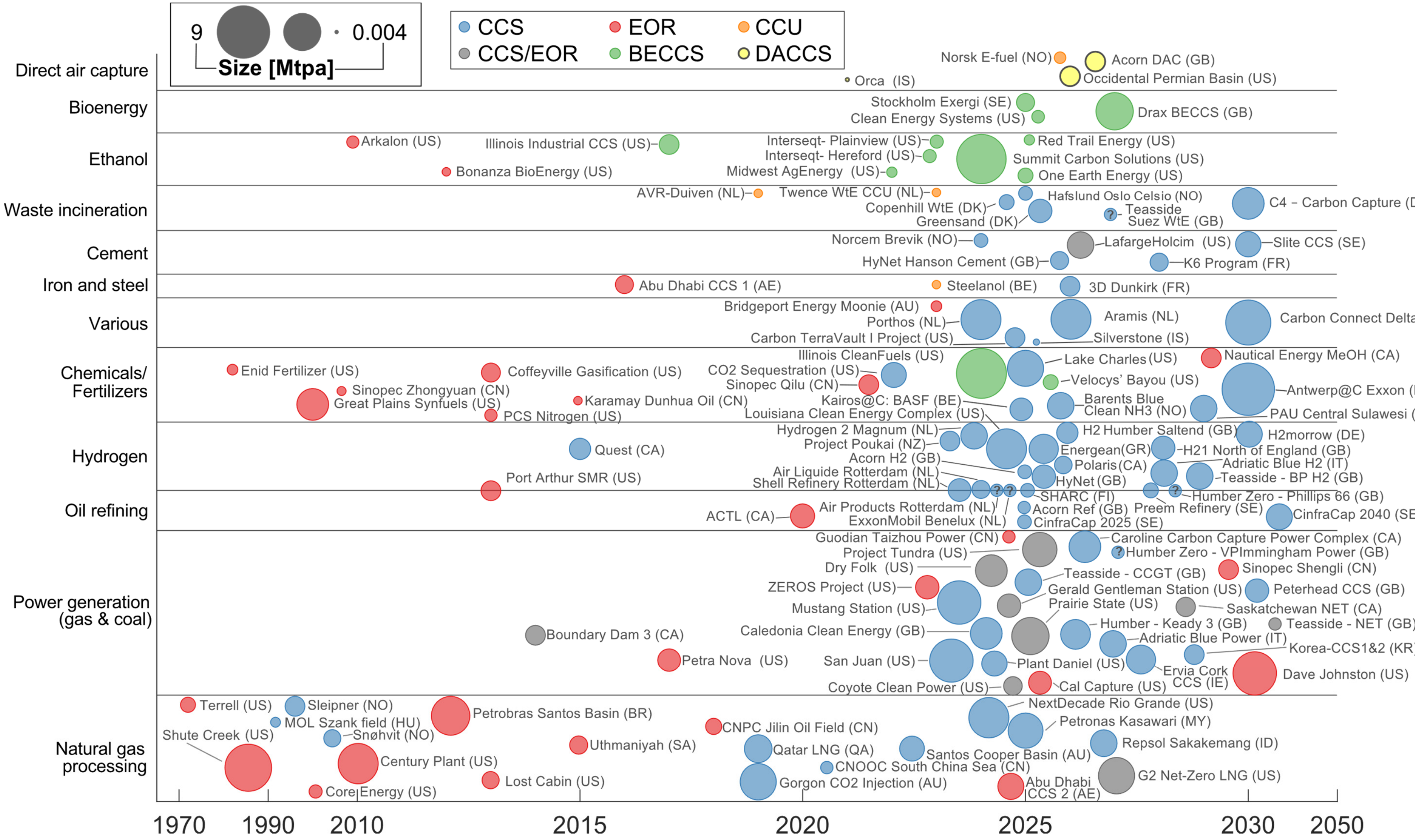

Figure 2-2: Timeline for the development of CCUS facilities. CCS, dedicated carbon capture and storage; EOR, enhanced oil recovery, CCU, carbon capture and utilization; CCS/EOR, combined approach or undecided; DACCS, direct air capture with carbon storage; BECCS, bioenergy with carbon capture and storage. Each bubble size is proportional to the communicated maximum capacity. The question mark indicates unknown size. All plants until Year 2022 are operational, with the exception of Petra Nova, the operation of which is suspended. The plot is adapted from [27] with data from [27][28][29], and various press releases collected until May 2022.

2.2 CO_2 capture via amine-based chemical absorption

The three main options for capturing CO_2 are: 1) separation of carbon from the bulk gas, i.e., from the process gas or flue gas (post-combustion), typically by means of absorption, adsorption or membranes; 2) removal of carbon from the fuel by partial oxidation/gasification of a hydrocarbon feedstock using oxygen/steam to produce a syngas, which is subsequently converted to a mixture of CO_2 and H_2 and from which CO_2 is separated, leaving hydrogen as the fuel. This was originally referred to as 'pre-combustion' but is nowadays more commonly associated with the term *blue hydrogen*; and 3) combustion in the absence of nitrogen, i.e., via oxygen instead of air, resulting in a flue gas that contains only CO_2 and water, with the latter being easily condensed. This is commonly termed *oxyfuel combustion*, and includes advanced forms of the process, such as chemical looping combustion, which uses metal oxides to provide the oxygen.

For a Brownfield site, separation from bulk gases is considered an add-on technology, whereas the processes leading to blue hydrogen and oxyfuels are retrofit technologies that require major adjustments/modifications of existing processes for their implementation [31], making realization in a new process (Greenfield) more likely. Both oxyfuel and blue hydrogen would impact the production process during the construction (downtime of production) and operational (possible impact on product quality, and increased integration may impact reliability) phases [36],[37]. Although separation from bulk gases requires more space at on-site [33], the equipment can be placed in a flexible manner [32]. The disadvantage of gas separation is that it has a high heat demand for solvent regeneration, which has been reported in academic cost estimates as leading to a higher capture cost (€/tCO_2) than oxyfuel combustion [31], [33], [34] and possibly also blue hydrogen production [34].

CO_2 separation from gases using chemical absorption with traditional aqueous amine solutions is a mature technology that has been used commercially in NG sweetening and fertilizer production processes for decades [35]. Moreover, it has been demonstrated as suitable for dedicated CO_2 capture and storage at full scale in coal-fired power plants in Canada and the US [36]. Therefore, it can be regarded as a proven technology with a technology readiness level (TRL) of 8–9 [22], and the knowledge and experience gained using this technology is generally transferable to process industries. However, there needs to be demonstration and verification of its performance, e.g., via pilot-scale testing at an industrial site. Such testing has been conducted for various non-power industries. including cement manufacturing, waste-to-energy plants, and refineries (flue gases from steam reformer and residual catalytic crackers) [37].

In both the industrial and academia settings, monoethanolamine (MEA) has been the traditional, non-proprietary solvent benchmark, and it is also used in the work of this thesis (see Section 3.1). However, given its rather high energy demand for solvent regeneration – called the specific reboiler duty (SRD) – of 3.5–4.1 MJ/kgCO_2 (see **Paper II** or [22]), it has been proposed in recent years to replace MEA as the benchmark with a solvent that is closer to industrial practice, e.g., an aqueous blend of 2-amino-2-methyl-1-propanol (AMP) and piperazine (PZ)

[38], [39]. This solvent has an SRD of 2.9–3.2 MJ/kgCO_2 [22], [40], [41]. For an overview of commercial solvents, many of which have an SRD <3.0 MJ/kgCO_2, see [22], [38].

2.3 Mitigation of industrial CO_2 emissions and the role of the CCS technology

The facilities of the process industry represent large point sources of CO_2. Table 2-1 characterizes the emissions at the site-level in terms of typical annual flows of CO_2 by sector, their source (stacks), and CO_2 concentration in the flue or process gases. Note that pulp and paper, ethanol, and waste-to-energy plants represent point sources of (mostly) biogenic CO_2. In the following section, a sector-specific background to CCS and alternative mitigation technologies are given.

Table 2-1: Characterization of industrial CO_2 sources by sector, indicative annual site-specific CO_2 emissions, and CO_2 concentration. Adapted from Garðarsdóttir et al. [42] **and Bains et al.** [43]**.**

Industry	Annual site-specific CO_2 emissions (Mtpa)	CO_2 sources at site	Concentration of CO_2 (vol.%)	% of site emissions	Reference
Iron and steel (integrated mill)	3–16	BFG - process gas	20–27	(70)[1]	[44], [45]
		Hot stoves flue gas	15–20	15–20	
		Power plant flue gas	25–30	40–60	
Cement (dry kiln)	0.6–1.5	Combined stacks	18–20	90	[32], [44], [46], [47]
Oil refining	0.5–4	H_2 - steam reformer flue gas	18–22	5-30	[31], [34], [48]
		Fluid cracker flue gas	13–15	20–50	
		Process heaters flue gas	8–10	30–60	
Petrochemicals	1–3	Ethylene cracker flue gas	7–12	~80	[34], [49]
		Ammonia CO_2 absorber	98–100	~60	[43], [50]
Pulp and paper	0.5–2	Recovery boiler flue gas	13	75	[51], [52]
		Power boiler flue gas	10–13	10–15	
		Lime kiln flue gas	20	10–15	
Waste-to-energy	0.1–0.5	Stack	~10	~100	[53]–[55]
Ethanol	0.1–1	Fermenter off-gas	98–99	~55–65	[27], [56], [57]

[1] Carbon content that is converted to CO_2 when combusted.

Iron and Steel: Most of the global primary steel is produced in large-scale, integrated steel mills where coal and coke are used primarily to reduce the iron ore and smelt the formed pig iron in the blast furnace (BF), which is followed by processing to steel. The carbon is oxidized to form CO_2 and CO, and ends up in the blast furnace gas (BFG). Together with the off-gases from other units, the BFG is combusted to produce heat, e.g., in CHP boilers, and in hot stoves, which supply the BF with hot air. The CO_2 emissions intensities of integrated steel mills that apply the best-available technology (BAT) in Europe have achieved levels of~1600–1700 kgCO_2/t of steel, which is close to what is technically and theoretically possible [58]. Many studies have, therefore, evaluated CCS as an option for the removal of CO_2 from the steel mill off-gases [59]–[63]. In summary, those studies have reported 50%–80% CO_2 emissions avoidance when the CO_2 is captured from the largest direct emission points on-site (stacks of CHPs, hot stoves, lime kilns, sinter plants, coke ovens), depending on the number of stacks included. Applying amine absorption to capture CO_2 from BFG alone could reduce emissions by 19%–30% [34], [59]. The introduction of biomass could theoretically deliver a 38%–55% reduction in emissions [64], [65]. In addition to the practical limitations and the biomass supply, a major restriction is the mechanical strength of coke required to support the burden in large BFs and to maintain gas permeability. If combined with CCS, bio-energy CCS (BECCS) could lead to negative emissions (i.e., CO_2 removal from the atmosphere) [66]–[68]. However, in recent years, CCS has not become the main emissions mitigation option for the steel industry in Europe. Instead, European steelmakers have announced plans [69] to mitigate emissions by employing direct reduction of iron (DRI) using 100% hydrogen (either immediately or after a period of NG use), preferably from renewable energy. The reduction of iron ore in a shaft reactor to sponge iron using NG or 100% renewable H_2 with subsequent melting in an electric-arc furnace (EAF) leads to emissions intensities of ~560–1,450[†] [58] and 25–50 $kgCO_2/t$ of steel [70], [71]. An alternative production route based on direct electrification that is being developed involves molten-oxide electrolysis of iron ore [72].

Cement: In a modern dry kiln process, a mix of limestone ($CaCO_3$) and other minerals is heated in preheaters and pre-calciners before the cement clinker is sintered at high temperatures in rotary kilns fired with fossil or biogenic fuels. About 600–1,000 $kgCO_2/t$ of clinker are emitted, of which ~50%–60% originate from the calcination reaction to lime (CaO), with the remainder attributed to the fuels that provide heat. Therefore, fuel switching to the greater use of biogenic fuels or electrification, either partly, e.g., via electric heating of the pre-calciner (e-LEILAC, see [73]) or fully, e.g., via plasma torches in the kiln [74], [75], can only mitigate the fuel-related share of emissions. CCS (or CCU) is, thus, widely regarded as a required technology for the cement industry, and it has been studied in detail [34], [47]. The interested reader is referred to the comprehensive TEA published by Voldsund et al. [32] and Garðarsdóttir et al. [76], who have shown that oxyfuel-based capture is a more-economic option than, for example, calcium looping or amine-based gas separation, while emphasizing the need for site-specific assessments. Jakobsen et al. [46] have studied the economic effects of partial capture based on residual heat from a Norwegian cement plant and have found similar full-chain CCS cost for partial and full capture. Interestingly, the first full-scale CO_2 capture from a cement factory in Brevik, Norway, which is planned to go online in 2024, is based on gas separation of ~50% of the site emissions powered by residual heat [77]. Additional mitigation can be achieved through the use of alternative binders (non-cement) or reduced clinker ratios, as well as the recarbonation of concrete during its lifetime [78].

Petroleum refining and petrochemicals: At refineries and petrochemical sites, CO_2 is emitted from various sources. Most of the CO_2 originates from on-site generation of electricity and process heat [34]. For refineries, catalytic crackers are the second-largest point sources, followed by hydrogen production units [47]. For petrochemicals, ethylene is one of the largest

---

[†] Fundamentally determined by the CO_2 intensity of the electricity and the scrap content.

point sources, which in Europe is predominantly produced from naphtha via steam cracking. This requires vast amounts of heat, typically provided by combustion, leading to ~1.5–2.1 tCO_2/t of ethylene [34]. The techno-economics of CO_2 capture from these sectors has been studied in detail [33], [34], [48], and the technical and operational challenges have been mapped [79]. Berghout et al. [31] have conducted a comprehensive assessment of a combination of measures, including energy efficiency and biomass. Johansson et al. [49], [80] and Andersson et al. [81] have studied heat supply options, including heat recovery for amine-based gas separation.

In essence, these studies have shown that refineries and petrochemical plants are highly heterogeneous in terms of their product portfolios, process layouts and levels of complexity. Gas separation from sources with relatively high CO_2 concentrations, such as gasifiers or hydrogen production, is attractive also due to its heat recovery potential. However, since a large fraction of the site emissions (up to 50% [48]) is scattered, full capture seems less-feasible. Partial capture from a hydrogen reformer syngas for storage/utilization has been demonstrated, e.g., at Port Arthur in the US [82] and Quest CCS in Canada [83]. While oxyfuels are less-developed, they can mitigate the emissions from boilers/furnaces [84] and the catalytic cracker [85], in a cost-effective manner [34].

Another emissions-intensive bulk chemical is ammonia (1.8–2.4 tCO_2/t of ammonia), which is typically produced from hydrogen via steam methane reforming of NG and nitrogen. The CO_2 is captured inherently (~60% of the site emissions [43]), and is commonly used as feedstock for urea production or sold off to other CO_2-utilization markets (food and beverages, enhanced oil recovery). This could be extended to include the more-dilute CO_2 streams in flue gases generated from process heat. Alternatively, ammonia production could be fully electrified via electrolysis of water and air separation [50].

Unlike the cement and steel plants, the refinery and petrochemical sectors produce hydrocarbons and emit most of the carbon during the use-phase (fuel, fertilizer) or at the end-of-life (materials ending up in landfills or being combusted). Thus, the CCUS of process emissions (or the electrification of the heat supply for that matter) has a limited mitigation effect on the entire value chain of the hydrocarbon industry. Electrification of, for example, transport and heating, the inclusion of biogenic carbon, and the circular use of carbon (thermochemical recycling [86], direct air capture) are necessary to reach net-zero emissions in the sectors that are currently coupled to hydrocarbon fuel usage.

Biogenic sources - pulp and paper, waste-to-energy and ethanol: These sectors have in common that their emissions are mostly biogenic and could, thus, supply negative emissions once captured (provided that their biogenic feedstock is not associated with a depletion of the carbon stock where it was grown). Waste-to-energy (WtE) plants emit about 60%–65% of the biogenic CO_2. Haaf et al. [53] have assessed the techno-economic impacts of capture with calcium looping and MEA on the generation and cost of electricity. Hammar [55] has assessed heat integration options and found that amine-based capture could retain ~80% and ~100% of the produced electricity and heat, respectively, when capturing 60% of the emissions. Similar results were found for capture of the fossil share of CO_2 by Öberg [54]. The first capture units

(0.1 Mtpa) for CCU are already operating or under construction in the Netherlands, and larger units designed for dedicated storage in Oslo (0.4 Mtpa) and Copenhagen (0.5 Mtpa) are planned to go online in Years 2025/2026 [87], [88].

Direct CO_2 emissions from corn fermentation plants (US) are about 55%–65% biogenic [57]. The ethanol fermenter off-gas is, however, entirely biogenic and has a CO_2 purity of 98–99%, which would allow capture and compression for pipeline transport at a cost of only ~25$/t$CO_2$ [56], which is less than the US tax credit for CCUS. A full-scale capture unit ethanol fermentation with dedicated storage has been operating in Illinois since 2017 at a scale of 1 Mtpa CO_2.

The emissions from modern pulp and paper mills are 75–100% biogenic, depending on the fuel type. In a Nordic context, residual biomass is a common fuel source. An excess of heat and electricity is common [51], and often sold as high revenue product. Residual heat is reported to be insufficient to cover full CO_2 capture [52] and the use of an auxiliary boiler and the importation of electricity are likely consequences of the implementation of CO_2 capture. To date, the lack of incentives for negative emissions has prevented the implementation of CCS in the pulp and paper industry. The Government of Sweden is preparing a first tender for reverse auctions in Year 2023 [89], [90]. The first pilot test campaigns in Europe are being prepared, e.g., in the ACCSESS project [91].

3 Applied and developed methods

Figure 1-1 provides an overview of the methods applied and developed in the appended papers.

- The main method is the *numerical process modeling of the amine-based CO_2 absorption*, which is used at the unit and process level to: 1) study the design of partial capture (**Papers I** and **II**); 2) study the ability to manage (heat and gas) variations depending on the design (**Papers A** and **B**); and 3) estimate the energy demand and provide the basis for equipment sizing for heat integration and the site-level assessment of partial capture (**Papers III–V**). To assess properly the dynamic behavior on an hourly scale, a dynamic model of the MEA absorption cycle developed by Montañés et al. [92], [93] was applied by G. Martinez Castilla in **Paper A**.
- The *pilot-scale test of CO_2 capture* from steam reformer flue gases conducted by Aker Carbon Capture AS at the Lysekil refinery and reported in **Paper II** supports and verifies the process modeling and the findings concerning the energy savings potentials of partial capture (when following one of the two general design pathways; see Section 3.1).
- The *cost-estimation* applied in **Papers I**, **IV**, **V**, and **B** adds an economic dimension to the evaluation of partial CO_2 capture, which is fundamentally motivated by the economic savings that it provides (see Section 4).
- The *heat integration and mapping of heat sources* in **Papers III** and **IV** to study the impact of CO_2 capture on the energy efficiency of a steel mill depending on the level of integration (choice of CO_2 and heat source) are based on a steel mill model described by Hooey et al. [94] and were performed by M. Sundqvist. The heat integration in **Paper V** is based on the analysis of site data on an hourly scale for an entire year, so as to deliver representative, time-dependent capacities for the identified heat sources to an optimization tool.
- The *multi-period optimization* in the form of a mixed-integer linear programming (MILP) model was developed by C. Langner, and is applied in **Paper V** to identify the most-cost-efficient or least-energy-intensive mix of heat sources to power the CO_2 capture unit, depending on the steam demand (site capture rate), steam temperature, and energy system-related and economic parameters.
- **Papers IV** and **V** use *site-level abatement cost curves* to identify partial capture scenarios. These curves incorporate the heat supply cost and CO_2 capture cost into a detailed resolution as a function of the site capture rate (amount of CO_2 captured).
- Finally, **Paper VI** applies *allocation schemes* for the assignment of avoided emissions to co-generated products, to explore the flexibility of allocation that manufacturers should or should not be granted by regulatory bodies.

The remainder of this Chapter briefly describes some of these methods and – where applicable – their contributions to the development of the field (see Aims in Section 1.1). For a description of the experimental setup of the MEA campaign in **Paper II**, the steel mill model in **Papers III** and **IV**, the MILP optimization in **Paper V**, and the dynamic model in **Paper A**, the reader is referred to the respective papers.

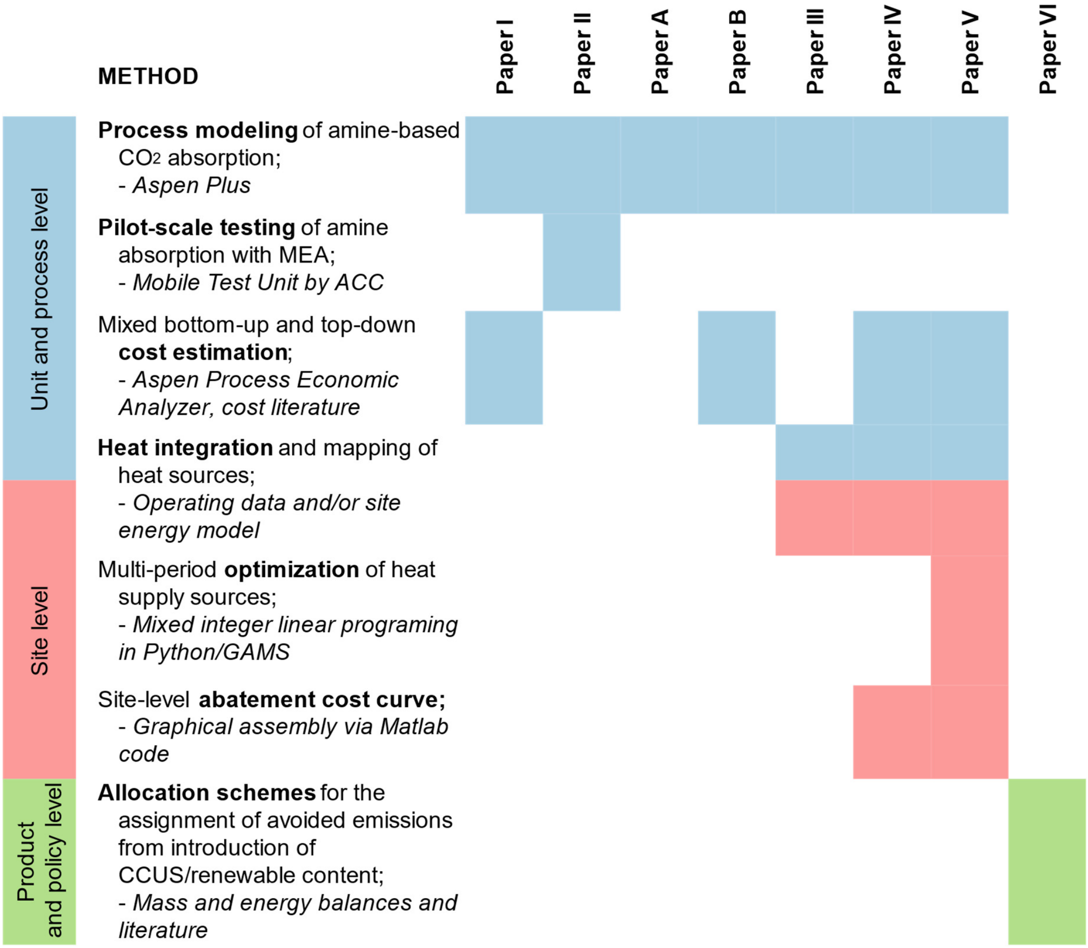

	METHOD	Paper I	Paper II	Paper A	Paper B	Paper III	Paper IV	Paper V	Paper VI
Unit and process level	**Process modeling** of amine-based CO_2 absorption; *- Aspen Plus*	🟦	🟦	🟦	🟦	🟦	🟦	🟦	
	Pilot-scale testing of amine absorption with MEA; *- Mobile Test Unit by ACC*		🟦						
	Mixed bottom-up and top-down **cost estimation**; *- Aspen Process Economic Analyzer, cost literature*	🟦			🟦		🟦	🟦	
Site level	**Heat integration** and mapping of heat sources; *- Operating data and/or site energy model*					🟦🟥	🟦🟥	🟦🟥	
	Multi-period **optimization** of heat supply sources; *- Mixed integer linear programing in Python/GAMS*							🟥	
	Site-level **abatement cost curve;** *- Graphical assembly via Matlab code*						🟥	🟥	
Product and policy level	**Allocation schemes** for the assignment of avoided emissions from introduction of CCUS/renewable content; *- Mass and energy balances and literature*								🟩

Figure 3-1: Overview of the applied methods and the relationships to the appended papers. The tools used are indicated in italics.

3.1 Process modeling of amine absorption

Figure 3-1 depicts the standard solvent process[‡] for CO_2 capture via gas separation in the context of an industrial site and the full CCS chain, including the downstream CO_2 conditioning, intermediate storage, transport and permanent geologic storage. The CO_2-rich gas is brought into contact with the liquid absorbent in a structured-packed column - the absorber - where the CO_2 is absorbed into the liquid phase. The CO_2-lean gas stream is vented, whereas the CO_2-rich liquid enters the desorber (or stripper). In the desorber, the CO_2 is released and the solvent is regenerated by increasing the temperature (to around 120°C). The warm CO_2-lean solvent is circulated back to the absorber via a cross-heat exchanger and cooler. The pure CO_2 stream exiting the top of the stripper is sent to the conditioning unit, which compresses the CO_2 depending on the transport mode.[§]

The capture process is modeled in the Aspen Plus software (Aspen Technology Inc., Bedford, MA, USA) using an aqueous solution of 30 wt.% MEA. The absorption/desorption of CO_2 in the respective columns follows rigorous rate-based calculations, i.e., the rate of mass transfer between the liquid and gas phases is estimated, rather than assuming vapor-liquid phase equilibrium (see [95]). In analogy to the work of Garđarsdóttir et al. [10], the model considers reaction rate constants for relevant reactions in the chemical absorption of CO_2 by MEA. The liquid-phase properties of the aqueous MEA system are estimated based on the non-random two-liquid (NRTL) activity coefficient model for electrolytes, while the Redlich-Kwong equation of state is used for gas-phase properties. The mass transfer and reaction rates are modeled according to the two-film theory of gas absorption [96]. Since the gas absorption rate is limited on the liquid side, the liquid film is discretized to consider both reactions in the liquid film and the mass transfer resistance [97]. The mass transfer coefficients and the interfacial area are estimated using the correlation derived by Bravo et al. [98], while the heat transfer coefficients are obtained using the Chilton and Colburn analogy [99] between mass and heat transfer. Further specifications are detailed in the respective papers, and vary to some extent because the original model settings of Garđarsdóttir et al. [10] were revised[**] in line with [100] for **Papers II** and **V**.

[‡] Common process modifications, such as absorber intercooling and rich solvent splitting, are described and evaluated for partial capture in **Paper I** and partly in **Paper II** but are outside the scope of this summary essay.

[§] **Papers I** and **III–IV** include compression to 110 bara, thus assuming specifications similar to pipeline transport. **Papers II** and **V**, and **Paper A** do not include the CO_2 conditioning in the modeling scope of the work, whereas **Paper B** includes the compression part for ship transport (15 barg) in the modeling scope and estimates the remaining duties of the CO_2 liquefaction based on Deng et al. [122].

[**] In line with the MEA model updated by AspenTech [100], the property data for the MEA system were updated, the property method was set to ENRTL (from ELECNRTL), and the two separate reaction sets for the absorber and desorber were implemented according to Zhang and Chen [173].

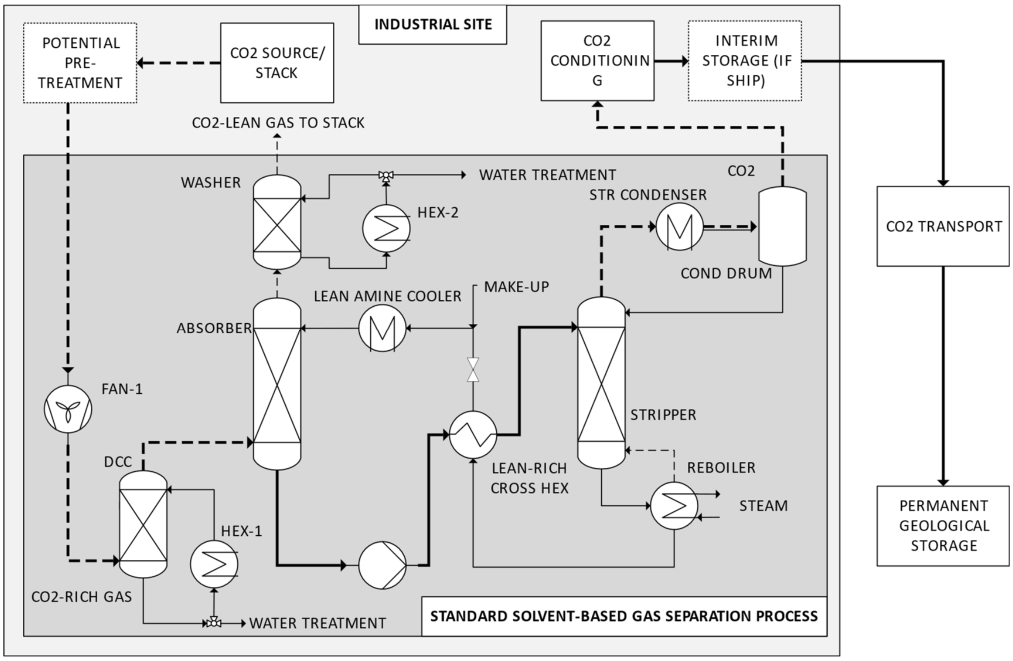

Figure 3-2: Process flow diagram of the standard gas separation solvent process placed in the context of the industrial site and the full CCS chain, i.e., including the off-site CO_2 transport and permanent geologic storage.

3.1.1 Design pathways for partial capture

Paper I describes two fundamental design pathways for partial capture and presents a formalized approach to modeling that allows a comparison of both pathways (see details on gas residence time in **Paper I**). It thereby extends the literature on partial capture [101]–[104], in which the modeling is often described only superficially.

In **Paper I**, a full capture reference is designed with liquid hold-up (~residence times) in line with those reported for pilot plants [105] [106], [107], with column heights representative of full-scale plants. All the equipment is simulated in design mode, i.e., it is sized to a targeted capture rate (e.g., 90%) in the absorber. The full capture design is optimized towards a minimum specific heat demand by varying the liquid-to-gas (L/G) ratio at a targeted capture rate. It should be noted that while the ubiquitous 90% capture target –originally an assumed techno-economic minimum [108], [109] –is useful as a standard for comparisons, it has become something of an academic artifact. This is because: 1) it is occasionally misunderstood as the feasible limit of CO_2 capture, see for example [110]; and 2) it has been superseded in that higher capture rates will eventually be needed to meet the net-zero targets, and recent research [109], [111], [112] points to a manageable cost increase of ≤10% for an additional 10% captured CO_2 [112].

Partial capture may be accomplished through two design pathways derived from the full capture design (Figure 3-3): 1) the *split stream path* (SSP), in which the capture rate is reduced by bypassing parts of the CO_2-rich gas flow, such that a slipstream is treated at a high separation rate of CO_2 in a downscaled absorber (i.e. ~90%); or 2) the *separation rate path* or *off-design* *path* (SRP/ODP)[††], whereby the entire gas flow is treated but a smaller fraction of the CO_2 in the gas flow is separated (i.e., <<90%). The SSP can be interpreted as representing a downscaled full capture design with the same specific reboiler duty per tonne of separated CO_2. The SRP/ODP is similar to full capture in terms of the sizes of the items of equipment (i.e., the absorber and desorber columns), although it has a lower solvent circulation rate, which means that it separates less CO_2 in the absorber while maintaining the gas flow (lower L/G). Table 3-1 summarizes the modeled design path for each of the papers and presents a short motivation for the scope. Concerning the SRP/ODP, **Paper II** extends the modeling approach of **Paper I** by not only setting the packing volume as constant in relation to the full capture design, but also the diameter and height, which implies that the SRP/ODP is operating in off-design mode. The reader is referred to the modeling approach of the design study in Section 3.2.3 of **Paper II.**

To conclude, **Papers I** and **II** have introduced design pathways for partial capture and describe the respective modeling approaches used to evaluate: 1) the ability of the capture unit to cope with variations as a function of the design (**Papers A** and **B**); and 2) the techno-economic performance of partial capture (**Papers III–V**).

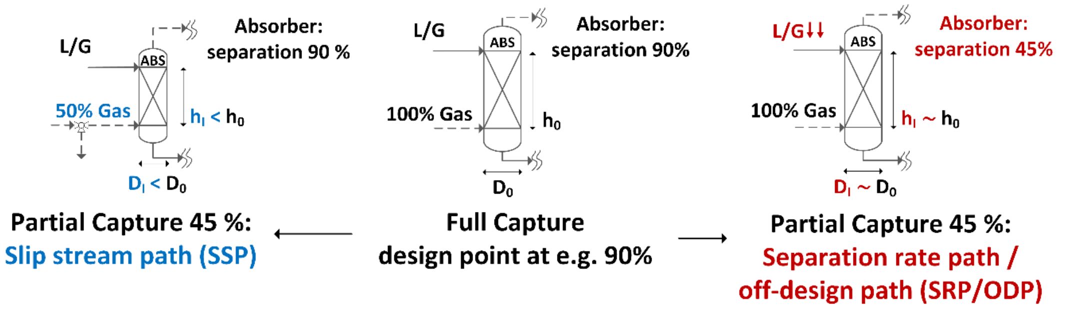

Figure 3-3: The SSP and SRP design pathways for partial capture of 45% of the CO_2, compared to full capture of 90% of the CO_2 in the feed gas. The indices "0" and "1" refer to the full-capture reference dimensions and the partial-capture design dimensions, respectively. Adapted from Paper I.

Table 3-1: Overview of the modeled design pathways for partial CO_2 capture in the appended papers.

Paper	**Split-stream path - SSP**	**SRP/off-design path**	**Comment on modeling/purpose**
Paper I	✓	✓	On-design comparison; gas residence time in absorber kept constant as a criterion for comparison of the pathways
Paper II	✗	✓	Experimental verification of model performance in quantifying SRP for high CO_2 concentrations; modeling study of off-design path concerning energy savings as a function of column design
Paper III + Paper IV	✗	✓	SRP chosen to minimize demand for heat supply
Paper V	✓	✗	Simple scaling of the plant for cost curves
Paper A	✗	✓	Steady-state design basis at peak heat load chosen to handle seasonal variations
Paper B	✓	✓	SRP/off-design for seasonally varying heat load compared to SSP for constant heat load

---

[††] To stress the equivalence to full capture design in terms of the column dimensions, Paper II refers to the SRP as "off-design partial". For the remainder of this thesis, this design path is referred to as SRP/ODP.

3.2 Heat integration – site-specific mapping of heat sources and the ECC method

Papers III–**V** adopt a site-specific approach to the techno-economic assessment (TEA) of the heat supply to the reboiler of the CO_2 capture unit (solvent regeneration), which explicitly includes the heat integration with the industrial process. The heat integration is performed by: 1) mapping the heat sources; and 2) quantifying their heat supply potentials depending on the temperature levels and the assumed minimum temperature differences, ΔT_{min}, for heat transfer based on site-specific data and/or a site energy model. These two steps are incorporated into the TEA approach, which is called the energy supply cost curve (ECC) in **Paper V** (detailed in Section 2.1 of the paper). The ECC can be summarized in four steps:

i. Mapping of heat sources, i.e., identification and classification of heat sources at the site level. Table 3-2 shows examples of heat sources and the applied classification in **Papers IV** and **V** (see **Paper V** for the exact definition) into residual heat (also referred to as 'excess heat' or 'waste heat') and existing and new steam-generating capacity, both of which require the importation of external energy.

ii. Quantification of usable heat (depending on the temperature level and ΔT_{min}), including representative temporal variations (e.g., on an hourly scale), the character of which may vary, as indicated in Table 3-2.

iii. Estimation of capital and operating expenditures and associated emissions (direct and indirect) for each heat source.

iv. Ranking (see **Paper IV**) or optimization (see **Paper V**) to obtain a mix of heat sources that provides the lowest cost or minimizes the use of imported energy (fuel, electricity).

Importantly, the ECC approach allows: 1) identification of a mix of heat sources as a function of the steam demand (CO_2 captured); 2) detailed assessment of the heat recovery potential, e.g., via bottom-up assessments of heat collection networks similar to those reported previously [81], [113], but also considering temporal variations in residual heat; 3) inclusion of the existing capacity of the site energy system to generate additional steam; and 4) incorporation of the indirect emissions associated with different energy carriers and, thus, the regional energy context. The approach thereby extends previous studies, which have often assumed that combined heat and power (CHP) plants are the only heat supply option, and as a consequence couple the economics of CO_2 capture at an industrial site to vast amounts of exported electricity [114], [115], or which have assessed heat recovery based on annually averaged heat load values [81] (also **Papers III** and **IV**), and compared heat recovery as a single measure to different CHP plants (on a one-to-one basis) [49], [80].

Concerning steps iii) and iv) of the ECC, the reader is referred to the following Section 3.3 on cost estimation and the MILP optimization procedure in **Paper V**. A primary output of the ECC is the energy supply cost as a curve plotted against the steam demand and this is an input to the site-level abatement cost described in Section 3.4.

Table 3-2: Classification of CCS heat supply sources at industrial facilities. "Intermittent" denotes strong, irregular fluctuations coupled to the industrial process; "Steady" denotes small fluctuations, which in principle follow the operation/production load of the industrial process; and "Variable" means manageable in the sense that steam generation could be adjusted more or less independently of the operation/production load of the industrial process. Adapted from Paper V.

Class of heat supply	Examples of heat supplying technologies	Character
I - Residual heat (heat recovery)	Vented steam	Intermittent
	Excess gas flaring (other than for safety purposes, start-up, shut down)	Intermittent
	Heat recovery steam generators (using, for example, hot flue gases)	Intermittent/ Variable
	Heat collection network (steam raising, hot water collection)	~Steady
	Heat collection network with heat pumping	~Steady
	Heat recovery from CO_2 conditioning unit; other planned processes	~Steady
II - Existing capacity (external energy)	Switching compressor/pump drive from steam turbine to electric motor;	Variable;
	Turbine back-pressure operation / turbine bleed steam	Variable
	Increase in load of steam boilers (often fossil fuel, such as oil or gas)	Variable
III - New heat capacity (external energy)	Installation of new steam boilers (fossil, biomass, electric)	Variable
	Installation of CHP plants (fossil, biomass)	Variable

3.3 Applied cost estimation

Concerning the estimation of capital expenditures (CAPEX), **Papers I** and **IV** follow the enhanced-detailed-factor (EDF) cost methodology developed by Nils Eldrup [116], whereas **Paper V** follows the methodology applied by SINTEF Energy [76], [117]. Both approaches are similar in that they: 1) apply a discounted cash flow method, in which the investment costs of the CCS units are annualized (as opposed to the net-present-value method or an exhaustive method, see [118]); and 2) represent a factorial bottom-up method, i.e., the equipment size is based on process simulations, the direct cost (equipment cost and installation cost) is estimated using commercial cost-estimating tools (or literature data) and subsequently multiplied by cost factors to obtain the total plant cost (TPC). Figure 3-4 illustrates this approach for the SINTEF Energy method, wherein the cost factors include process contingencies (technology maturity), the indirect cost (engineering, yard improvement, service facilities), and project contingencies (level of cost estimate). In addition to the TPC, the owner's costs and contingencies for spare parts and modifications, as well as the interest accrued during construction are included to obtain the total capital requirement (TCR), which is discounted and annualized (CAPEX). Note that the quotas/literature data for an entire unit (top-down approach) can also be incorporated, so that a mixed approach is possible (useful for non-standard equipment). In contrast, the EDF method adopts a (more-detailed) itemization of individual pieces of equipment and assigns individual cost factors that include the material type based on the type (solids/fluids handling) and the equipment cost (see installation factor sheet in the appendix to [116]). However, the inclusion of data for an entire unit (top-down) seems less-intuitive.

The work presented in this thesis mainly applies cost estimation, and when possible aspires to follow the documented guidelines (see, for example, [119], [120]), and it does not contribute to the development of the costing method per se. However, cost functions for the direct cost of heat-supplying equipment, as well as for CO_2 capture equipment were regressed using polynomial functions or the power-law function ($\text{cost} = a + \text{size}^b$, [121]) and appended to **Paper V,** which may be valuable for others as input. Thus, once simulated, gas-separation processes and heat exchanger networks can be cost-estimated using the cost functions in **Paper V** to obtain the direct cost. Examples and reference values for the cost factors needed to obtain the CAPEX according to Figure 3-4 are listed in Table 3-3, together with cost assumptions that are commonly made to estimate operating expenditures – both fixed (maintenance, labor) and variable (energy, chemicals, sludge disposal, process water).

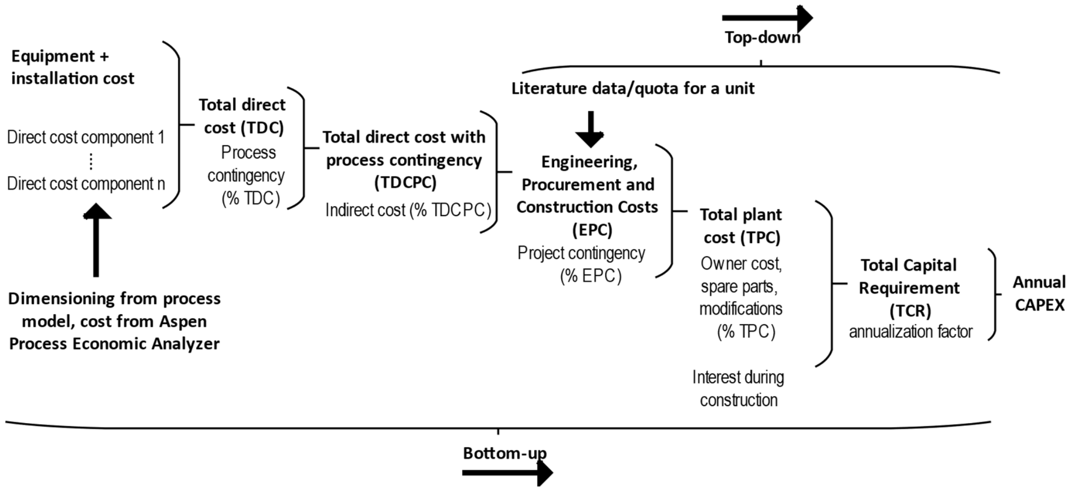

Figure 3-4: Capital cost estimation using a mixed bottom-up and top-down methodology. Arrows indicate the entry point and direction of cost scaling (factors). Source: Paper V, therein adapted from [53], [76], [122].

Table 3-3: Common assumptions for the CAPEX and OPEX estimations in techno-economic estimations for CCS, as adapted from Paper V. The cost factors refer to the nomenclature depicted in Figure 3-4.

CAPEX	Unit	Value	Comment/Reference
Cost year	-	2018	Example value; important to communicate in TEAs.
Techno-economic lifetime	Years	25	Typically applied in academic studies; technical lifetime can be much longer.
Cost index	-	PCD	Adapt cost years; Price index reflecting central European chemical plants [123]; for discussion of cost index, see [119].
Location factor (2018)	-	0.995	Adapt to countries; example of Sweden relative to Netherlands [116] (adjusted to cost in Year 2018); see [119].
Construction time	Years	3 (4)	See [117].
Discount rate	%	8 (5–10)	Average discounted cash flow rate (no inflation).
Annualization factor	TCR/CAPEX	10.67	Depends on rate and lifetime, calculated according to [116].
Process contingencies	%TDC	0–70	Reflects technology maturity (TRL), e.g., commercial (TRL 9) 0%–10%; full-sized modules have been operated (TRL 7–8) 5%–20%; small pilot-plant data (TRL 5–6) 20%–35%; see [124], [125].
Indirect cost	%TDCPC	25	See [115].
Project contingency	%EPC	40	Reflects level of cost estimate. For academic studies: simplified level of 30%–50%; assessed according to [124].
Owner's cost and contingency	%TPC	9.5	See [115].
Interest during construction	%TPC	~9	Depends on construction years and allocation of interest, as well as interest rate; see [117], [124].
OPEX			
Availability (capacity factor)	h/a	8,500	Site-specific; for typical values in industry; see [126].
Maintenance plus insurance	%TPC/a	4 (2–6)	Annual fixed cost; % of total plant cost [117].
Operating labor cost	k€$_{2018}$/a	411	Example (SE): 6 operators, 1 engineer; Swedish labor cost based on average wages [127], extended to full-burdened cost [128].
Natural gas price	€$_{2018}$/MWh	41.4	Example (SE): industrial in Year 2018; no VAT [129].
Electricity price	€$_{2018}$/MWh	58.40	Example (SE): non-household in Year 2018; no VAT [129].
MEA price	€$_{2018}$/t	1,700	[130], Best estimates based on experimental makeup: 1.0–1.6 kg/tCO$_2$.
Cooling water makeup	€/m^3	0.4	[76]; refers to estimated losses, see [131].
Reclaimer sludge disposal	€/t	300	[130]; see IEAGHG report on reclaiming [132].
Caustic soda (NaOH) price	€/t	400	[76]; amount ~1 kg/tCO$_2$; see [32].
Process water makeup	€/m^3	6.65	[76]; amount ~300–500 kg/tCO$_2$ (process simulation).

3.4 Site-level abatement cost curves

Abatement cost curves (ACCs) can help to identify the most-cost-effective level of CCS implementation. At a systems level, marginal ACCs can identify industrial facilities that can achieve low mitigation costs, as illustrated by Garðarsdóttir [42] and Johnson et al. [8] for the process industry and by Beiron et al. [133] for CHP plants.

To provide sufficient detail for such systems-level analyses or decarbonization roadmaps for industrial sites, the graphical approach of site-level ACC (illustrated in Figure 3-5 and applied in **Papers IV** and **V**) can be useful. In essence, the site-level ACC graphically superimposes cost curves for the on-site CO_2 capture and conditioning units onto the cost for energy supply as a function of the level of abatement, i.e., the amount of CO_2 captured (minus direct and indirect emissions).[‡‡] Although the underlying bottom-up assessments of CO_2 and heat sources require some effort, the site-level ACC provides: 1) an enhanced level of detail covering the entire span from partial to full capture at a site; 2) adaptability for sensitivity analyses, provided that the computation of the site-level ACC is sufficiently embedded in a numerical tool; and 3) rapid visual identification of cost-effective levels of CO_2 capture. The site-level ACC approach extends previous work that used marginal ACCs to identify the most-cost-effective stacks (or mitigation technology) [31], [48], in that it can: 1) resolve the degree of capture within a stack and does not treat an entire stack as an increment in a marginal ACC; 2) incorporate site- and scale-dependent costs for the energy supply, which can influence the overall level of cost effectiveness (see Section 6.3.3); and 3) compare and grade different mitigation options.

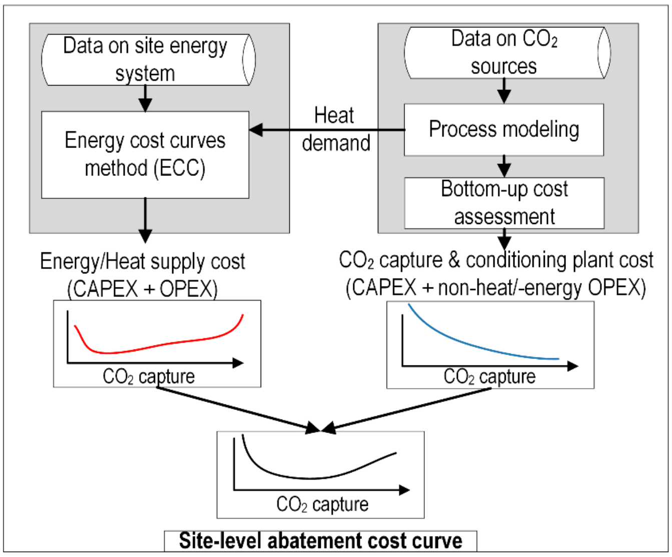

Figure 3-5: Graphical illustration of the approach to the site-level abatement cost curve that incorporates the TEA of CCS units placed at the site (CO_2 capture, conditioning, etc.) and a dedicated TEA of the heat/energy supply cost, e.g., via the ECC method.

[‡‡] Note that the scope of **Paper IV** is limited to direct emissions, while **Paper V** excludes the CO_2 conditioning. In addition, **Papers IV** and **V** focus exclusively on the heat supply, although the approach can be extended to other scale- and site-dependent forms of energy or consumables, such as process cooling.

3.5 Product carbon intensity and carbon allocation

Since a major policy instrument for climate mitigation is carbon pricing, emissions-based metrics such as €/tCO_2 are commonly applied in studies of CCS. Still, the historic levels of carbon pricing in the EU/US have often been considered insufficient to initiate CCS. Thus, downstream policies focused on the product and its value chain have been suggested by, for example, Agora Energiewende [9]. For this, the impact of CCS activities is more clearly expressed in terms of product cost (and thus, price), energy intensity and the carbon intensity, i.e., CO_2 emissions per unit of product. Relevant equations are given in **Papers V** and **VI**, which consider aspects such as the Scope 1–2 emissions[§§] from the CCS chain[***] and Scope 1–3 emissions from the products.

Figure 3-6 introduces the role of carbon allocation as a measure to assign the renewable content and avoided emissions (due to mitigation efforts) to products from an industrial facility. So-called *allocation schemes* for co-processing determine the assignment between the products, for which **Paper VI** fundamentally distinguishes between *physical allocation* and *attribution*. *Physical allocation* is defined as the assignment of avoided emissions (e.g., CCS activity) or renewable content (e.g., biomass use) based on consistent physical relationships between the inputs/outputs and the co-products and their carbon mass, energy content or energy consumption levels. This proximity to physical relationships would give results close to the actual measurements of, for example, C^{14} isotopes (see Dell'Orco et al.[134] for an overview of the measurement techniques for biogenic carbon), for most processes [135]. *Attribution* goes beyond physical representativeness and is a free-choice assignment to any co-product formed in a process into which biogenic carbon has been introduced or from which CO_2 has been captured, provided that the total biogenic carbon input is not exceeded (on a mass or energy basis). See Figure 5 in **Paper VI** for an illustration of the allocation schemes for the co-processing of biogenic and fossil feedstocks, with the example of a blast furnace into which biochar is injected.

Figure 3-6 also illustrates the so-called *within-product allocation* [135], which determines the assignment within a specific product *subsequent* to any allocation or attribution between products. To exemplify this, consider aviation fuel that is produced using a mix of biogenic and fossil feedstocks. A share of the produced fuel can be sold with a renewable content of 100%, while the remainder is sold with 0% to less than 100% renewable content, provided that the

---

[§§] Scope 1 emissions are direct greenhouse gas emissions from sources owned by a company. Scope 2 emissions relate to indirect greenhouse gas emissions from the generation of purchased energy, e.g., electricity. Scope 3 emissions represent indirect emissions that are not owned or controlled by the company, such as the extraction/production/transport of materials/fuels, and the distribution/use of products [174]. Scope 3 emissions were applied where relevant, e.g., to the ethanol product in **Paper VI**, and are used here for the refinery product petrol.

[***] Emissions from CO_2 transport were not included either here or in the Papers. A report by the Norwegian Ministry of Petroleum and Energy [175] estimated ship transport emissions to be 1.3%–2.9% of the transported amount of CO_2 (LNG-fuelled). The lower value is for quay-to-quay transport, whereas the higher value is for direct injection from the vessel.

total renewable content in the feedstock (on a mass or energy basis) - allocated or attributed to the aviation fuel - is not exceeded.

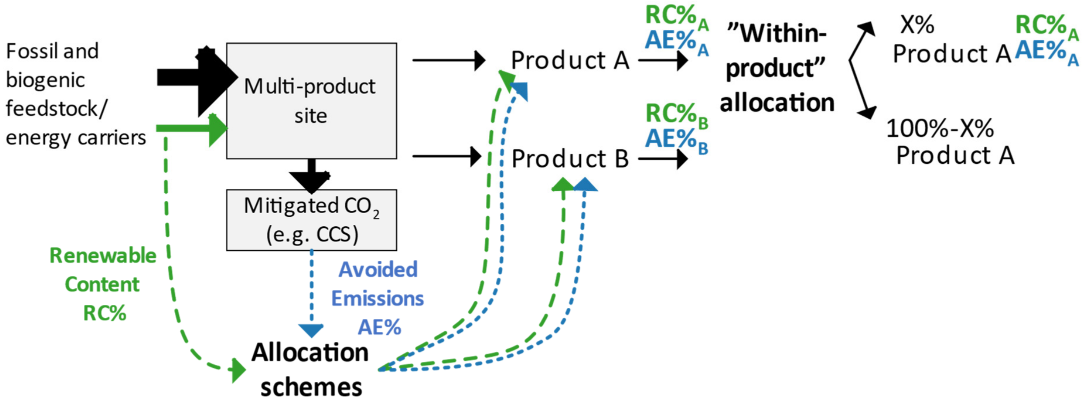

Figure 3-6: Carbon allocation: illustration of *allocation schemes* for the assignment of avoided emissions and renewable content between products, and the *within-product* allocation.

4 The concept of partial capture

Partial capture of carbon aims, for specific market or site conditions, to capture a fraction of the CO_2 available on-site. A list of the conditions that would favor initial implementation of partial capture in process industry over immediate implementation of a full capture process is presented in Table 4-1 (as extension to the list in **Paper I**). Included are examples from the literature and from the papers included in this work. In principle, partial capture is economically motivated. Nonetheless, the specific conditions/motivating aspects can be grouped as:

- Site condition-dependent, i.e., specific to the on-site process characteristics, site energy systems, and process layout, as well as the location of the site, i.e., in the contexts of a regional energy system (energy supply capacities, energy cost regimes) and accessibility to a CO_2 transport and storage infrastructure.
- Product- and market-related, i.e., sector-specific markets; and
- Policy landscape- and funding scheme-derived.

Partial capture differs from full capture in that the lower capture rate confers additional technical degrees of freedom that can be used in the application of a solvent-based process. These can include different pathways for column design, and different degrees of integration at the site (choice of heat and CO_2 source), and allow the process to be designed for market conditions that will vary over time and that value flexibility. As illustrated in Figure 4-1, partial capture sites have the potential to achieve full decarbonization together with co-mitigation measures, and to evolve towards full capture over time. Thus, partial capture can may represent a low-risk starting point towards the final destination in the “roadmap” for industrial decarbonization.

Table 4-1: Motivations and conditions for partial capture in process industry, as compared to immediate implementation of full capture. Extended from Paper I.

Site condition-dependent	Product/market	Policy & funding	Motivating aspect/condition for partial capture over immediate implementation of full capture	Example
×			Site has multiple stacks of varying quality and, thus, different capture costs.	Paper V; Arasto [61]
×			Site has available residual heat, albeit in limited quantity.	Paper III - V Brevik plant [77] Kuramochi [114]
×			Co-mitigation of partial capture with other measures, such as fuel change (biomass), improvements in energy and material efficiency.	Paper VI
×	×		Continuous optimization of the product portfolio. Examples: volatility in energy prices, temporal variations in the production (e.g., seasonal district heating).	Paper A & B; [18]
	×		Emerging markets for high-value, low-carbon products with relatively small volumes.	Paper VI
	×	×	Adherence to an emissions performance standard.	[18]; Clean Power Act [136]
	×	×	Sites co-process biogenic and fossil carbon and the mitigation of either of these is valued higher than the other under the condition that partial capture can mitigate only one.	see Section 5.3
		×	Economic risk reduction (reduction of absolute cost).	Boundary Dam; Port Arthur [82]
		×	Funding gap (carbon price or other policy measure insufficient for full capture).	see Section 7

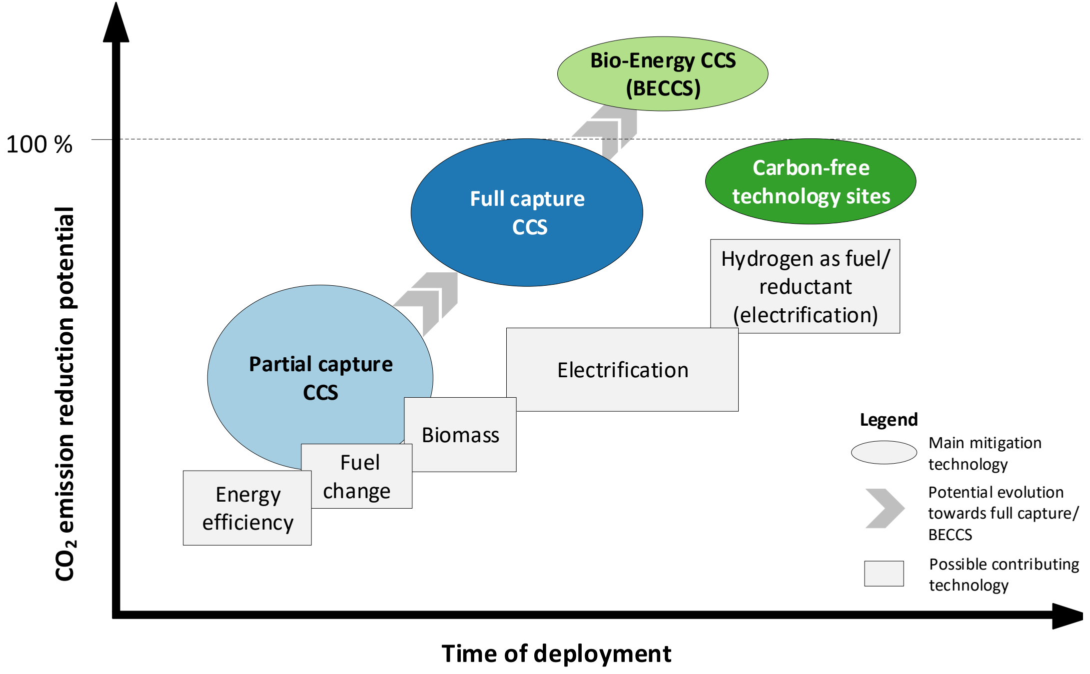

Figure 4-1: Partial capture on an industrial-system level in the context of the decarbonization of process industry over time. The arrows indicate the potential evolution towards full capture/BECCS, though they do not imply partial capture or full capture as prerequisites for BECCS. The timeline is indicative, and carbon-free technologies may very well be available earlier. Adapted from Paper I.

5 Carbon intensities of industrial products and the impact of carbon allocation

The prospect of markets for low-carbon products will incentivize investments in mitigation technologies. This section discusses how the carbon intensities of industrial products are affected by (partial) CO_2 capture and storage (Section 5.1), as well as by carbon allocation (Section 5.2). The concept of sequestered biogenic CO_2 acting as a product to supply negative emissions is discussed in Section 5.3, as a preview of future research.

5.1 Taking the product perspective

Figure 5-1 assigns the impact of CCS to the energy intensity, carbon intensity, and cost of (a single) main product. The case studies of an integrated steel mill and an oil refinery from **Papers IV** and **V**, respectively, are used here as examples. For the steel mill, the single product assumed is a tonne of steel slabs, whereas for the oil refinery it is a GJ or one liter of petrol. Figure 5-1 illustrates how carbon capture allows one to adjust the carbon intensities of industrial products in favor of energy intensity (see the difference between full capture and the reference case). When applying partial capture powered exclusively by residual heat, the carbon intensity may be reduced without significantly increasing the use of primary energy for heat supply at the site. In the case of steel production, the energy intensity with partial capture is even lower than the reference, due to a more-energy-efficient distribution of the steel mill off-gases (see Section 6.3.1). For the steel product, the bulk emissions occur during production [137], which CCS effectively mitigates, thereby reducing the carbon intensity of the product (here, Scope 1). For the petroleum derivatives, only a small fraction of the emissions (here, ~4.4 $kgCO_2$/GJ fuel are emitted at the refinery) can be mitigated by CCS. Even if the full capture case mitigates ~70% of the site emissions, the effect on the fuel's emissions (here, Scope 1–3) is limited to <4%. The role that CCS can play, albeit at similar scale, could include the supply of negative emissions for refineries that replace their fossil feed with sustainable alternatives (biogenic carbon, direct air capture).

Similarly, the impact of CCS on product cost is minor for refinery products, whereas if the cost impact of CCS is assigned to the price of steel, partial and full capture would lead to price increases of ~6% and 15%, respectively. If the EU ETS cost of 100 €/tCO_2 is fully assigned to the steel price, i.e., without any free allowances (and protection from carbon leakage to locations outside of the EU), the price increases by 30% for the reference case. Any implementation of CCS below that cost level would reduce the impact of the EU ETS.

From the perspectives of the end-product and consumers, the additional cost due to CCS (or other mitigation measures) is often low: for refineries, the small cost increase per liter of petrol would scarcely be noticed at the filling station. Short downstream value chains (petrol retailers), some of which are controlled by the refining companies, might help to pass on the extra cost to the customer. For base commodities that are not as close to the consumer, such as steel, mechanisms are needed to distribute the cost to end-products/consumers, e.g., a buyers' coalition [138] or a climate surcharge on material-intensive final products [9]. If passed along the value chain successfully, the cost of low-carbon steel (the CCS cost and EU ETS of 100 €/tCO_2, as in Figure 5-1) would increase the cost for a mid-sized passenger car by <0.5%, as identified by Rootzén et al. [139]. Similarly, pulp and paper products could incentivize BECCS investments for product cost increases of <0.7% [138], and a cost increase for residual buildings of <1% could offset the CO_2 abatement cost of cement [140].

To conclude, the industry- and site-specific impacts of CCS can be better understood by taking the product perspective in addition to emissions-based metrics (€/tCO_2), especially in connection to the value chains in industry and the opportunity to finance CO_2 mitigation of base commodities through the willingness to pay of the consumer (climate surcharge) or public procurement [9].

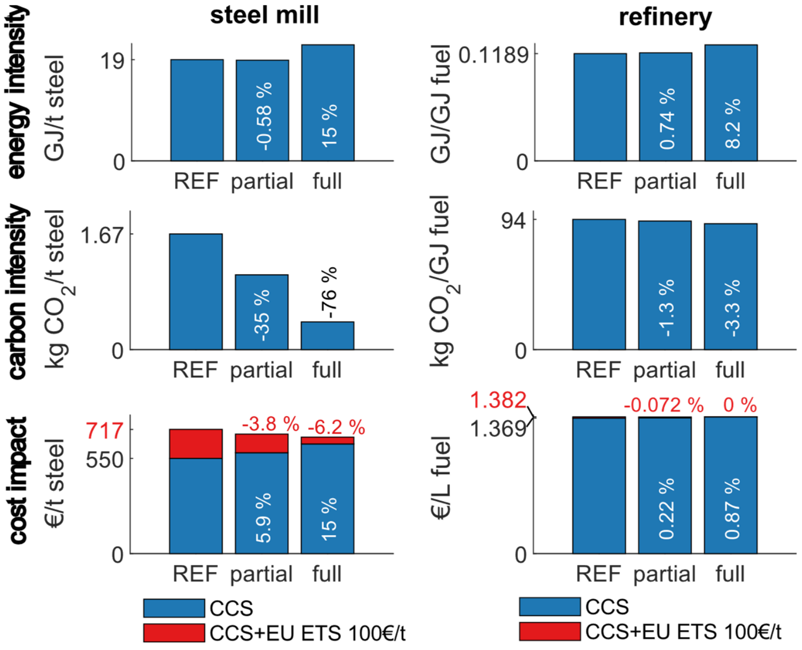

Figure 5-1: Impacts of the degree of CCS implementation from the product perspective, in terms of energy consumption (top panel), emissions intensity (middle panel), and cost impact (bottom panel: with or without an EU ETS cost of 100 €/t) per unit of bulk product from a steel mill (left column) and a refinery (right column). A reference case without CCS (REF) is shown, together with the partial and full capture cases, adapted from Paper IV and Paper V, which correspond to the cases in Figure 6-13. The indicated percentages refer to the changes that result from CCS, as compared to the reference case. The percentages in red refer to the changes that result from CCS, as compared to the reference case, which includes the EU ETS allowance price of 100 €/tCO_2 (no free allowances) for the emission of CO_2 (uncaptured). The cost year is €2018.

5.2 The impacts of carbon allocation on the carbon intensities of products

The impact of carbon allocation on the carbon intensity is illustrated in this section regarding two aspects: 1) within-product allocation; and 2) carbon allocation for multi-product sites that are co-processing biogenic and fossil feedstocks.

To illustrate the first aspect, the steel mill example in the above section is revisited. Figure 5-2 shows that within-product allocation of the avoided emissions (here, through partial capture) would allow the sale of a share of the product as a low- or zero-carbon product, whereas the remaining share would have the same carbon intensity as the reference prior to the installation of the mitigation technology.

The assignment of emissions savings to a single bulk product (petrol or steel slabs) is illustrative, albeit simplified. In practice, most sites have multiple products. Figure 5-3 illustrates the second aspect, using the example of a steel mill that mitigates emissions by applying CCS (capture from the blast furnace gas) and injecting biochar into the blast furnace while co-generating ethanol, as described in **Paper VI**. The figure demonstrates the impact of the allocation scheme on the assigned biogenic content of the product. The *allocation by carbon mass* in Figure 5-3a mimics the physical realities by assigning each carbon-containing effluent stream of the blast furnace the same share of biogenic carbon, corresponding to the ratio of the biogenic to fossil feedstocks entering the BF. Since most of the effluent streams relate to steel production units, the majority of the biogenic carbon is allocated to the steel product. As explained in **Paper VI**, this allocation of biogenic carbon and the allocation of avoided emissions via CCS to ethanol (also on mass basis) are not sufficient to allow the ethanol to qualify as bioethanol (criterion: 65% reduction, as compared to 94 gCO_{2eq}/MJ for petrol). A *free-choice attribution* of biogenic carbon to ethanol in Figure 5-3b and an attribution of avoided emissions via CCS would, however, enable qualification as bioethanol. **Paper VI** further highlights the roles of electricity grid intensities, heat integration, and extent of biochar injection and CCS in the carbon intensity of co-generated ethanol.

These two aspects highlight the impacts of carbon allocation schemes and shed light on the issue as to the level of flexibility that manufacturers should have in allocating emissions savings linked to verifiable and quantifiable mitigation actions. The list below includes the motivation for increased flexibility in carbon allocation, e.g., through attribution or within-product allocation, as well as the risks (adapted from the discussion in **Paper VI**).

The motivation for increased flexibility in carbon allocation includes:

- The degree of mitigation (emissions savings) is independent of the choice of carbon allocation (provided that no double counting of emissions savings occurs).
- Emissions savings can be assigned to high-value products that raise revenue and could, thus, increase the return on an investment made in a mitigation technology. Furthermore, the creation of low-carbon products and additional mitigation technologies may be incentivized.

- Physical representation allocates emissions savings to products produced in large volume. For manufacturers of base materials (steel, cement), the co-generation of high-value, low-carbon products aimed at other sectors (fuels, chemicals) in relatively small volumes may be disincentivized. To qualify as bioethanol, the biochar from the example given in Figure 5-3 could have been gasified in a dedicated plant without co-processing and its synergetic effects (displacing fossil carbon in the blast furnace, biomass impurities from waste wood ending up in slag, heat integration, use of existing equipment), thus leading to a higher cost.
- The length of time required to implement any mitigation measure (even the most ambitious kind) at-scale at large industrial sites could be significant. An example is the large steel mill at Ijmuiden (NL) with annual emissions of 12 $MtCO_2$, which will most likely be mitigated in a stepwise fashion over several years. Within-product allocation might allow the creation of revenue streams for each step taken in that mitigation procedure.

The possible consequences and risks associated with allowing increased flexibility comprise:

- Some products sold will have an assigned biogenic content that is greater (and some products correspondingly will have one that is lower) than the actual physical biogenic content (if measured).
- Flexible attribution and revenues from low-carbon products imply settling for low-levels of mitigation (e.g., partial capture) while maintaining unabated fossil fuel consumption, as opposed to incentivizing immediate, full mitigation.
- Ambiguity and non-transparency with respect to product labeling for the consumer may arise if ‘green’ products (suggesting the avoidance of fossil feedstocks/energy in production) and low-carbon products are labeled as equal, which might be perceived as greenwashing.

Taken together, the findings and discussions laid out here and in **Paper VI** emphasize that policymakers need to address the issue of carbon allocation in a clear way. Ultimately, the regulatory body is left with a political choice when deciding which allocation schemes are valid. If granted, freedom with regards to the choice of allocation may help to create additional value, and thereby, incentivize mitigation. To mitigate the risks, policy measures could reward ambitious mitigation measures, e.g., by remitting a collected climate surcharge depending on the mitigation degree and by mandating labeling that makes a clear distinction between low-carbon and zero-carbon (‘green’) products.

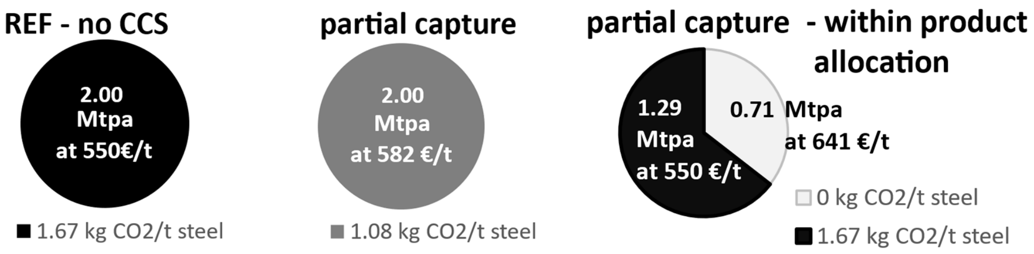

Figure 5-2: Impacts of "within-product"-allocation on the carbon intensity and cost of produced steel (right panel), as compared to: partial capture, where the emissions savings and cost are all allocated to steel (middle panel); and the reference case without CCS (left panel). The values shown are per tonne of steel.

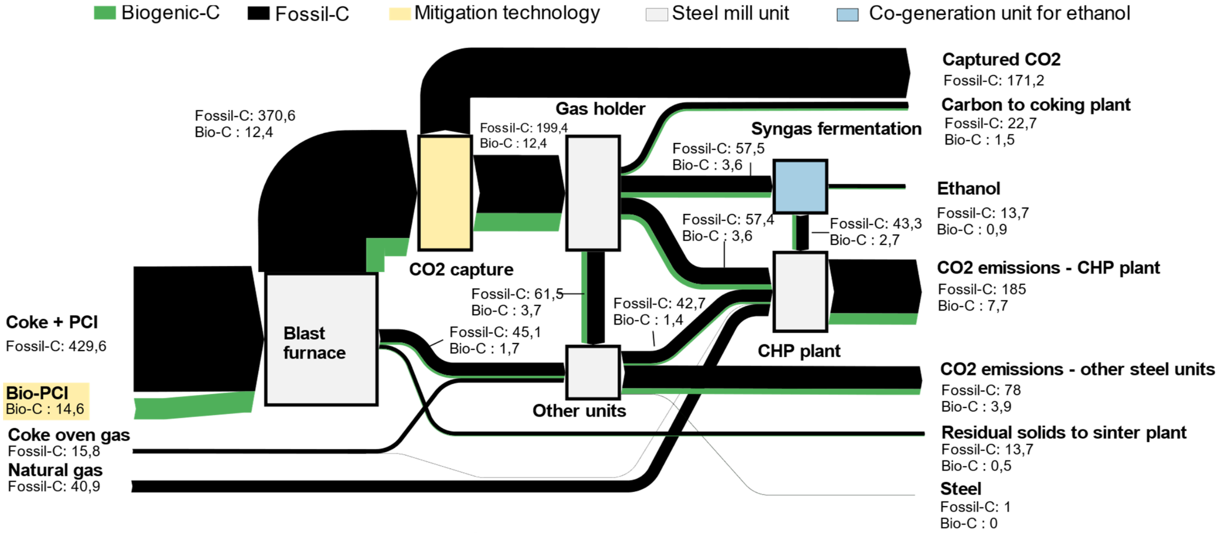

a) Allocation by carbon mass

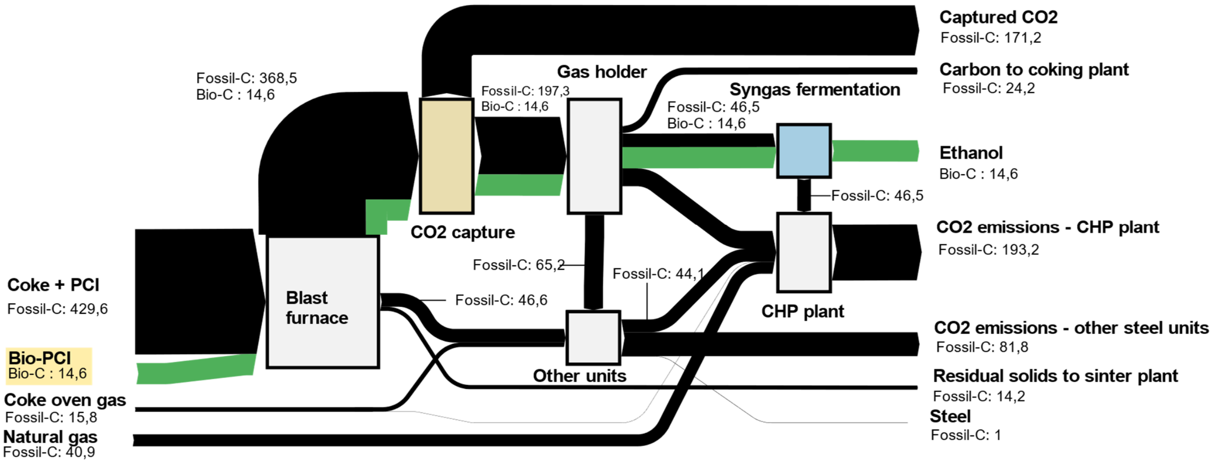

b) Attribution (free-choice) to ethanol

Figure 5-3: Flow of biogenic carbon (green arrows) through a steel mill that has ethanol production and CCS. The allocation between streams is determined through allocation according to the carbon mass (a) and free-choice attribution to ethanol (b). The green arrows are enhanced for visualization purposes (5:1) relative to the black arrows. The values given are kg of carbon per tonne of hot-rolled coil of steel. Note that biogenic carbon is not captured due to the assumption of "fossil carbon first". Adapted from Paper VI.

5.3 Capturing green or black carbon – need for a systems perspective regarding policy and the allocation question

Paper VI reports that the attribution of emissions savings beyond a carbon intensity of 0 kgCO_2/unit product would require robust off-setting mechanisms via the products. However, “carbon-negative” products are less-intuitive than the alternative of selling negative CO_2 as a product. The allocation of biogenic carbon to captured CO_2 as product is exempted from the scope of **Paper VI** (it is assumed instead that fossil carbon is captured first, as shown in Figure 5-3). Thus, the following discussion extends that paper and concerns the application of the product perspective to CO_2 and the roles of policies on carbon allocation in incentivizing CCS and early CCS systems.

Figure 5-4 illustrates a simplified example of carbon allocation for CO_2 capture from a site that emits a blend of biogenic and fossil CO_2 [such as waste-to-energy (WtE) plants, cement plants fired with biomass, refineries ramping up bio feedstock, steel plants injecting biochar]. The figure assumes that negative emissions can occur at the unit level and be sold even if the site-level net-emissions remain positive. In this context, it should be debated as to whether negative emissions relate in scope to the unit, site, corporation, national or even global level. At what point does the captured CO_2 from a biogas-fed steam-reformer in a refinery resemble negative emissions? Is it immediately or only first when the refinery net emissions are zero, or the Scope 1–3 emissions of the manufacturer are zero? The regulations answering these questions will influence incentives for negative emissions. Returning to Figure 5-4 assuming unit-level negative emissions: Different allocation schemes for biogenic carbon to the flow of stored CO_2 are imaginable. Irrespective of whether these schemes follow physical principles (allocation by mass) or attribution (favoring fossil or biogenic carbon),the net-mitigated emissions are the same. Still, the monetization of mitigation efforts may value captured fossil and biogenic carbon differently, for example, in a case where the EU ETS and policy mechanisms for negative emissions (such as reverse auctioning) are not coupled to price, or separate markets allow the sale of negative emissions at much higher prices (e.g., sale on the LCFS credit market in California, which values CO_2 higher than the EU ETS for example; see Figure 2-1). This means that any viable allocation scheme will influence the monetization/revenue from mitigation as soon as fossil carbon and biogenic carbon are valued differently. Some inferred hypotheses exemplify this for the case of high-value negative emissions markets: a physical allocation will favor sites with large biogenic shares in the feedstock, since the amount of fossil carbon that is allocated to stored CO_2 is low and, thus, less fossil carbon must be co-mitigated at a lower value. Attribution that favors biogenic carbon would instead maximize revenues. Attribution that requires fossil carbon to be captured first would minimize the allocation of the biogenic feedstock to captured CO_2, and, thus, minimize the revenues from the high-value, negative emissions market. A possible solution that would enable competition between sites and not favor one over the other, and thereby possibly providing a lower system cost, is to allow flexible allocation (since the origin of a CO_2 molecule emitted to the atmosphere initially does not matter – the warming potential is the same). However, there is interest in maximizing mitigation per investment, especially for early CCS systems, which also may be publicly funded.

Allocation schemes that favor biogenic capture (BECCS) could lead to a more costly systems solution (typically higher capture cost and often lower scale as compared to fossil capture, with the exception of large pulp and paper sites) and the somewhat odd effect of providing vast negative emissions while fossil emissions continue unabated. In addition, there is the risk that biomass could be locked into BECCS schemes rather than being processed into materials, e.g., substituting fossil carbon in the petrochemical industry.

This discussion and the hypotheses illustrate the need for more research in the areas of policy measures, valuation of negative emissions, and carbon allocation, to identify the high-level ramifications on the CCS systems level. The first steps concerning CCS systems modeling and policy measures for BECCS are being conducted by Karlsson et al.[141].

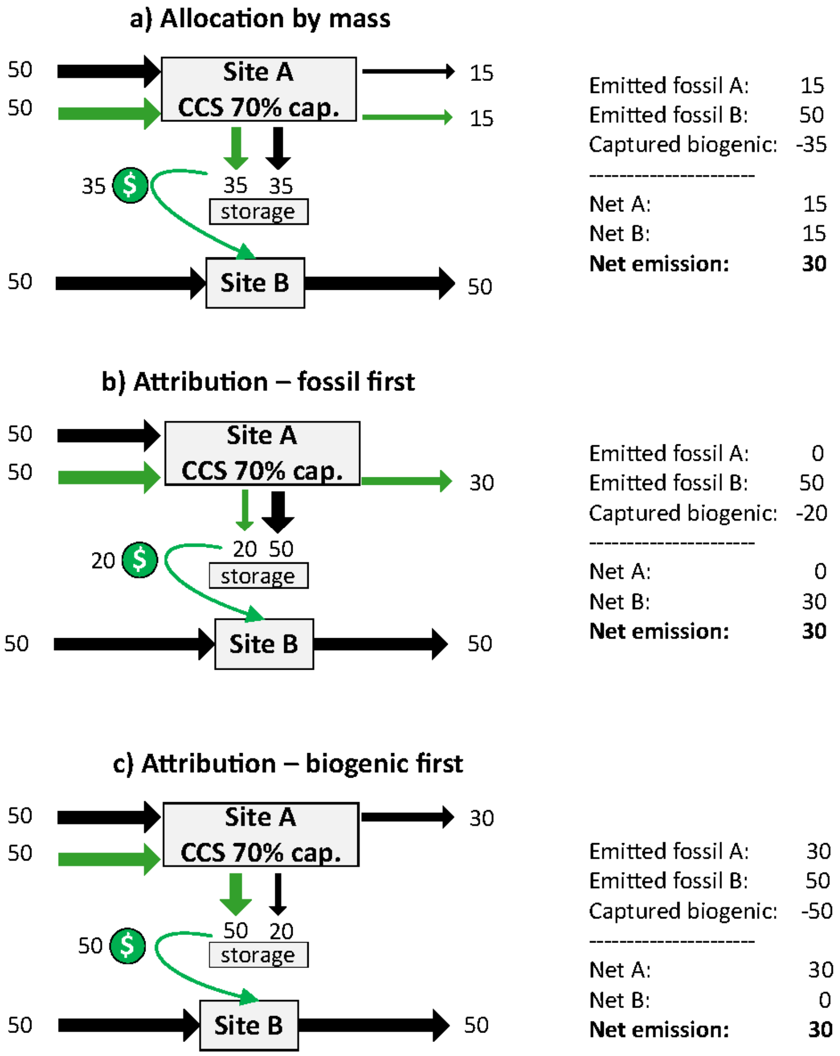

Figure 5-4: Simplified schematic of the allocation of captured biogenic CO_2 and the sale of negative emissions. The numbers refer to unit of carbon dioxide (e.g. tCO_2).

6 Techno-economic assessments - demonstrating the application of partial capture

This Chapter summarizes the key findings for the techno-economic performance of partial capture regarding: the process design of partial capture (Section 6.1), the management of temporal variations in heat supply (Section 6.2), and the importance of heat recovery (Section **Error! Reference source not found.**). In relation to the method development aims, Section 6.3 also illustrates the usefulness of site-level abatement cost curves for identifying partial capture scenarios.

6.1 Process design of partial capture

6.1.1 Techno-economic comparison of design pathways

Figure 6-1 shows the energy performances of the two design pathways for partial capture (see Section 3.1) studied in **Paper I**: the split-stream path (SSP), and the separation rate or off-design path (SRP/ODP) for gases with high CO_2 concentrations (20 vol%). Since it is only down-scaled, the SSP has the same energy performance as the full capture design. For the SRP/ODP, both the specific reboiler duty (SRD) and specific cooling demand decrease while the power demand increases (dominated by the flue gas fan, since the gas flow remains constant) when the separation rate in the absorber is lowered (reduced solvent flow).

Figure 6-2 reveals the mechanism underlying the reduced reboiler duty of the SRP/ODP. It shows that the SRP/ODP (~60% capture) leads to an absorber operation that is characterized by a tendency towards a rich-end pinch rather than a lean-end pinch (*cf.* difference in partial CO_2 pressure between the gas phase and gas/liquid interface) and a bulge temperature of lower magnitude (~73°C) that is located slightly closer to the top of the column than is the case for on-design full capture of 95% of CO_2 (~85°C). The lower temperature and the lower L/G ratio, thus, lead to increased uptake of CO_2 at the top of the column, which leads to a higher loading of the solvent leaving the absorber, ultimately causing a lower SRD in the stripper.

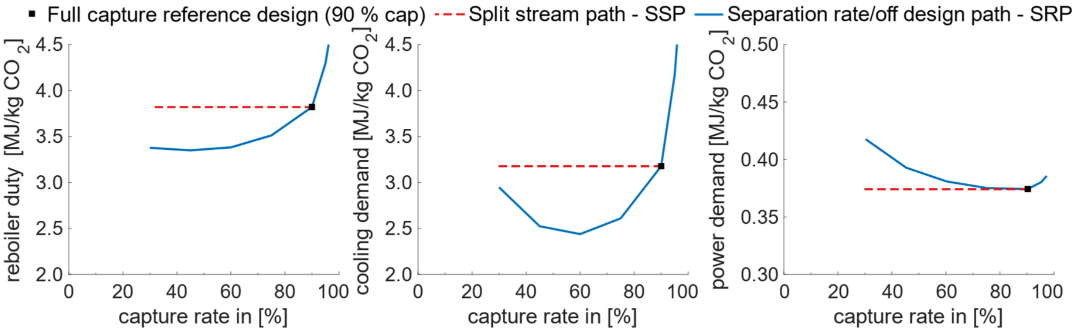

Figure 6-1: Comparison of design pathways for partial capture showing the specific reboiler duty, cooling demand and the power demand for the split-stream path (SSP) and the separation-rate/off-design pathway (SRP/ODP), as compared to a 90% full capture design. The CO_2 concentration in the absorber feed is 20 vol.%$_{wet}$. Note that the ordinates do not start from zero. Adapted from Paper I.

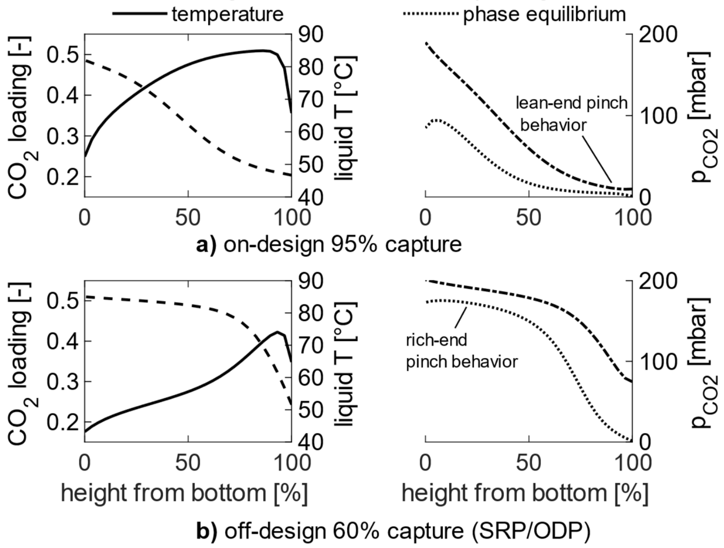

Figure 6-2: Absorber profiles for liquid temperature and molar CO_2 loading (left panels), and McCabe-Thiele plots of the partial CO_2 pressure (right panels) for on-design full capture (a) and SRP/ODP (b) for a fixed absorber design (20 m packing height, design factor of 80% at 95% capture) and a CO_2 concentration of 20 vol%$_{wet}$. Adapted from Paper II.

Depending on the market conditions and, thus, the underlying OPEX-to-CAPEX ratio (*cf.* Figure 17 in **Paper I**), the energy savings may be sufficiently large for the specific capture cost (per tCO_2) of the SRP/ODP to be lower than that for SSP or even full capture. Figure 6-3a shows that: 1) the cost savings linked to the SRP/ODP, given the assumptions made in **Paper I**, can be up to 10% lower than the full capture cost; and 2) the cost advantage diminishes for lower scales/capture rates. Figure 6-3b illustrates the underlying cost structure and identifies the largest savings due to the lower cost for steam supply (for a default value of 17 €/t steam), followed by lower expenses for chemicals and cooling, all of which are coupled to the reduced energy demand and lower L/G ratio of the SRP/ODP. **Paper I** also emphasizes the importance of the CO_2 concentration, and identifies that the reduction in reboiler duty, and consequently the lower specific cost of the SRP/ODP, diminishes for concentrations below 13–17 vol.%$_{wet}$ (depending on the separation rate; *cf.* Figures 11 and 15 in **Paper I**). This is in line with the literature [103], [142], [143] on CO_2 capture from coal power plants (~13 vol.%$_{wet}$), which implies that the SSP is the more-cost-effective design path for partial capture.

To conclude, the chosen design path has ramifications for the energy consumption level and the cost structure of partial CO_2 capture. It is important to emphasize that the cost comparison made here assumes equivalent costs for steam used for partial capture and full capture – an assumption that is challenged (and rightly so) in Section 6.3. Finally, an essential characteristic of the SRP/ODP design is not accounted for in the analyses of **Papers I** and **II**, and that is the flexibility in managing variations when operating in off-design mode. This is further examined in Section 6.2.

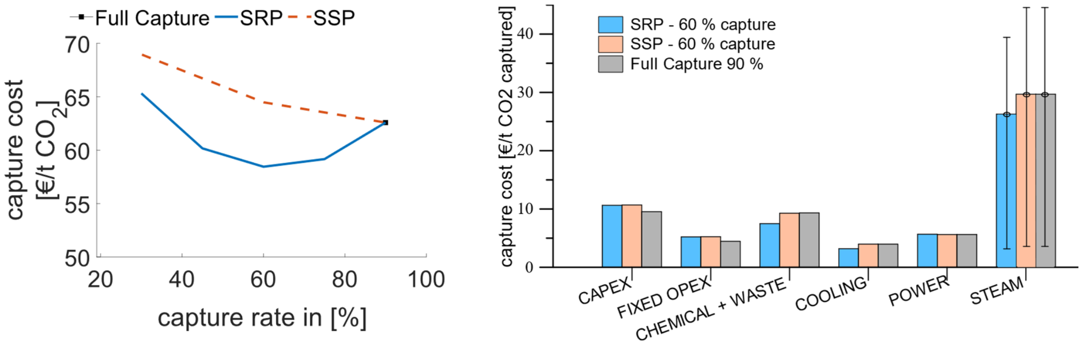

a) b)

Figure 6-3: Capture costs for the partial capture design pathways (a), and the underlying cost structures (b). The reference design is for 90% capture from the flue gas of 200 kg/s with a CO_2 concentration of 20 vol%$_{wet}$ (~1.3 MtCO$_2$ p.a. captured). The range (whiskers) indicated for the steam cost corresponds to 2–25 €/t steam (at 130°C) and the colored bar is for a steam cost of 17 €/t steam.

6.1.2 Experimental verification of off-design partial capture and the impact of column design

The pilot-scale test of CO_2 capture from steam reformer flue gases (18%–20 vol.%$_{wet}$) using MEA reported in **Paper II** is significant in that: 1) no performance results for capture from such CO_2-rich gases using MEA at similar scale have been reported previously; and 2) the energy savings for partial capture via the SRP/ODP, as modeled in **Paper I**, could be verified experimentally. Figure 6-4 shows the experimental SRD and the SRD obtained from numerical modeling in **Paper II** versus the capture rate. Despite the presence of outliers (see Section 5.1 in **Paper II**), the SRD savings for reducing the capture rate from ~90%–95% to 60% are 7% (modeled in **Paper II**), 7–10% (experimental), and 11% (modeled **Paper I**), and these values are in good agreement for a gas with a CO_2 concentration of ~20 vol.%$_{wet}$.

The numerical modeling in **Paper II** further finds that the SRD savings for partial capture via the SRP/ODP depend on the column design (absorber packing height and design factor, i.e., the approach to flooding) and the CO_2 feed concentration, as illustrated in Figure 6-5. The SRD savings decrease when the columns are designed more generously with larger specific packing volumes (greater absorber height, lower design factors, i.e., less-stringent approach to flooding). Furthermore, the share of SRD savings that occurs at a capture rate <90% increases with increasing CO_2 concentrations (coupled to higher absorber temperatures), making off-design partial capture especially interesting for large point sources with high CO_2 concentrations (thus, both **Paper I** and **Paper II** point to lower energy savings for the SRP/ODP at capture rates below 90%).

To conclude, **Paper II** experimentally verifies the energy performance of the SRP/ODP and generalizes by studying its dependence upon column design. Finally, the paper introduces the concept of partial capture with inherent full-capture ready design (see Section 5.3 in **Paper II**).

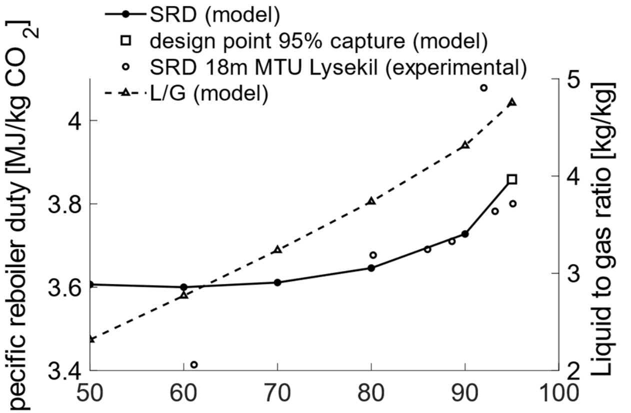

Figure 6-4: Specific reboiler duty (SRD) and liquid-to-gas (L/G) ratio versus absorber CO_2 capture rate for 20 vol.%$_{wet}$ CO_2 for a fixed column design with 95% capture, packing height of 20 m, and design factor of 80%. The experimental values from the pilot-scale campaign are included for comparison (packing height of 18 m, 18–20 vol% CO_2). Note that the ordinates do not start from zero.

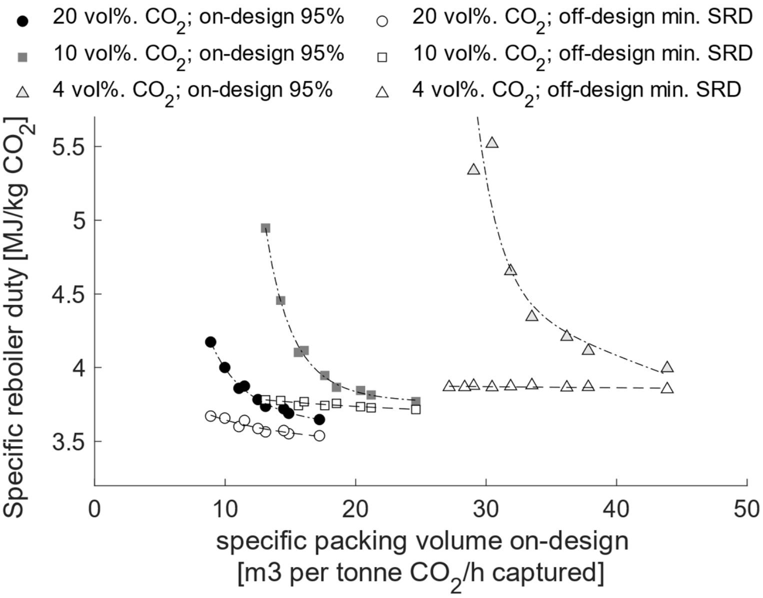

Figure 6-5: The SRD savings, i.e., the vertical difference between on-design (filled symbols) and off-design SRP/ODP (non-filled symbols) as a function of the specific packing volume (on-design, 95% capture) for various CO_2 concentrations.

6.2 Management of temporal variations in heat supply

Typically, the production of base materials occurs at a rather constant load throughout the year, with regular maintenance periods (annual, biennial, or longer) during which production is shut down. Therefore, the amount of residual heat that can be made available for CCS often follows the production load. There can also be an induced seasonality to the availability of residual heat due to varying production levels or energy exports. Figure 6-6 shows two examples of heat that is available for CCS at: a) a rather constant load throughout the year (with hourly-to-monthly variations around an annual average); and b) a seasonally varying load due to district heating export (which is high during wintertime and low during summertime, leading to reciprocally inverse loads of available heat for CCS, as shown in the figure).

This section describes the possibilities to manage such variations in the regime of the capture plant or within the industrial site's energy system. A properly designed capture plant can cope with variations in the amount of heat to the reboiler (and of feed gas to the absorber) on an hour-to-day-scale (see Section 6.2.1), and can also be operated with seasonally-varying load at low-to-moderate cost (see Section 6.2.2). Variations can also be managed within the existing site energy system through the use of additional heat sources with sufficient capacity to back-up a constant load of steam supply to the reboiler (see Section 6.2.3).

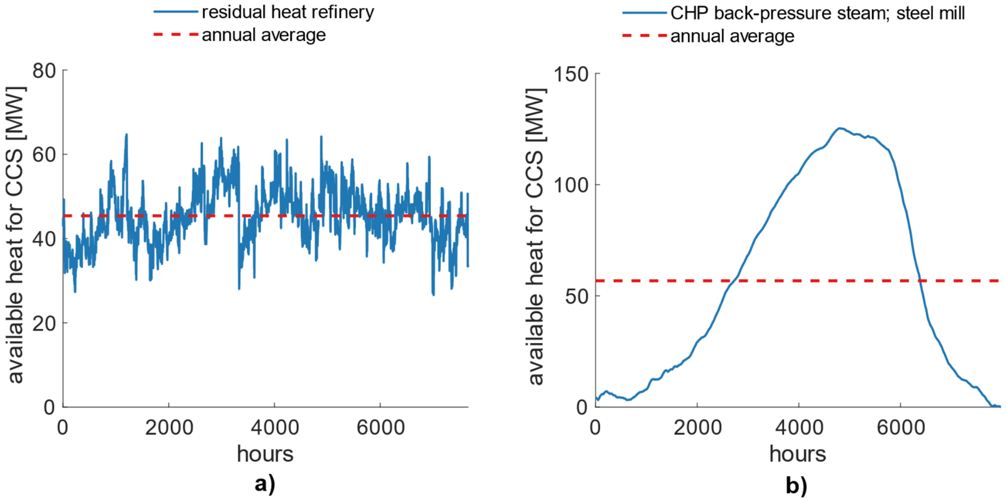

Figure 6-6: Heat available for CCS at a rather constant load (a) and with a seasonally varying load (b) over the course of a year (0 hours = January). The blue curves indicate the assessed heat recovery potentials from residual heat sources (at 131°C) at a complex refinery (a) and the assessed potential of back-pressure steam (at 125°C) of a CHP plant fired with steel mill off-gases that supplies district heating during the winter months.

6.2.1 Impacts of hour-to-day-scale variations in heat and gas supply to the capture unit

The behavior of the MEA absorption cycle in terms of its response time and capture performance is simulated dynamically when variations to the feed gas flow and heat supply are present, as laid out in **Paper A**. Based on a steady-state model of the standard process, the plant is sized to a peak heat load of 155 MW in summer to capture 90% from the BFG gas stream.

The heat supply originates from back-pressure steam (CHP plant) and from the combustion of flare gases. Apart from the underlying seasonal variation in the amount of heat from the CHP (*cf.* Figure 6-6b), variations in the BFG flow and gas flaring occur frequently throughout the year, although they often last for <2 or <8 hours (*cf.* Figures 5 and 6 in **Paper A**).

Figure 6-7 compares the capture performance of a dynamic plant that follows the actual variations to a steady-plant that uses the same averaged amount of heat during a 2-week period in summer. The dynamic plant, in fact, captures 1% more CO_2 than the steady-state plant over the designated time period. Implementing a feedback control strategy that controls the stripper bottom temperature by manipulating the solvent circulation rate increases by an additional 1.2% the amount of captured CO_2. The reason why the dynamic plant performs so well is the non-linearity of the response to changes in heat load. Figure 6-8 shows the absorbed (absorber) and released (stripper) CO_2 levels for a periodic variation in heat load (±30 MW around the baseline of 110 MW) depending on the duration of one cycle. This demonstrates that the increase in CO_2 production in response to a heat increase is both faster and of greater magnitude than the drop in CO_2 production caused by a decrease in heat of the same magnitude. The figure also reveals a buffering capacity for the solvent between the absorber and stripper, which allows for temporary CO_2 release from the stripper even when no gas enters the absorber. This buffering capacity is a function of the size and location of the solvent buffer tank and the solvent circulation rate. It affects the response time of the plant, which, for example, is slower in winter due to lower solvent circulation (lower heat load). **Paper A** concludes that the dynamic MEA capture plant copes well with the described variations within the reference steel mill and can deliver a capture performance that is similar to that of a steady-state plant, as assumed in **Papers III–V**. The prerequisite for this is that the absorption process is designed so as to be sufficiently large (i.e., SRP/ODP) to cope with the entire span of the experienced variations of the heat load.

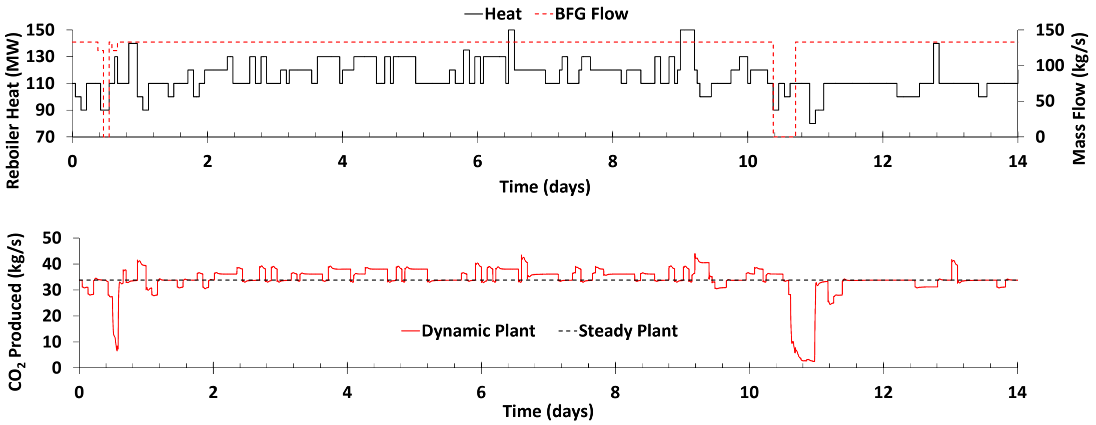

Figure 6-7: Capture performance of a blast furnace gas (BFG) during a 2-week period. Upper panel: Historic variations in the BFG flow and available heat from back-pressure operation and flare gases. Lower panel: Transient responses in CO_2 production to variations for a dynamic plant, as compared to a steady-state plant that utilizes the same average heat at constant load. For details regarding the origins of the historic data, see Paper A. Source: Paper A.

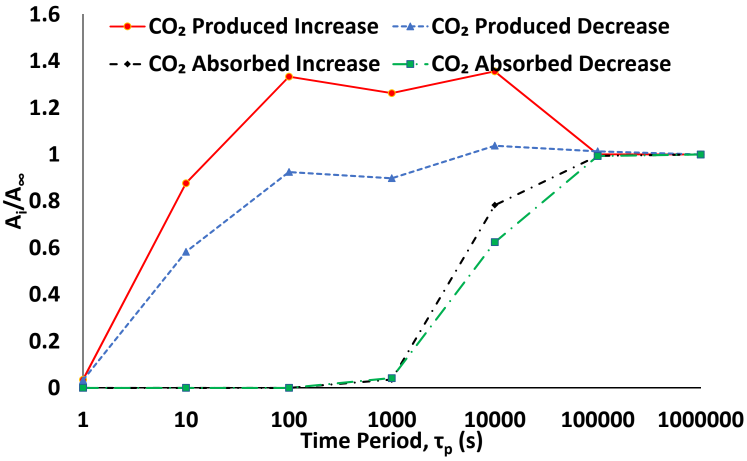

Figure 6-8: Relative amplitudes of CO_2-produced (stripper) and CO_2-absorbed (absorber) depending on the period of sinusoidal variation (±3 0MW around the 110-MW baseline) in the reboiler heat duty. The maximum (Increase) and minimum (Decrease) values of the responses are plotted separately. Source: Paper A.

6.2.2 Seasonal variation in residual heat – are district heating and CCS competing for industrial residual heat?

The ability to cope with seasonal variations by adapting the size of the capture plant (SRP/ODP) to the peak heat load (in summer in the district heating context) will lead to lower utilization of the plant (higher CAPEX per captured tCO_2) during the periods of lower heat load, assuming that the plant follows the load of available heat (blue curve in Figure 6-6b). To estimate the cost impact, **Paper B** compares this type of seasonal operation (steady-state model) to a plant that operates at a constant load and that is sized (SSP) to avoid the same amount of CO_2 (similar to the red line in Figure 6-6b). The constant load operation requires an additional heat supply during periods of low residual heat (increased OPEX). **Paper B** concludes that the increased CAPEX due to low utilization cannot compensate for the OPEX savings and, thus, that the seasonal operation is more costly than the constant operation[†††]. Figure 6-7 demonstrates that the increase in cost of seasonal operation is heavily dependent upon the degree of utilization and the scale. For utilization >~50% and for scales >~400 $ktCO_2$ per annum, the cost increase is <10 €/tCO_2.

Seasonal operation of CCS is a way to retain levels of district heating supply from industrial sites or WtE plants whilst applying CCS. However, in the context of decarbonizing industry, residual heat could be put to better use for CCS, depending on how a reduced district heating supply could be compensated for in the local/regional energy system's context. From the cost perspective, the revenue loss from a reduced district heating supply would be substantial, and could lead to a capture cost similar to that for retaining the district heating supply loads (*cf.* cases D1 and A/B in Figure 11b in **Paper B**). It should be noted that ~25%–38% of the heat

---

[†††] Paper B assumes biomass with 0 gCO_2/kWh for the generic study, and natural gas with 50 gCO_2/kWh in the steel case study. Accounting for indirect emissions or assuming more-carbon-intense fuels will identify a smaller or negative expense for seasonal operation when striving for equal CO_2 avoidance between seasonal and constant operation (increased capture is needed to compensate for higher direct and indirect emissions from the additional fuel used to supply the heat that enables constant CCS operation).

dispatched to the reboiler at 120°–130°C can be directly recovered and utilized for district heating (for details, see the paper by Eliasson et al. [144] and the thesis work of Abrami [145]) (this notion was not included in **Paper B**). Even levels in the range of 89%–126% of the district heating supply can be retained by vigorous heat integration or the use of advanced hybrid heat pumps at the expense of electricity generation, as illustrated for WtE-CHP plants by Hammar [55] and Abrami [43], respectively.

To conclude, both the capture plant's potential for heat recovery and seasonal operation (if properly designed) should be considered when planning the combined implementation and operation of district heating and CCS at industrial sites or WtE plants.

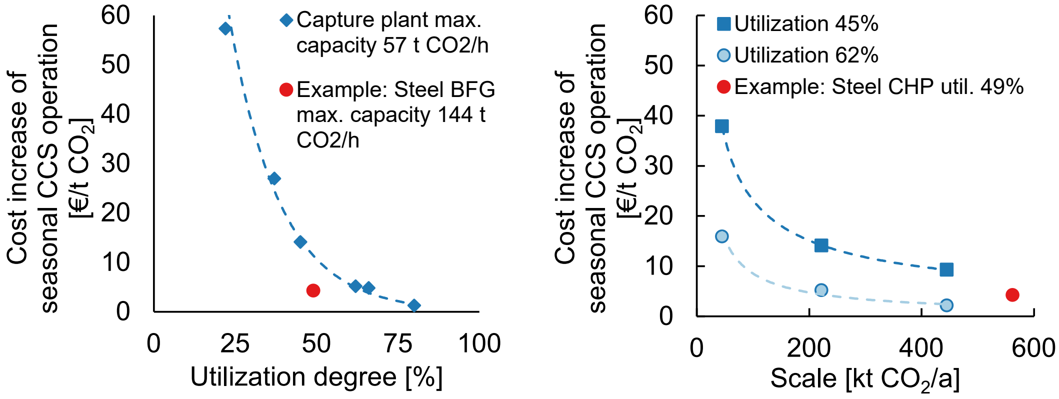

a) b)

Figure 6-9: The cost increase of seasonal operation of the capture plant depending on the degree of plant utilization (a) and the scale (b), as compared to constant operation of the capture plant with 100% utilization to achieve the same annual level of captured CO_2. The blue dashed lines indicate the results of a generic study (13 vol.% CO_2), whereas the red single-dot describes the CO_2 capture from the blast furnace gas (24 vol.% CO_2) with heat from the CHP plant being fed together with the steel mill off-gases. Adapted from Paper B.

6.2.3 Potential of on-site industrial energy systems to manage variations and to supply a constant load to the capture unit

In an industrial energy system (IES), additional reserve heat sources are required if the objective is to supply a constant load of steam to the reboiler in a situation where the available residual heat sources (e.g., excess steam, heat collection networks, heat recovery boilers) are insufficient to meet the targeted heat level due to their temporal variations. For this, either the existing boiler load can be increased (if the capacity is sufficient) or new steam-generating capacities (boilers) need to be installed, both of which entail the expense of increased fuel consumption and emissions. **Figure** 6-10a shows the available heat sources (blue and green) and the managing heat source (red) – in this case natural gas steam boilers – for a refinery case study, as detailed in **Paper V**. The managing heat source is topped-up whenever the (more-economic) heat sources are unavailable. **Figure** 6-10b depicts the alternative of instead managing the variations in heat load in the capture plant, and **Figure** 6-10c illustrates a case of constant heat load when variations in heat sources are omitted from the analysis. Table 6-1 summarizes these three cases. It is evident that: 1) managing the variations in the IES so as to achieve a constant load with additional fuel entails a considerable cost and increased emissions; 2) a proper characterization of the temporal variations in heat sources from IES units is essential for obtaining a representative cost for heat supply, and thus capture cost (omitting variations underestimates the capture cost by 12% in this example); and 3) management of variations in the capture plant versus in the IES may lead to a similar capture cost (~+4 €/tCO_2 compared to a constant load without variations). However, the downstream impact of a variable capture plant load is not assessed here. Ultimately, the capabilities of the capture unit and of the site-specific IES in managing variations in heat supply need to be evaluated in terms of their technical and economic feasibility levels.

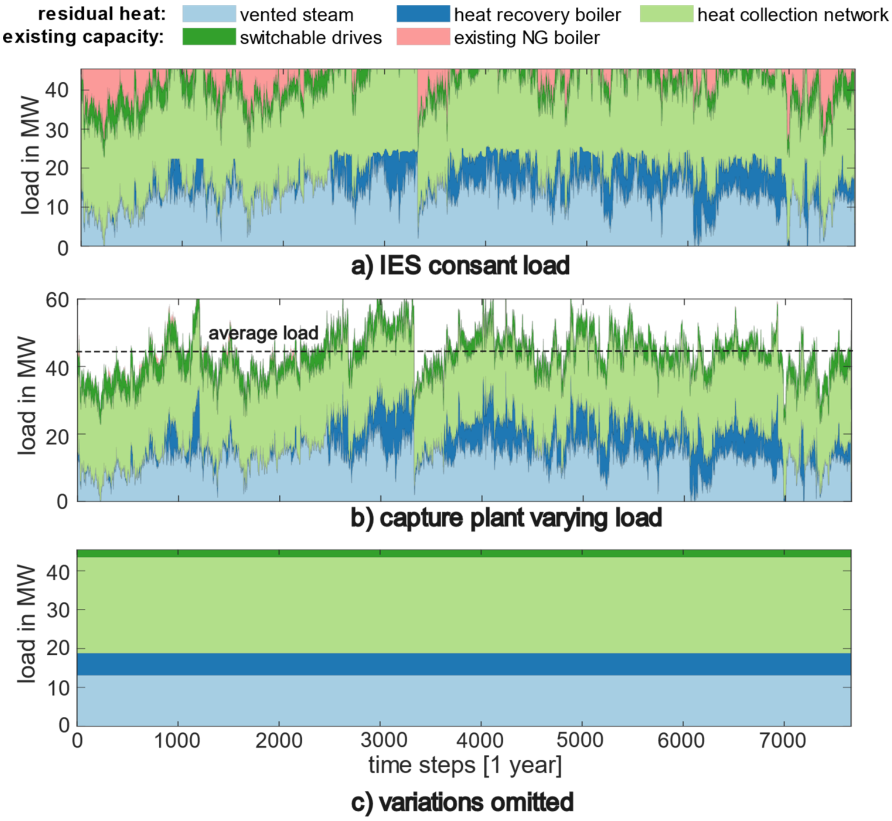

a) IES consant load

b) capture plant varying load

c) variations omitted

Figure 6-10: Load distributions of the heat sources that power the capture of CO_2 from the flue gas of a refinery steam reformer. The management of variations occurs via the industrial energy system (IES) to provide a constant load of 45 MW (a), or via the capture plant (varying reboiler load of 45 MW on average) (b). Plot c) shows the case when omitting variations in the heat sources and instead assuming annually averaged values per heat source.

Table 6-1: Comparison of variation management strategies via a) the industrial energy system (IES) or b) the capture plant. Case c) is when variations are omitted from the analysis (annual average). Cost assumptions are according to Paper V; abs/str columns designed for 20/10 m packing, flooding approach of 80%, 95% capture (SRD ~3.86 MJ/kgCO_2); off-design performance according to model output in Paper II. Util., utilization degree. Capture cost is shown in €/tCO_2 avoided.

Example	Managed by	Variations [MW] min / mean / max	Reboiler [MW]	Captured ktCO_2/a	Capture cost €/tCO_2	Util. [%]
a) IES constant load	IES	27 / 45 / 65	45	360	38.3	100
b) Varying load	Capture plant	27 / 45 / 65	27-65	384	37.7	75
c) Variations omitted	-	45 / 45 / 45	45	360	33.8	100

6.3 Heat recovery and abatement cost curves for CO_2 capture

CCS requires a significant amount of energy, and this demand may even dominate the site energy system. This energy is, however, required at a specific and relatively low temperature level, and efficient integration with the site is crucial. This section illustrates the usefulness of site-level abatement costs for identifying partial capture scenarios in the examples of two case studies: – an integrated steel mill (Section 6.3.1) and a refinery (Section 6.3.2) – and highlights the importance of heat recovery for CCS in industries (Section 6.3.3).

6.3.1 Lessons learned from the integrated steel mill case study

The heat recovery potential from an integrated steel mill is assessed in **Paper III,** which finds heat sufficient to capture 40%–45% of the CO_2 emissions of the site (3.4 Mtpa). The assessed CO_2 sources and identified heat sources are listed in Figure 6-6. **Paper III** demonstrates that high-level integration of CO_2 capture from a process gas, instead of end-of-pipe capture from a flue gas, can positively affect the industrial process. In the steel mill case, capture from the BFG (which feeds into the CHP and the hot stoves) will increase its heating value and facilitate redistribution of the steel mill off-gases, allowing more residual heat to be recovered at higher temperature and entailing a lower primary energy usage by the steel mill. Together with the more-energy-efficient solvent regeneration due to a higher partial CO_2 pressure in the BFG, this leads to an overall more-cost-efficient CO_2 capture, as compared to end-of-pipe capture from flue gases. Abatement cost curves, such as those in Figure 6-11, illustrate the difference in heat integration between the cases: the blue line for BFG capture is consistently lower than the light-blue or red line for flue gas capture. The steps in the curves are caused by the installation of the next ranking heat source (*cf.* Figure 8 in **Paper IV**). Provided that the underlying mapping of heat sources (**Paper III**) and the bottom-up cost estimations of heat supply cost and capture plant cost **(Paper IV)** are done in sufficient detail, such abatement cost curves that incorporate the heat supply cost can effectively compare the capture costs for different CO_2 sources and combinations thereof (via the use of combined strippers; *cf.* Table 3 and Figure 4, **Paper IV**), as a function of the capture rate.

Table 6-2: Assessment of CO$_2$ and heat sources from the case study of an integrated steel mill (2.0 Mt of primary steel slabs p.a.) in Papers III and IV.

CO$_2$ source	**Type**	**c(CO$_2$)** vol.%$_{wet}$	**pressure** bara	**CO$_2$ flow** kt/a	**SRD** MJ/kg CO$_2$[1] @ separation rate (%)
Blast furnace gas	Process gas high-level integration	24.6	1.81	1,410[2]	2.80–2.98 (46–90%)
CHP flue gas	End-of-pipe low-level integration	29.6	1.05	1,910	3.08–3.23 (32–90%)
Hot stoves flue gas	Flue gas/end-of-pipe low-level integration	25.1	1.05	740	3.4 (90%)
Heat source		**Class**	**Pre-ranking**[3]	**Cost** €$_{2015}$/t steam	**Capacity** MJ/kg CO$_2$[4]
Back-pressure steam		I/II	1	<2	0.59
Excess gas flaring (other than safety)		I	2	7	0.4
Heat recovery steam generators (hot stoves)		I	3	2–4	0.09
Coke dry quenching (CDQ) + recovery boiler		I	4	45–55	0.11
Dry slag granulation (DSG) + recovery boiler		I	5	5	0.24
New biomass-fired CHP plant		III	6	18–28	1.08

[1] 30 wt.% MEA with intercooling and rich-solvent split in partial capture off-design (if capture rate is <90%).

[2] The CO$_2$ in the blast furnace ends up in the flue gas of hot stoves and the CHP plant (cf. Figure 2 in **Paper IV**).

[3] Ranking prior to cost estimation based on accessibility/technology maturity.

[4] Related to site emissions of 3.4 Mtpa CO$_2$.

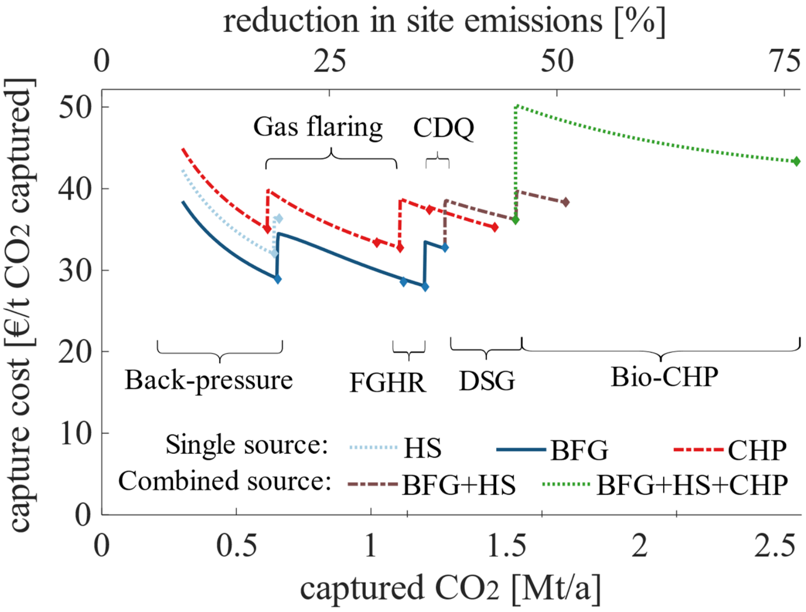

Figure 6-11: Annualized capture cost for CO$_2$ capture from steel mill off-gases in relation to heat source (indicated by brackets) and achieved capture rate at the site level. Cost includes capture plant and heat supply cost (CAPEX and OPEX). Abbreviations: BFG, blast furnace gas; Bio-CHP, additional biomass-fired CHP plant; CDQ, coke dry quenching; CHP, existing combined heat and power plant flue gas; DSG, dry slag granulation; FGHR, flue gas heat recovery; HS, hot stoves flue gas. Source: Paper IV.

6.3.2 Lessons learned from the refinery case study

The case study of a complex, medium-sized refinery in **Paper V** illustrates the methodological advances made in heat supply assessments for CCS (see Section 3.2). Instead of assuming pre-ranked heat sources based on an annually averaged load (**Paper IV**), a mix of heat sources is considered that is optimized (cost or energy minimization) and that accounts for the temporal variations. Figure 6-11 shows the origin of the heat, i.e., the class according to Table 3-2, the heat supply cost curve, and the impact on the capture cost of a mix of heat sources with minimum importation of external energy carriers. In addition to the previous section, the following is a list of the findings that can be extracted from these detailed, site-level abatement cost curves:

- The connection between the class of heat supply and its cost can be illustrated effectively – the heat supply cost increases with the capture rate once the potential of residual heat is exploited, and external energy needs to be imported.
- The approach helps to identify areas with a flat response in cost, i.e., where additional heat can be made available at very little marginal cost – provided that the underlying capacity of the IES and cost structures have been included in sufficient detail.
- For sites with multiple stacks, Figure 6-11 c (blue line) demonstrates that the economy of scale can be negatively affected by the addition of less-suitable stacks (low CO_2 concentration/flow, high level of impurities): the specific capture cost is falling with the capture rate, as expected, when capturing from the first stack. However, when less-suitable stacks are added, the specific capture cost may increase or plateau. Clustering, i.e., sharing equipment or even blending CO_2 sources may improve this situation, albeit only to a limited extent (see [146]).
- Site-level abatement cost curves can also reflect the impacts that indirect emissions from external energy carriers (grid CO_2 emissions, natural gas supply emissions) have on the avoidance of CO_2 and its cost, as shown in in Figure 10 in **Paper V**.

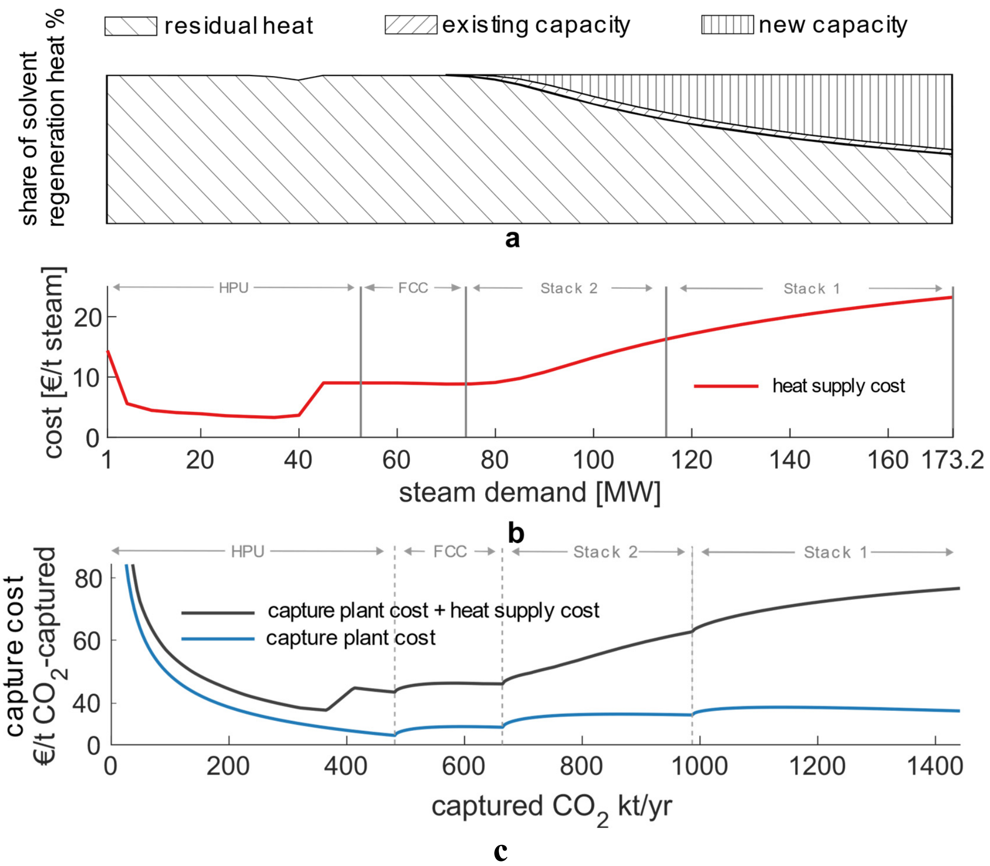

Figure 6-12: Sources of heat for amine solvent regeneration (a), the resulting heat supply cost curve when minimizing the external energy demand (b), and the impacts of heat supply cost on the capture cost (CAPEX & OPEX) of the amine capture plant. The capture plant costs represent one separate capture unit for each stack. Note that the abscissa is the same for panels a and b, but is different for panel c. Adapted from Paper V, and published in [147]**.**

6.3.3 The cost impact of heat supply on the CCS chain as a motivation for partial capture

As illustrated above, detailed site-level abatement cost curves can help to identify cost-efficient partial capture scenarios. These can then be placed in the context of the full CCS chain, i.e., including the conditioning[‡‡‡], transport, and permanent storage of CO_2, and compared with full capture scenarios. Figure 6-13 shows such contextualization for the above-described case studies. It is apparent that: 1) the heat supply for amine capture has a substantial cost impact on the full chain cost; 2) partial capture powered by recovered residual heat can lead to significant cost savings, as compared to full capture (which relies more on external energy), and these cost savings are larger than the economy-of-scale effects; and 3) heat recovery is essential for cost-efficient implementation of CCS. Furthermore, full capture will often require additional primary energy, thus leading to a cost structure that is more-sensitive to external changes in the energy system and market volatility.

To conclude, the use of detailed site-level abatement cost curves that incorporate the heat or energy supply cost based on rigorous bottom-up, techno-economic assessments can assist in identifying the most-economic degree of CO_2 capture for the implementation of CCS at industrial sites.

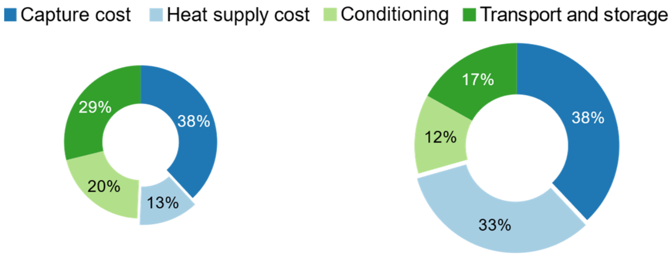

a) partial capture - refinery
78 €/tCO$_2$
482 ktCO$_2$/a

b) full capture - refinery
102 €/tCO$_2$
1 442 ktCO$_2$/a

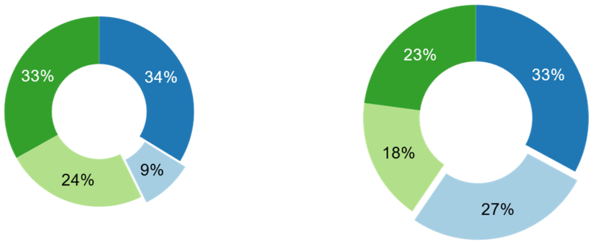

c) partial capture - steel mill
54 €/tCO$_2$
1 202 ktCO$_2$/a

d) full capture - steel milll
65 €/tCO$_2$
2 581 ktCO$_2$/a

Figure 6-13: CCS full-chain cost structure for identified partial capture scenarios a) and c), as compared to full-capture scenarios b) and d) for a Swedish refinery and a Swedish steel mill, respectively. The partial capture scenarios represent capture from a single stack – a steam reformer (a) and the blast furnace gas (c). The full capture scenarios represent capture from all the major stacks at the respective site. Costs shown are in €2018, assuming ship transport at 7 barg to permanent storage below the seabed of the North Sea. Adapted from Papers IV and V.

[‡‡‡] The conditioning unit as well as buffer storage for CO_2 ship transport or the CO_2 compression unit for pipeline transport) could be included into the site-level abatement cost curve to capture economy-of-scale effects (as in **Paper IV**). This was, however, not done in the refinery case study in **Paper V** to simplify the approach.

7 Partial capture as a strategic component of the transition to net-zero emissions

This Chapter discusses the opportunity that partial capture may present with respect to the transition of process industry to its operation within a net-zero GHG framework. Ultimately, partial capture will have to lead to full capture or co-mitigation with other measures or will need to be replaced by a manufacturing technology that avoids the use of carbon entirely (CDA) by the time that the articulated climate targets shall be reached around the middle of the 21st Century. Apart from the techno-economic potential of partial capture laid out in the previous chapters, the following aspects regarding the timeline, alternative mitigation and policy framework will likely influence decision as to near-term partial capture. These aspects are further illustrated in the form of sector-specific narratives that integrate the findings of this thesis and suggest potential applications for partial capture. Lastly, final remarks are presented from a systems perspective.

The additional aspects for consideration regarding the adoption of near-term partial capture are:

- Lead-times for the on-site implementation of CO_2 capture and conditioning units of 4–5 years (~1 year for feasibility study, ~1 year for front-end engineering and design, and ~2–3 years for construction and commissioning) [147].
- Long investment cycles for manufacturing processes of typically 20–70 years [9] will need to be considered and may allow only one opportunity to invest in new manufacturing processes before the net-zero targets need to be reached. As add-on technology, (partial) CO_2 capture is not bound to these cycles directly but would be affected if CO_2 or heat sources are altered by the implementation of a new technology.
- Regarding the scale of the issue, and bearing in mind that some carbon flows at industrial sites are so massive (e.g., Ijmuiden steel plant with 12 Mtpa CO_2) that any full mitigation will require time and substantial investments, there is a need for clear, comprehensive, and robust decarbonization strategies.
- Maturity of alternative production/mitigation technologies and availability of required infrastructure (electricity transmission capacity, hydrogen production/transport, natural gas/biomass access).
- Availability of CO_2 transport and storage infrastructure and coordination with its operators. The first infrastructure facilities in Europe will come online in the period 2024–2026.
- The need to meet EU-wide or corporate near-term climate targets – often articulated for Year 2030.
- The establishment of policy frameworks, e.g., reverse auctions for carbon removal, carbon contracts for difference (CCfD) and the carbon border adjustment mechanism (CBAM), which are required to trigger investments and to guarantee price levels in

combination with the existing EU ETS. It is worth mentioning, however, that emissions allowances under the EU ETS have reached price levels that are probably sufficient to justify economically (partial) CO$_2$ capture. This is illustrated in Figure 7-1, where the indicative full-chain cost for CCS is shown in comparison to the historic EU ETS price and a span of possible future carbon prices based on scenarios taken from the IEA World Energy Outlook 2021.

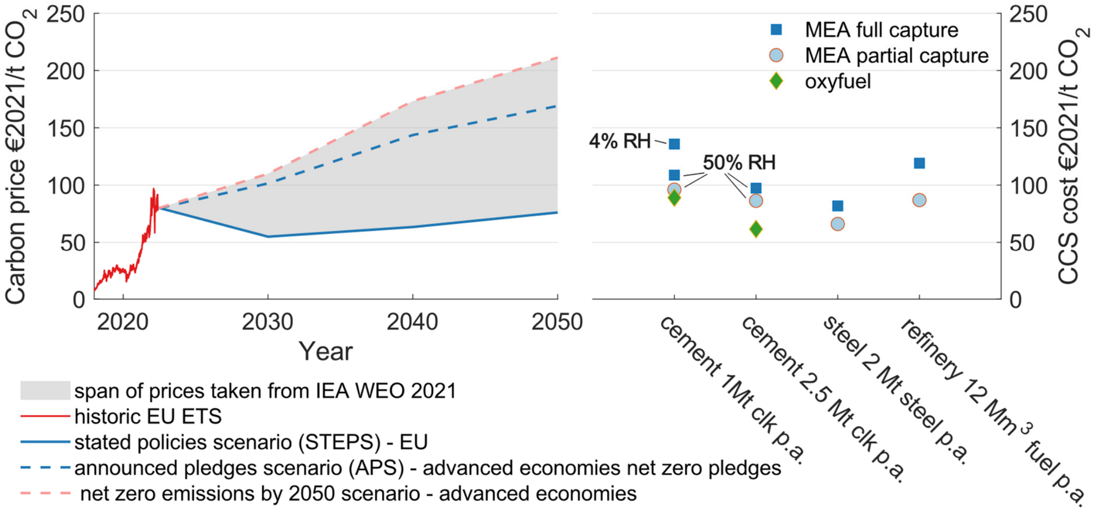

Figure 7-1: Comparison of carbon prices with CCS full-chain costs from steel, refinery, and cement facilities adapted from Paper V, Paper IV, and Garðarsdóttir et al. [76], **respectively (techno-economic lifetime of 25 years assumed). The cost year adaption to €$_{2021}$ is based on the PCD index for CAPEX and fixed OPEX** [148], **the electricity and natural gas prices with the EU average prices for non-household consumers, including taxes and levies** [149], **and other non-energy OPEX for the harmonized index of consumer prices** [150]. **For cement, different degrees of clinker production (clk) and residual heat (RH) availability are shown. The carbon prices include historic EU ETS prices until May 2022** [26] **and a span of scenario prices taken from the IEA's World Energy Outlook 2021** [151]. **The Stated Policies Scenario (STEPS) "*does not take for granted that governments will reach all announced goals. Instead, the STEPS explores where the energy system might go without additional policy implementation*". The Announced Pledges Scenario (APS) "*takes account of all of the climate commitments made by governments around the world, including Nationally Determined Contributions, as well as longer-term net-zero targets, and assumes that they will be met in full and on time.*" The net-zero emissions by 2050 scenario "*shows a narrow but achievable pathway for the global energy sector to achieve net-zero CO$_2$ emissions by 2050, with advanced economies reaching net-zero emissions in advance of others*".**

Narrative 1: The European steel sector – a narrowing window of opportunity for partial capture?

Figure 7-2 summarizes indicative pathways for the primary production of steel[§§§] in the transition to net-zero by Year 2050. The time window for implementation of partial capture at integrated steel mills (BF route) in Europe is closing and or has closed for sites that require re-investment (e.g., BF relining every 15–20 years) before Year 2030, which represents 48% of the primary steel production in the EU [9]. These sites should invest in DRI technologies that initially use natural gas and eventually (or immediately) hydrogen from renewable/low-carbon sources [152]. For sites that continue BF operation for more than 10–15 years, partial capture represents an opportunity to initiate decarbonization in the near-term, before these sites apply either full capture or undertake a transition to the DRI technology. Once the already-invested

---

[§§§] Other mitigation options not shown include increased scrap use (recycling), import of DRI (switch to secondary steelmaking) and direct electrification (electrowinning).

BF reaches its end of lifetime, the invested CO_2 infrastructure can be further used for DRI reactors that run on hydrocarbons (gas, coal) or to generate hydrogen from hydrocarbons with CCS in combination with hydrogen from renewable sources. The recent geopolitical disruption between Russia and the EU (and other Western states) caused by the Russian war of aggression on Ukraine challenges the short- to mid-term gas supply to Europe and, thus, will make the gas-bridge for steelmaking more costly. Using the existing coal supply infrastructure at the sites to generate the reducing gas for a DRI reactor (DRI based on coal gasification is commercial [153]) with inherent CO_2 capture and subsequent storage might be an option to consider that ensures a timely shift to DRI technology (although this needs further detailed investigation). To conclude, the application of partial CO_2 capture in the steel industry will only be of interest for sites that: 1) remain vested in the existing BF technology because of the long investment cycles and/or cannot switch to hydrogen-based DRI immediately[****]; and 2) want to reduce emissions from DRI operation based on hydrocarbons.

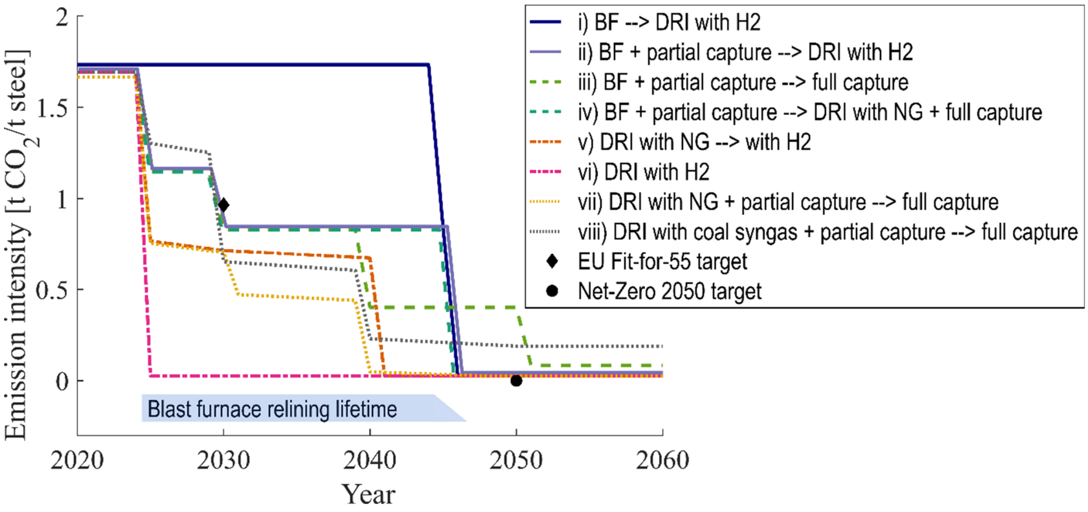

Figure 7-2: Timelines of indicative decarbonization pathways for primary steelmaking in the transition to net-zero. Assumptions: investment/implementation in Year 2025; EU grid electricity with 265 gCO_2/kWh in Year 2020 falling to zero by Year 2050 [154]; hydrogen from dedicated renewable electricity (0 gCO_2/kWh). Descriptions of pathways: i) BF relining (business-as-usual), then transition to DRI/EAF with H_2; **ii)** BF relining and partial capture first from BF, then HS, then transition to DRI/EAF with H_2; **iii)** BF relining and partial capture first from BF, then HS, then CHP plant, then full capture also from minor stacks (**Paper IV**); **iv)** BF relining and partial capture first from BF, then HS, then transition to DRI/EAF with NG and full capture; **v)** DRI/EAF with NG [155], then transition to H_2 in Year 2040; **vi)** immediate implementation of DRI/EAF with H_2 at full scale [70], [71]; **vii)** DRI/EAF with NG, then partial capture [156] (inherent CO_2 removal from reducing gas) from Year 2030 onwards and full capture (95% CO_2 capture from heating) by Year 2050; **viii)** DRI/EAF with syngas from coal gasification as reducing gas [157] with partial capture (inherent CO_2 removal from syngas and reducing gas) from Year 2030 onwards and full capture by Year 2050 (95% CO_2 capture from heating); EU Fit-for-55 target, assumes 55% reduction from 1,968 kgCO_2/t of crude steel for integrated steel mills in EU-27 countries in Year 1990 [158]. Abbreviations: BF, integrated steel mill close to BAT; DRI, gas-based direct reduced iron in shaft furnace with subsequent electric arc furnace (EAF); NG, natural gas; H2, hydrogen from electrolysis; HS, hot stoves; CHP, combined heat and power.

[****] Possible hurdles can be: hydrogen/renewable energy supply (production, transmission, if grid: CO_2 intensity); ore-quality required for DRI operation [176].

Narrative 2: Hydrogen production – partial capture to ramp up the low-carbon hydrogen supply

So-called blue hydrogen, i.e., hydrogen generated from steam reforming of hydrocarbons with CCS, has been heavily debated as to whether it has a sufficiently low-carbon character comparable to that of so-called 'green hydrogen', i.e., hydrogen from the electrolysis of water using renewable electricity, or is merely a distraction, i.e., its mitigation of emissions is insufficient due to the high level of fugitive methane emissions and low capture rates (e.g., from reformer syngas) and, therefore, simply a means for the fossil industry to continue their business model, as claimed by Howarth and Jacobsen [110]. Recent studies [159]–[161], however, have confirmed that blue hydrogen can have GHG emission levels comparable to hydrogen from electrolysis that is powered with renewable energy to 90%, provided that high capture rates >90% and minimal fugitive methane emissions (<1%) are achieved. Thus, for dedicated greenfield blue hydrogen plants, partial capture does not seem intuitive. For existing plants in the petrochemical and fertilizer industries, however, partial capture is a possibility for near-term mitigation, and it can be either ramped up to full capture or complemented with green hydrogen over time. This hybrid approach of combining electrolysis and steam reforming with CO_2 capture is especially interesting for ammonia production coupled to the fertilizer industry, where CO_2 is a feedstock for urea synthesis [162].

Narrative 3: Cement manufacturing – partial capture and co-mitigation to reach net-zero emissions

Partial CO_2 capture can be combined with other mitigation options to reach net-zero GHG emissions in the cement manufacturing. These co-mitigation options (see Section 2.3) include energy efficiency measures, switching to biofuels and/or kiln electrification, new cementious or less-clinker-intense products, carbonization of concrete structures during their lifetimes, and recycling of concrete, as shown in Figure 7-3. Although the first project currently under construction targets partial capture (see Section 2.3), the immediate implementation of full CO_2 capture may be preferred because: 1) it would unlock potential negative emissions (once the biofuel share is >~25% [9]); 2) it is likely that current EU ETS prices are already sufficiently high to cover its extra cost; and 3) it would maximize CO_2 mitigation prior to the target years and minimize the risk of possible delays in the ramping up of co-mitigation measures. For example, early plans for the Slite site in Gotland, Sweden consider the full capture of all direct emissions (1.8 Mtpa) by Year 2030 [163]. Partial capture may, thus, only be relevant with inherent full-capture ready design (as suggested in **Paper II**) at sites that aim to implement full capture in a stepwise manner, e.g., to minimize the initial investment or due to initial restrictions on the energy supply.

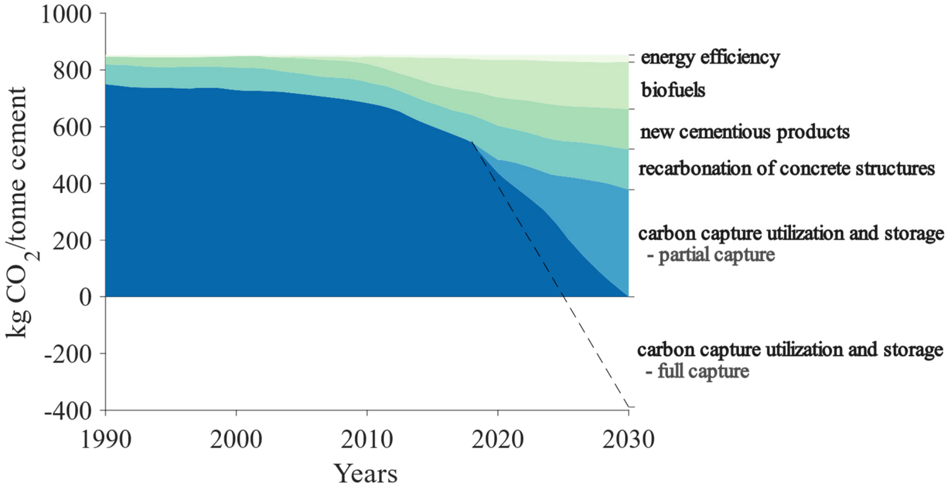

Figure 7-3: Roadmap for cement manufacturing adapted from the net-zero vision communicated by Cementa AB in 2018 [164]. **The dashed line indicates the potential for achieving negative emissions.**

Narrative 4: Waste-to-energy – partial capture as an opportunity to expand and flexibly manage the product portfolio

WtE plants could apply partial capture (SRP/ODP) to adapt flexibly the capture rate to the energy market. For example, the capture rate can be increased during summertime when the district heating demand is low. If heat recovery from the capture and conditioning units (see Section 6.2.2) allows a minimum capture rate corresponding to the fossil share of the fuel in wintertime without substantial penalties being imposed on the supply of district heating, then the increased capture rate during summertime could provide negative emissions at the site level on an annual basis. Thus, the product portfolio could be expanded to include carbon removal and to allow flexible management throughout the year depending on the regional energy and carbon markets. As illustrated in Section 5.3, the valid carbon allocation scheme and the valorisation of carbon removal may affect the attractiveness of such a strategy.

Narrative 5: Kraft pulp mill – partial capture as a first step to cost-efficient BECCS

Given the flow and concentration of biogenic CO_2 at kraft pulp mills in Sweden (see Section 2.3), partial CO_2 capture could be key to providing carbon removal via BECCS at low cost and to win reverse auction rounds initiated by the public authorities. Similar to the techno-economic assessment in this thesis (see Section 6.3), energy supply via heat recovery is likely to influence the level of cost-effective CO_2 capture on-site and would allow minimization of the additional combustion of scarce biogenic resources.

Narrative 6: Petroleum refineries – a first step in mitigation for 'Big Oil' in line with carbon takeback obligations

Petroleum refineries have in essence an unsustainable business model in selling fossil carbon. Biomass resources are limited relative to fossil carbon sources, and only a fraction of today's refining capacity may be needed for refining biofuels. Many refineries will face closure and European oil refineries are already experiencing overcapacity problems [165] and a declining demand for their products. Partial capture of carbon at refinery sites with good prospects for transitioning to bio-refining represents a possibility for early CO_2 mitigation and for complementing the transition of the refinery site. Many refineries are located close to relevant sea ports and have the prerequisites of relatively low-cost CO_2 (e.g., from steam reformers) and knowledgeable staff to help accumulate volumes from several industries so as to form CO_2 hubs, as planned for example in Rotterdam [166].

Finally, (partial) CO_2 capture from refineries could present the starting point for the major oil companies to deploy CCS within their own corporations (Scope 1) or along their value chains (Scope 3). Oil companies, some of which have communicated ambitious net-zero goals including Scope 3 (such as Equinor [167]), will have to apply CCS (and DACCS) or stop extracting carbon from the earth's crust altogether. Interestingly, such a goal is in perfect alignment with a CCS obligation policy that mandates fossil fuel suppliers to sequester an increasing percentage of the CO_2 associated with their supply to a jurisdiction, for example the UK, as suggested by Oxburgh et al. [168] to the UK government in 2016. This type of progressive carbon takeback obligation (CTBO) has been elaborated in the works of Jenkins et al. [169] and reflects the simple fact that the ratio of carbon extracted to carbon sequestered needs to reach a value of 1 by the time global warming is to stop, i.e., once 1.5°C or 2°C of global warming is reached, as indicated in Figure 7-4. Jenkins et al. have reported that a CTBO can mitigate emissions at a comparable or potentially lower cost for Society as conventional integrated assessment models (IAMs) that employ a global carbon price. In a nutshell, (partial) capture from refineries (or other point sources) can be a cost-effective starting point for oil companies to mitigate in the current policy regime of EU carbon pricing and can also present a head start to get onto pathways consistent with CTBO policies if these are implemented in the future. This complementary motivation for partial capture and the CTBO as useful policy are captured also in the title image of this thesis.

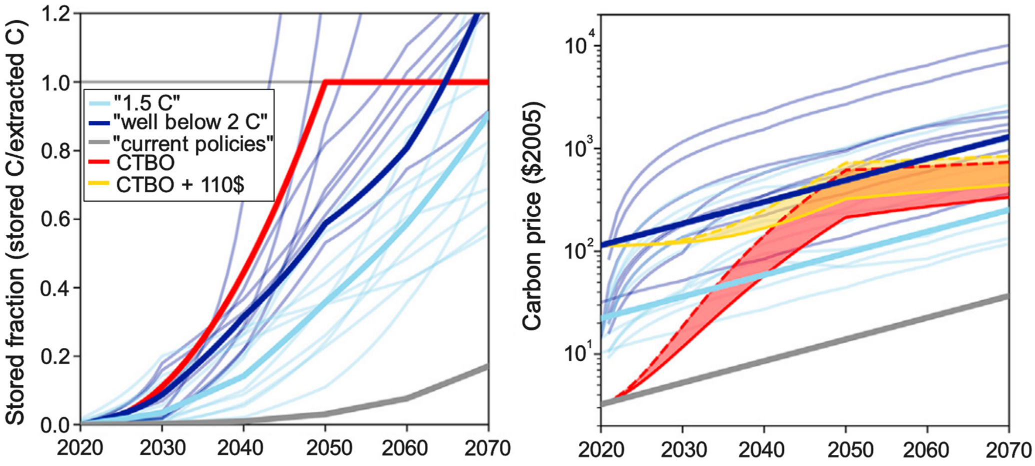

Figure 7-4: Comparison of conventional mitigation scenarios from IAMs (blue lines) with a global carbon takeback obligation (CTBO; red and yellow lines). The two levels of climate ambition of "1.5°C" and "well below 2°C" relate to the shared socioeconomic pathways SSPX-1.9 and SSPX-2.6. The "current policies" scenario (SSPX-4.5) is shown in gray. The left-hand panel shows the ratio of stored to extracted carbon (produced global energy and process emissions), while the right-hand panel shows the carbon price driving the mitigation in the IAMs compared to the cost of compliance with the CTBO. The yellow line indicates an alternative CTBO that includes a constant carbon price of 110 $ per tonne CO_2 in addition to the CTBO compliance cost, which results in cumulative emissions consistent with the "1.5°C" scenario at similar or lower cost. Reprinted from Jenkins et al. [169].

Final remarks from a systems perspective – time is of the essence

From a systems perspective, partial capture can be a piece in the puzzle to accomplish a timely transition to net-zero in the process industry. In the near-term, it can take on a share of the mitigation and relieve pressure on the electricity system and the ramping up of renewable electricity generation that is needed to expand and mitigate fossil emissions in all sectors, such as transport, residential heating, and industrial sectors, in which CCS is less-feasible and electrification presents a reasonable (if not the only feasible) option. Since humanity apparently did not heed early warnings (e.g., the testimony given by Dr. Hansen before the US Senate in 1988, which did initiate political work on climate change [170], [171] but did not prompt any stringent policy or resolute mitigation action) to reduce emissions in time, carbon removal from the atmosphere is now a necessity to limit global warning to 1.5°C [3]. Since natural mechanisms are limited, BECCS and DACCS will be needed at large scale, and these technologies will require a CO_2 transport and storage infrastructure. Partial capture can help to initiate the ramping up of point-source CCS, to ensure that a CO_2 transport and storage industry is established at a scale that can also handle negative emissions.

Finally, the widespread, near-term implementation of partial capture would initiate large-scale emissions reductions and decrease the risk of new production technologies failing to arrive on time and at scale to meet reductions targets. This is an important argument in favor of partial capture, since it is the accumulated CO_2 emissions that govern whether or not the world will comply with the Paris Agreement of staying well below 2°C global warming compared to pre-industrial levels. Reductions rates of 1–2 $GtCO_2/a$ [5] are needed and every tonne of CO_2 emitted into the atmosphere needs to be removed again as long as we fail to reduce emissions at those rates [172]. Thus, unless full capture or CDA manufacturing processes can be made available economically and technically in the near term, partial capture constitutes a first drastic cut in emissions, which can contribute to significantly lowering the accumulated emissions and help to meet climate targets, e.g., for Year 2030.

8 Conclusions

This thesis investigates the use of partial CO_2 capture from large point sources as a near-term mitigation option for carbon-intensive industries in their transition to operating within a net-zero emissions framework. Techno-economic and policy-related aspects relevant to the facilitation of near-term implementation of carbon capture are elaborated, with the focus on the site-level perspective. The work refines and develops the application of process models of absorption cycles to include design options for partial capture and methods to incorporate real site conditions (such as temporally varying the heat availability) into techno-economic assessments. The developed method enhances the representativeness of actual operation and allows for the identification of cost-effective levels and designs for initial part-load implementation of CO_2 capture.

The findings emphasize that partial capture is a stepping stone for the widespread implementation of CCS in the process industry. Its cost-effective implementation is paramount in the following aspects:

- *Energy and cost-effective design of partial capture*. Amine absorption cycles can be designed for CO_2 separation rates <<90% (e.g., 50%–70%), so to allow for more energy-efficient operation, which may lower the specific capture cost by up to 10% as compared to full capture (≥90%).
- *The potential savings in energy and in both absolute and specific costs achieved when operating off-design at lower separation rates*. The savings are particularly pronounced for gases with high CO_2 concentrations (~>17 vol.%$_{wet}$). Furthermore, they are determined by the fundamental geometry of the packed column, i.e., the packing height and flooding approach.
- *The ability to cope with variations in heat supply and feed gas flow* (caused by production) either via: 1) the capture plant design, e.g., through the inertia in the solvent system (hourly scale variation) or by varying the capture rate (seasonal variation); and/or 2) the site energy system, by using a reserve heat source to guarantee a certain heat supply. For a refinery, the extra costs of variation management in these two approaches are similar at ~+4 €/tCO_2. For a utilization rate of >~50% and for scales >~400 ktCO_2 per annum, the cost increase for seasonally varying operation in a district heating context is <10 €/tCO_2, as compared to constant load operation.
- *Extensive heat integration to minimize the costs and emissions from the import of additional energy carriers to power the capture unit.* Partial capture predominantly powered by residual heat leads to cost savings of 17%–24% (corresponding to 11–24 €/tCO_2) along the full CCS chain, as compared to the cost of full capture. This requires a systematic mapping and techno-economic assessment of the heat sources located at the site. Site-level abatement cost curves that incorporate both CO_2 and heat sources in detail as a function of captured CO_2 can graphically illustrate the most-economic degree of capture.

- *Policy instruments that incentivize emissions reduction*, for example, by considering flexible allocation of emissions reductions to high-value, low-carbon products and recognizing different levels of climate ambition (e.g., differentiating between fossil-free and low-carbon). Furthermore, policy instruments, such as carbon contracts for difference, are needed to guarantee reliable carbon price levels, even if EU ETS prices have likely reached levels sufficient to trigger (partial) CO_2 capture. Finally, a carbon takeback obligation should be considered as a backstop to guarantee the required sequestration of fossil carbon emissions.
- *The recognition of the narrow window of opportunity of ~30 years for partial capture* in line with the climate targets of the Paris Agreement and with regards to the lifetime of existing plant infrastructure, alternative production and (co-)mitigation technologies, and the regional context regarding energy systems and emerging CO_2 transport and storage infrastructure.

In conclusion, this thesis finds that partial capture of CO_2 is a readily available and economically viable mitigation option for process industry. Implementation before Year 2030 could help to achieve the reduction targets for Year 2030 articulated at a corporate/national level, and would provide a response to the required initiation of large-scale emissions reductions via CCS in line with the aspiration of a 1.5°C or 2.0°C global warming limit.

8.1 Considerations for future research

The topics explored in this thesis can be extended to pose new research questions on the following topics:

- Concerning partial capture design: a techno-economic (net-present value) analysis of off-design partial capture that is full-capture ready, as suggested in the discussion section of **Paper II**, including the adoption of a more-advanced solvent, e.g., an AMP/PZ blend.
- The impacts of policy measures regarding fossil CO_2 (EU ETS) and negative emissions (BECCS → reversed auctions) on the timely establishment and constitution of CCS infrastructure systems (see Section 5.3).
- Regarding variation management via the capture plant/seasonal operation: a full techno-economic assessment that includes CO_2 compression and liquefaction units as well as buffer storage on site.
- Research on policy measures regarding flexible carbon allocation, the incentivization of mitigation depending on the ambition level (low-carbon vs fossil free), and respective product certification (consumer-related transparency).
- The application of site-level abatement curves that incorporate a detailed techno-economic assessment of process cooling for CO_2 capture at industrial sites.

References

[1] United Nations Framework Convention on Climate Change, “The Paris Agreement,” Paris, 2015. [Online]. Available: https://unfccc.int/sites/default/files/english_paris_agreement.pdf.

[2] IPCC *et al.*, “IPCC, 2018: Summary for Policymakers. In: Global warming of 1.5°C. An IPCC Special Report on the impacts of global warming of 1.5°C above pre-industrial levels and related global greenhouse gas emission pathways, in the context of strengthening the global,” World Meteorological Organization, Geneva, Switzerland, 2018.

[3] P. R. Shukla *et al.*, “Summary for Policymakers. In: Climate Change 2022: Mitigation of Climate Change. Contribution of Working Group III to the Sixth Assessment Report of the Intergovernmental Panel on Climate Change,” Cambridge, UK and New York, NY, USA., 2022. doi: 10.1017/9781009157926.001.

[4] F. Hans, T. Kuramochi, R. Black, T. Hale, and J. Lang, “Net Zero Stocktake 2022 - Assessing the status and trends of net zero target setting across countries, sub-national governments and companies,” *NewClimate Institute Oxford Net Zero Energy & Climate Intelligence Unit and Data-Driven EnviroLab*, 2022. https://zerotracker.net/analysis/net-zero-stocktake-2022.

[5] C. Le Quéré *et al.*, “Fossil CO_2 emissions in the post-COVID-19 era,” *Nat. Clim. Chang.*, vol. 11, no. 3, pp. 197–199, Mar. 2021, doi: 10.1038/s41558-021-01001-0.

[6] International Energy Agency, “Tracking Clean Energy Progress,” 2018. https://www.iea.org/tcep/.

[7] IEA, “Tracking Industry 2021,” *Paris*, 2021. https://www.iea.org/reports/tracking-industry-2021 (accessed Jul. 05, 2022).

[8] F. Johnsson, F. Normann, and E. Svensson, “Marginal Abatement Cost Curve of Industrial CO_2 Capture and Storage – A Swedish Case Study,” *Front. Energy Res.*, vol. 8, no. August, pp. 1–12, 2020, doi: 10.3389/fenrg.2020.00175.

[9] Agora Energiewende and Wuppertal Institut, “Breakthrough Strategies for Climate-Neutral Industry in Europe: Policy and Technology Pathways for Raising EU Climate Ambition.” 2021, [Online]. Available: https://www.agora-energiewende.de/en/publications/breakthrough-strategies-for-climate-neutral-industry-in-europe-study.

[10] S. Ó. Garđarsdóttir, F. Normann, K. Andersson, and F. Johnsson, “Postcombustion CO_2 Capture Using Monoethanolamine and Ammonia Solvents: The Influence of CO_2 Concentration on Technical Performance,” *Ind. Eng. Chem. Res.*, vol. 54, no. 2, pp. 681–690, Jan. 2015, doi: 10.1021/ie503852m.

[11] Global CCS Institute, “The Global Status of CCS: 2018,” Australia, 2018. [Online]. Available: https://www.globalccsinstitute.com/resources/global-status-report/.

[12] G. P. Peters *et al.*, “Key indicators to track current progress and future ambition of the Paris Agreement,” *Nat. Clim. Chang.*, vol. 7, no. 2, pp. 118–122, Feb. 2017, doi: 10.1038/nclimate3202.

[13] IChemE Energy Centre, “A Chemical Engineering Perspective on the Challenges and Opportunities of Delivering Carbon Capture and Storage at Commercial Scale,” 2018.

[14] P. Stigson, A. Hansson, and M. Lind, “Obstacles for CCS deployment: an analysis of discrepancies of perceptions,” *Mitig. Adapt. Strateg. Glob. Chang.*, vol. 17, no. 6, pp. 601–619, 2012, doi: 10.1007/s11027-011-9353-3.

[15] K. Witte, “Social Acceptance of Carbon Capture and Storage (CCS) from Industrial Applications,” *Sustainability*, vol. 13, no. 21, p. 12278, Nov. 2021, doi: 10.3390/su132112278.

[16] A. N. Hildebrand and H. J. Herzog, “Optimization of carbon capture percentage for technical and economic impact of near-term CCS implementation at coal-fired power plants,” *Energy*

Procedia, vol. 1, no. 1, pp. 4135–4142, Feb. 2009, doi: 10.1016/j.egypro.2009.02.222.

[17] S. Singh *et al.*, “China baseline coal-fired power plant with post-combustion CO_2 capture: 2. Techno-economics,” *Int. J. Greenh. Gas Control*, vol. 78, no. July, pp. 429–436, 2018, doi: 10.1016/j.ijggc.2018.09.012.

[18] IEA Greenhouse Gas R&D Programme (IEAGHG), “Partial Capture of CO_2.” 2009/TR2, 2009.

[19] M. A. Schnellmann, C. K. Chyong, D. M. Reiner, and S. A. Scott, “Deploying gas power with CCS: The role of operational flexibility, merit order and the future energy system,” *Int. J. Greenh. Gas Control*, vol. 91, no. October, p. 102838, 2019, doi: 10.1016/j.ijggc.2019.102838.

[20] S. Roussanaly *et al.*, “Techno-economic comparison of three technologies for pre-combustion CO 2 capture from a lignite-fired IGCC,” 2020, doi: 10.1007/s11705-019-1870-8.

[21] S. Rezvani, D. McIlveen-Wright, Y. Huang, A. Dave, J. D. Mondol, and N. Hewitt, “Comparative analysis of energy storage options in connection with coal fired Integrated Gasification Combined Cycles for an optimised part load operation,” *Fuel*, vol. 101, pp. 154–160, 2012, doi: 10.1016/j.fuel.2011.07.034.

[22] M. Bui *et al.*, “Carbon capture and storage (CCS): the way forward,” *Energy Environ. Sci.*, vol. 11, no. 5, pp. 1062–1176, 2018, doi: 10.1039/C7EE02342A.

[23] European Commission, “EU Innovation Fund - Awarded large-scale projects,” 2022. https://ec.europa.eu/clima/eu-action/funding-climate-action/innovation-fund/large-scale-projects_en.

[24] S. McCulloch and IEA, “Carbon capture in 2021: Off and running or another false start?,” 2021. https://www.iea.org/commentaries/carbon-capture-in-2021-off-and-running-or-another-false-start.

[25] K. Broecks, C. Jack, E. ter Mors, C. Boomsma, and S. Shackley, “How do people perceive carbon capture and storage for industrial processes? Examining factors underlying public opinion in the Netherlands and the United Kingdom,” *Energy Res. Soc. Sci.*, vol. 81, p. 102236, 2021, doi: https://doi.org/10.1016/j.erss.2021.102236.

[26] International Carbon Action Partnership, “ICAP Allowance Price Explorer,” 2022. https://icapcarbonaction.com/en/ets-prices.

[27] Global CCS Institute, “The Global Status of CCS: 2021,” *Australia*, 2021. https://www.globalccsinstitute.com/resources/global-status-report/.

[28] International Association of Oil & Gas Producers, “Map of CCUS Projects in Europe - Overview of existing and planned CCUS facilities - as of January 2022,” 2022. https://iogpeurope.org/resource/map-of-eu-ccus-projects/ (accessed May 02, 2022).

[29] Global CCS Institute, “CO_2RE - Facility Database public version,” 2022. https://co2re.co/FacilityData (accessed May 02, 2022).

[30] Carbon Capture Coalition, “Inflation Reduction Act of 2022 Makes Monumental Enhancements to the Foundational 45Q Tax Credit,” 2022. https://carboncapturecoalition.org/inflation-reduction-act-of-2022-makes-monumental-enhancements-to-the-foundational-45q-tax-credit/.

[31] N. Berghout, H. Meerman, M. van den Broek, and A. Faaij, “Assessing deployment pathways for greenhouse gas emissions reductions in an industrial plant – A case study for a complex oil refinery,” *Appl. Energy*, vol. 236, pp. 354–378, 2019, doi: 10.1016/j.apenergy.2018.11.074.

[32] M. Voldsund *et al.*, “Comparison of technologies for CO 2 capture from cement production—Part 1: Technical evaluation,” *Energies*, vol. 12, no. 3, p. 559, Feb. 2019, doi: 10.3390/en12030559.

[33] N. Berghout, M. van den Broek, and A. Faaij, “Techno-economic performance and challenges of applying CO_2 capture in the industry: A case study of five industrial plants,” *Int. J. Greenh. Gas Control*, vol. 17, pp. 259–279, 2013, doi: 10.1016/j.ijggc.2013.04.022.

[34] T. Kuramochi, A. Ramírez, W. Turkenburg, and A. Faaij, "Comparative assessment of CO_2 capture technologies for carbon-intensive industrial processes," *Prog. Energy Combust. Sci.*, vol. 38, no. 1, pp. 87–112, 2012, doi: 10.1016/j.pecs.2011.05.001.

[35] Global CCS Institute, "Technology Readiness and Costs of CCS," no. March, p. 49, 2021, [Online]. Available: https://www.globalccsinstitute.com/wp-content/uploads/2021/04/CCS-Tech-and-Costs.pdf.

[36] H. C. Mantripragada, H. Zhai, and E. S. Rubin, "Boundary Dam or Petra Nova – Which is a better model for CCS energy supply?," *Int. J. Greenh. Gas Control*, vol. 82, pp. 59–68, Mar. 2019, doi: 10.1016/j.ijggc.2019.01.004.

[37] I. Askestad *et al.*, "Towards full-scale carbon capture – Results from the Mobile Test Unit in various industry sectors," *15th Int. Conf. Greenh. Gas Control Technol. GHGT-15*, no. March, pp. 1–8, 2021, [Online]. Available: https://ssrn.com/abstract=3811352.

[38] P. H. M. Feron, A. Cousins, K. Jiang, R. Zhai, and M. Garcia, "An update of the benchmark post-combustion CO_2-capture technology," *Fuel*, vol. 273, p. 117776, 2020, doi: https://doi.org/10.1016/j.fuel.2020.117776.

[39] IEAGHG, "Further Assessment of Emerging CO 2 Capture Technologies for the Power Sector and their Potential to Reduce Costs," vol. 2019–09, no. September, 2019, [Online]. Available: www.ieaghg.org.

[40] M. van der Spek, R. Arendsen, A. Ramirez, and A. Faaij, "Model development and process simulation of postcombustion carbon capture technology with aqueous AMP/PZ solvent," *Int. J. Greenh. Gas Control*, vol. 47, pp. 176–199, 2016, doi: https://doi.org/10.1016/j.ijggc.2016.01.021.

[41] P. Moser *et al.*, "ALIGN-CCUS: Results of the 18-month test with aqueous AMP/PZ solvent at the pilot plant at Niederaussem – solvent management, emissions and dynamic behavior," *Int. J. Greenh. Gas Control*, vol. 109, no. March, p. 103381, 2021, doi: 10.1016/j.ijggc.2021.103381.

[42] S. Ó. Garðarsdóttir, F. Normann, R. Skagestad, and F. Johnsson, "Investment costs and CO_2 reduction potential of carbon capture from industrial plants – A Swedish case study," *Int. J. Greenh. Gas Control*, vol. 76, no. October 2017, pp. 111–124, 2018, doi: 10.1016/j.ijggc.2018.06.022.

[43] P. Bains, P. Psarras, and J. Wilcox, "CO_2 capture from the industry sector," *Prog. Energy Combust. Sci.*, vol. 63, pp. 146–172, Nov. 2017, doi: 10.1016/j.pecs.2017.07.001.

[44] T. Zitscher, U. Neuling, and A. Habersetzer, "Analysis of the German Industry to Determine the Resource Potential of CO 2 Emissions for PtX Applications in 2017 and 2050," 2020.

[45] Global Energy Monitor, "Global Steel Plant Tracker," 2022. https://globalenergymonitor.org/projects/global-steel-plant-tracker/tracker-map/ (accessed Jul. 06, 2022).

[46] J. Jakobsen, S. Roussanaly, and R. Anantharaman, "A techno-economic case study of CO_2 capture, transport and storage chain from a cement plant in Norway," *J. Clean. Prod.*, vol. 144, pp. 523–539, 2017, doi: https://doi.org/10.1016/j.jclepro.2016.12.120.

[47] D. Leeson, P. Fennell, N. Shah, C. Petit, and N. Mac Dowell, "A Techno-economic analysis and systematic review of carbon capture and storage (CCS) applied to the iron and steel, cement, oil refining and pulp and paper industries," *Int. J. Greenh. Gas Control*, vol. In press, pp. 71–84, 2017, doi: 10.1016/j.ijggc.2017.03.020.

[48] J. van Straelen, F. Geuzebroek, N. Goodchild, G. Protopapas, and L. Mahony, "CO_2 capture for refineries, a practical approach," *Int. J. Greenh. Gas Control*, vol. 4, no. 2, pp. 316–320, 2010, doi: 10.1016/j.ijggc.2009.09.022.

[49] D. Johansson, J. Sjöblom, and T. Berntsson, "Heat supply alternatives for CO_2 capture in the process industry," *Int. J. Greenh. Gas Control*, vol. 8, pp. 217–232, May 2012, doi:

10.1016/j.ijggc.2012.02.007.

[50] IEA, “Ammonia Technology Roadmap,” *Paris*, 2021. https://www.iea.org/reports/ammonia-technology-roadmap (accessed Jul. 06, 2022).

[51] K. Kuparinen, S. Lipiäinen, E. Vakkilainen, and T. Laukkanen, “Effect of biomass-based carbon capture on the sustainability and economics of pulp and paper production in the Nordic mills,” *Environ. Dev. Sustain.*, no. 0123456789, Jan. 2022, doi: 10.1007/s10668-021-02074-9.

[52] K. Onarheim, S. Santos, P. Kangas, and V. Hankalin, “Performance and costs of CCS in the pulp and paper industry part 1: Performance of amine-based post-combustion CO_2 capture,” *Int. J. Greenh. Gas Control*, vol. 59, pp. 58–73, Apr. 2017, doi: 10.1016/j.ijggc.2017.02.008.

[53] M. Haaf, R. Anantharaman, S. Roussanaly, J. Ströhle, and B. Epple, “CO_2 capture from waste-to-energy plants: Techno-economic assessment of novel integration concepts of calcium looping technology,” *Resour. Conserv. Recycl.*, vol. 162, no. July, p. 104973, 2020, doi: 10.1016/j.resconrec.2020.104973.

[54] S. Öberg, “Design of Partial CO_2 Capture from Waste Fired CHP Plants,” Chalmers University of Technology, 2017.

[55] C. Hammar, “Heat integration between CO_2 Capture and Liquefaction and a CHP Plant: Impact on Electricity and District Heating Delivery at Renova’s CHP Plant in Sävenäs.” Masters’ Thesis; Chalmers University of Technology, 2022, [Online]. Available: https://hdl.handle.net/20.500.12380/304511.

[56] D. L. Sanchez, N. Johnson, S. T. McCoy, P. A. Turner, and K. J. Mach, “Near-term deployment of carbon capture and sequestration from biorefineries in the United States,” *Proc. Natl. Acad. Sci. U. S. A.*, vol. 115, no. 19, pp. 4875–4880, 2018, doi: 10.1073/pnas.1719695115.

[57] K. Y. Hornafius and J. S. Hornafius, “Carbon negative oil: A pathway for CO_2 emission reduction goals,” *Int. J. Greenh. Gas Control*, vol. 37, pp. 492–503, Jun. 2015, doi: 10.1016/j.ijggc.2015.04.007.

[58] M. Kirschen, K. Badr, and H. Pfeifer, “Influence of direct reduced iron on the energy balance of the electric arc furnace in steel industry,” *Energy*, vol. 36, no. 10, pp. 6146–6155, 2011, doi: https://doi.org/10.1016/j.energy.2011.07.050.

[59] M. T. Ho, A. Bustamante, and D. E. Wiley, “Comparison of CO_2 capture economics for iron and steel mills,” *Int. J. Greenh. Gas Control*, vol. 19, pp. 145–159, 2013, doi: 10.1016/j.ijggc.2013.08.003.

[60] IEAGHG, “Iron and Steel CCS study (Techno-economics integrated steel mill),” 2013/04, July, 2013.

[61] A. Arasto, E. Tsupari, J. Kärki, E. Pisilä, and L. Sorsamäki, “Post-combustion capture of CO_2 at an integrated steel mill – Part I: Technical concept analysis,” *Int. J. Greenh. Gas Control*, vol. 16, pp. 271–277, Aug. 2013, doi: 10.1016/j.ijggc.2012.08.018.

[62] E. Tsupari, J. Kärki, A. Arasto, and E. Pisilä, “Post-combustion capture of CO_2 at an integrated steel mill – Part II: Economic feasibility,” *Int. J. Greenh. Gas Control*, vol. 16, pp. 278–286, Aug. 2013, doi: 10.1016/j.ijggc.2012.08.017.

[63] C.-C. Cormos, “Evaluation of reactive absorption and adsorption systems for post-combustion CO_2 capture applied to iron and steel industry,” *Appl. Therm. Eng.*, vol. 105, pp. 56–64, 2016, doi: 10.1016/j.applthermaleng.2016.05.149.

[64] J. G. Mathieson, H. Rogers, M. A. Somerville, S. Jahanshahi, and P. Ridgeway, “Potential for the use of biomass in the iron and steel industry,” *Chemeca 2011 - Eng. a Better World*, no. November 2014, p. 1065, 2011, [Online]. Available: http://search.informit.org/browsePublication;isbn=9780858259676;res=IELENG;subject=Zoology.

[65] T. Norgate, N. Haque, M. Somerville, and S. Jahanshahi, “Biomass as a Source of Renewable Carbon for Iron and Steelmaking,” *ISIJ Int.*, vol. 52, no. 8, pp. 1472–1481, 2012, doi: 10.2355/isijinternational.52.1472.

[66] H. Mandova *et al.*, “Achieving carbon-neutral iron and steelmaking in Europe through the deployment of bioenergy with carbon capture and storage,” *J. Clean. Prod.*, vol. 218, pp. 118–129, May 2019, doi: 10.1016/j.jclepro.2019.01.247.

[67] M. Biermann, A. Alamia, F. Normann, and F. Johnsson, “Evaluation of Steel Mills as Carbon Sinks,” 2018.

[68] S. E. Tanzer, K. Blok, and A. Ramírez, “Can bioenergy with carbon capture and storage result in carbon negative steel?,” *Int. J. Greenh. Gas Control*, vol. 100, no. June, p. 103104, Sep. 2020, doi: 10.1016/j.ijggc.2020.103104.

[69] V. Vogl *et al.*, “Green Steel Tracker,” 2021. https://www.industrytransition.org/green-steel-tracker/ (accessed Jul. 05, 2022).

[70] V. Vogl, M. Åhman, and L. J. Nilsson, “Assessment of hydrogen direct reduction for fossil-free steelmaking,” *J. Clean. Prod.*, vol. 203, pp. 736–745, 2018, doi: https://doi.org/10.1016/j.jclepro.2018.08.279.

[71] HYBRIT Development AB, “HYBRIT Fossil free steel - Summary of findings from HYBRIT Pre-Feasibility Study 2016–2017,” 2018. [Online]. Available: http://www.hybritdevelopment.com/.

[72] James Temple, “A new way to make steel could cut 5% of CO_2 emissions at a stroke,” *MIT Technology Review*, 2018. https://www.technologyreview.com/2018/09/24/2024/this-mit-spinout-could-finally-clean-up-steel-one-of-the-globes-biggest-climate-polluters/ (accessed Jul. 05, 2022).

[73] LEILAC consortium, “LEILAC - Low emissions Intensity Lime & Cement,” 2022. https://www.project-leilac.eu/the-core-technology (accessed Jul. 05, 2022).

[74] B. Wilhelmsson, C. Kollberg, J. Larsson, J. Eriksson, and M. Eriksson, “CemZero - A feasibility study evaluating ways to reach sustainable cement production via the use of electricity,” 2018. https://www.cementa.se/sv/cemzero (accessed Jul. 05, 2022).

[75] J. Petersson, “Thermal Plasma in a Rotary Kiln for Cement Production: An Investigation of the Heat Transfer Mechanisms,” Chalmers University of Technology, 2022.

[76] S. O. Gardarsdottir *et al.*, “Comparison of technologies for CO 2 capture from cement production—Part 2: Cost analysis,” *Energies*, vol. 12, no. 3, p. 542, Feb. 2019, doi: 10.3390/en12030542.

[77] Norcem and Heidelberg Cement Group, “Norwegian CCS Demonstration Project - Norcem FEED - Redacted version of FEED Study (DG3) Report,” 2019. https://ccsnorway.com/wp-content/uploads/sites/6/2020/07/NC03-NOCE-A-RA-0009-Redacted-FEED-Study-DG3-Report-Rev01-1.pdf.

[78] IEA, “Technology Roadmap - Low-Carbon Transition in the Cement Industry,” *Paris*, 2018. https://www.iea.org/reports/technology-roadmap-low-carbon-transition-in-the-cement-industry (accessed Jul. 05, 2022).

[79] N. Berghout, M. van den Broek, and A. Faaij, “Techno-economic performance and challenges of applying CO 2 capture in the industry: A case study of five industrial plants,” *Int. J. Greenh. Gas Control*, vol. 17, no. 2013, pp. 259–279, 2013, doi: 10.1016/j.ijggc.2013.04.022.

[80] D. Johansson, P. Å. Franck, and T. Berntsson, “CO_2 capture in oil refineries: Assessment of the capture avoidance costs associated with different heat supply options in a future energy market,” *Energy Convers. Manag.*, vol. 66, pp. 127–142, 2013, doi: 10.1016/j.enconman.2012.09.026.

[81] V. Andersson, P. Å. Franck, and T. Berntsson, “Techno-economic analysis of excess heat driven

post-combustion CCS at an oil refinery," *Int. J. Greenh. Gas Control*, vol. 45, pp. 130–138, 2016, doi: 10.1016/j.ijggc.2015.12.019.

[82] G. Power, A. Busse, and J. MacMurray, "Demonstration of Carbon Capture and Sequestration of Steam Methane Reforming Process Gas Used for Large-Scale Hydrogen Production," Pittsburgh, PA, and Morgantown, WV (United States), May 2018. doi: 10.2172/1437618.

[83] L. Rock *et al.*, "The Quest CCS Project: 1st Year Review Post Start of Injection," *Energy Procedia*, vol. 114, pp. 5320–5328, 2017, doi: https://doi.org/10.1016/j.egypro.2017.03.1654.

[84] A. I. Escudero, S. Espatolero, and L. M. Romeo, "International Journal of Greenhouse Gas Control Oxy-combustion power plant integration in an oil refinery to reduce CO 2 emissions," *Int. J. Greenh. Gas Control*, vol. 45, pp. 118–129, 2016, doi: 10.1016/j.ijggc.2015.12.018.

[85] L. F. De Mello, R. Gobbo, G. T. Moure, and I. Miracca, "Oxy-combustion technology development for Fluid Catalytic Crackers (FCC) - Large pilot scale demonstration," *Energy Procedia*, vol. 37, pp. 7815–7824, 2013, doi: 10.1016/j.egypro.2013.06.562.

[86] I. Cañete Vela, T. Berdugo Vilches, G. Berndes, F. Johnsson, and H. Thunman, "Co-recycling of natural and synthetic carbon materials for a sustainable circular economy," *J. Clean. Prod.*, vol. 365, no. November 2021, p. 132674, Sep. 2022, doi: 10.1016/j.jclepro.2022.132674.

[87] The City of Oslo, "The City of Oslo ensures realisation of carbon capture and storage (CCS) - Press release," 2022. https://www.oslo.kommune.no/politics-and-administration/politics/press-releases/the-city-of-oslo-ensures-realisation-of-carbon-capture-and-storage-ccs#gref (accessed Jul. 06, 2022).

[88] ARC, "ARC - Company webpage: Waste-to-energy and CCS at Amager Bakke," 2022. https://a-r-c.dk/about-arc/carbon-capture/ (accessed Jul. 06, 2022).

[89] Swedish Energy Agency, "The reversed auction for bio-CCS will be postponed," 2022. https://www.energimyndigheten.se/en/news/2022/the-reversed-auction-for-bio-css--will-be-postponed/ (accessed Jul. 06, 2022).

[90] Swedish Prime Minister's Office, "Press release: Norway and Sweden agree to intensify cooperation on carbon capture and storage," 2022. https://www.government.se/articles/2022/04/norway-and-sweden-agree-to-intensify-cooperation-on-carbon-capture-and-storage/ (accessed Jul. 07, 2022).

[91] CORDIS, "ACCSESS - Providign access to cost-efficient, replicable, safe and flexible CCUS," 2021. https://cordis.europa.eu/project/id/101022487 (accessed Jul. 07, 2022).

[92] M. R. Montañés, E. N. Flø, and O. L. Nord, "Dynamic Process Model Validation and Control of the Amine Plant at CO_2 Technology Centre Mongstad," *Energies*, vol. 10, no. 10. 2017, doi: 10.3390/en10101527.

[93] R. M. Montañés, N. E. Flø, and L. O. Nord, "Experimental results of transient testing at the amine plant at Technology Centre Mongstad: Open-loop responses and performance of decentralized control structures for load changes," *Int. J. Greenh. Gas Control*, vol. 73, pp. 42–59, 2018, doi: https://doi.org/10.1016/j.ijggc.2018.04.001.

[94] P. L. Hooey, A. Bodén, C. Wang, C.-E. Grip, and B. Jansson, "Design and Application of a Spreadsheet-based Model of the Blast Furnace Factory," *ISIJ Int.*, vol. 50, no. 7, pp. 924–930, 2010, doi: 10.2355/isijinternational.50.924.

[95] R. Taylor, R. Krishna, and H. Kooijman, "Real-World Modeling of Destillation," no. July, pp. 28–39, 2003, [Online]. Available: https://www.aiche.org/resources/publications/cep/2003/july/real-world-modeling-distillation.

[96] W. G. Whitman, "The two film theory of gas absorption," *Int. J. Heat Mass Transf.*, vol. 5, no. 5, pp. 429–433, May 1962, doi: 10.1016/0017-9310(62)90032-7.

[97] Y. Zhang, H. Chen, C.-C. Chen, J. M. Plaza, R. Dugas, and G. T. Rochelle, "Rate-Based Process

Modeling Study of CO_2 Capture with Aqueous Monoethanolamine Solution," *Ind. Eng. Chem. Res.*, vol. 48, no. 20, pp. 9233–9246, Oct. 2009, doi: 10.1021/ie900068k.

[98] J. L. Bravo, J. A. Rocha, and J. R. Fair, "Mass transfer in gauze packings," *Hydrocarb. Process.*, vol. 64, no. 1, pp. 91–95, 1985.

[99] T. H. Chilton and A. P. Colburn, "Mass transfer (absorption) coefficients prediction from data on heat transfer and fluid friction," *Ind. Eng. Chem.*, vol. 26, no. 11, pp. 1183–1187, 1934.

[100] AspenTech, "ENRTL-RK Rate-Based Model of the CO_2 Capture Process by MEA using Aspen Plus - Version 10.0." 2017.

[101] L. E. Øi, E. Sundbø, and H. Ali, "Simulation and Economic Optimization of Vapour Recompression Configuration for Partial CO_2 capture," in *Proceedings of the 58th Conference on Simulation and Modelling (SIMS 58) Reykjavik, Iceland, September 25th - 27th, 2017*, Sep. 2017, no. 138, pp. 298–303, doi: 10.3384/ecp17138298.

[102] F. Normann, S. Ó. Garðarsdóttir, R. Skagestad, A. Mathisen, and F. Johnsson, "Partial Capture of Carbon Dioxide from Industrial Sources - A Discussion on Cost Optimization and the CO_2 Capture Rate," 2017, vol. 00, pp. 14–18.

[103] A. B. Rao and E. S. Rubin, "Identifying cost-effective CO_2 control levels for amine-based CO_2 capture systems," *Ind. Eng. Chem. Res.*, vol. 45, no. 8, pp. 2421–2429, 2006, doi: 10.1021/ie050603p.

[104] R. Anantharaman, S. Roussanaly, S. F. Westman, and J. Husebye, "Selection of Optimal CO_2 Capture Plant Capacity for Better Investment Decisions," *Energy Procedia*, vol. 37, pp. 7039–7045, 2013, doi: 10.1016/j.egypro.2013.06.640.

[105] N. Enaasen Flø, H. Knuutila, H. M. Kvamsdal, and M. Hillestad, "Dynamic model validation of the post-combustion CO_2 absorption process," *Int. J. Greenh. Gas Control*, vol. 41, pp. 127–141, 2015, doi: 10.1016/j.ijggc.2015.07.003.

[106] N. E. Flø, "Post-combustion absorption-based CO_2 capture : modeling , validation and analysis of process dynamics," Norwegian University of Science and Technology, 2015.

[107] N. E. Flø, H. M. Kvamsdal, M. Hillestad, and T. Mejdell, "Dominating dynamics of the post-combustion CO_2 absorption process," *Comput. Chem. Eng.*, vol. 86, pp. 171–183, 2016, doi: 10.1016/j.compchemeng.2015.11.003.

[108] A. B. Rao and E. S. Rubin, "Identifying cost-effective CO_2 control levels for amine-based CO_2 capture systems," *Ind. Eng. Chem. Res.*, vol. 45, no. 8, 2006, doi: 10.1021/ie050603p.

[109] P. Brandl, M. Bui, J. P. Hallett, and N. Mac Dowell, "Beyond 90% capture: Possible, but at what cost?," *Int. J. Greenh. Gas Control*, vol. 105, no. July 2020, p. 103239, Feb. 2021, doi: 10.1016/j.ijggc.2020.103239.

[110] R. W. Howarth and M. Z. Jacobson, "How green is blue hydrogen?," *Energy Sci. Eng.*, vol. 9, no. 10, pp. 1676–1687, 2021, doi: 10.1002/ese3.956.

[111] P. Feron *et al.*, "Towards Zero Emissions from Fossil Fuel Power Stations," *Int. J. Greenh. Gas Control*, vol. 87, no. May, pp. 188–202, Aug. 2019, doi: 10.1016/j.ijggc.2019.05.018.

[112] D. Danaci, M. Bui, C. Petit, and N. Mac Dowell, "En Route to Zero Emissions for Power and Industry with Amine-Based Post-combustion Capture," *Environ. Sci. Technol.*, vol. 55, no. 15, pp. 10619–10632, Aug. 2021, doi: 10.1021/acs.est.0c07261.

[113] H. Ali *et al.*, "Cost estimation of heat recovery networks for utilization of industrial excess heat for carbon dioxide absorption," *Int. J. Greenh. Gas Control*, vol. 74, pp. 219–228, 2018, doi: https://doi.org/10.1016/j.ijggc.2018.05.003.

[114] T. Kuramochi, A. Ramírez, W. Turkenburg, and A. Faaij, "Comparative assessment of CO_2 capture technologies for carbon-intensive industrial processes," *Prog. Energy Combust. Sci.*, vol. 38, no. 1, pp. 87–112, Feb. 2012, doi: 10.1016/j.pecs.2011.05.001.

[115] IEAGHG, "Understanding the Cost of Retrofitting CO_2 capture in an Integrated Oil Refinery," vol. 2017-TR8, no. August, 2017.

[116] H. Ali, N. H. Eldrup, F. Normann, R. Skagestad, and L. E. Øi, "Cost Estimation of CO_2 Absorption Plants for CO_2 Mitigation – Method and Assumptions," *Int. J. Greenh. Gas Control*, vol. 88, pp. 10–23, 2019, doi: https://doi.org/10.1016/j.ijggc.2019.05.028.

[117] R. Anantharaman *et al.*, "DECARBit - Enabling advanced pre-combustion capture techniques and plants - D 1.4.3 European best practice guidelines for assessment of CO_2 capture technologies," 2011. https://www.sintef.no/globalassets/project/decarbit/d-1-4-3_euro_bp_guid_for_ass_co2_cap_tech_280211.pdf.

[118] S. Roussanaly, "Calculating CO_2 avoidance costs of Carbon Capture and Storage from industry," *Carbon Manag.*, vol. 10, no. 1, pp. 105–112, Jan. 2019, doi: 10.1080/17583004.2018.1553435.

[119] M. van der Spek, S. Roussanaly, and E. S. Rubin, "Best practices and recent advances in CCS cost engineering and economic analysis," *Int. J. Greenh. Gas Control*, vol. 83, pp. 91–104, Apr. 2019, [Online]. Available: http://www.sciencedirect.com/science/article/pii/S175058361930101X.

[120] S. Roussanaly *et al.*, "Towards improved guidelines for cost evaluation of carbon capture and storage," Mar. 2021, doi: 10.5281/ZENODO.4940264.

[121] G. Towler and R. Sinnott, *Chemical Engineering Design: principles, practice, and economics of plant and process design*, 2nd Editio. Butterworth-Heinemann, 2012.

[122] H. Deng, S. Roussanaly, and G. Skaugen, "Techno-economic analyses of CO_2 liquefaction: Impact of product pressure and impurities," *Int. J. Refrig.*, vol. 103, pp. 301–315, 2019, doi: 10.1016/j.ijrefrig.2019.04.011.

[123] Chemietechnik and Hüthig GmbH, "PCD - Preisindex für Chemieanlagen in Deutschland 2010-2019," 2020. https://www.chemietechnik.de/wp-content/uploads/2019/08/Preisentwicklung-Okt-1.jpg (accessed Nov. 15, 2021).

[124] E. S. Rubin *et al.*, "A proposed methodology for CO_2 capture and storage cost estimates," *Int. J. Greenh. Gas Control*, vol. 17, pp. 488–503, 2013, doi: 10.1016/j.ijggc.2013.06.004.

[125] S. Roussanaly *et al.*, "Towards improved guidelines for cost evaluation of carbon capture and storage," Mar. 2021, doi: https://doi.org/10.5281/zenodo.4940264.

[126] S. Ó. Garðarsdóttir, F. Normann, R. Skagestad, and F. Johnsson, "Investment costs and CO_2 reduction potential of carbon capture from industrial plants – A Swedish case study," *Int. J. Greenh. Gas Control*, vol. 76, pp. 111–124, Sep. 2018, doi: 10.1016/j.ijggc.2018.06.022.

[127] SCB, "Salary search," 2020. https://www.scb.se/en/finding-statistics/sverige-i-siffror/salary-search/ (accessed Nov. 09, 2020).

[128] Tillväxtverket, "Verksamt.se - räkna ut vad en anställd kostar," 2020. https://www.verksamt.se/alla-e-tjanster/rakna-ut/rakna-ut-vad-en-anstalld-kostar (accessed Nov. 09, 2020).

[129] SCB, "Energy prices on natural gas and electricity," 2020. https://www.scb.se/en/finding-statistics/statistics-by-subject-area/energy/price-trends-in-the-energy-sector/energy-prices-on-natural-gas-and-electricity/ (accessed Nov. 09, 2020).

[130] M. Biermann, H. Ali, M. Sundqvist, M. Larsson, F. Normann, and F. Johnsson, "Excess heat-driven carbon capture at an integrated steel mill – Considerations for capture cost optimization," *Int. J. Greenh. Gas Control*, vol. 91, no. April, p. 102833, Dec. 2019, doi: 10.1016/j.ijggc.2019.102833.

[131] D. W. Green and R. H. Perry, *Perry's Chemical Engineers' Handbook - 8th Edition*. McGraw-Hill, 2007.

[132] IEAGHG, "Evaluation of Reclaimer Sludge Disposal from Post-combustion CO_2 Capture," no.

2014/02, 2014, doi: 10.1016/j.egypro.2014.11.102.

[133] J. Beiron, F. Normann, and F. Johnsson, “A techno-economic assessment of CO_2 capture in biomass and waste-fired combined heat and power plants – A Swedish case study,” *Int. J. Greenh. Gas Control*, vol. 118, no. September 2021, p. 103684, Jul. 2022, doi: 10.1016/j.ijggc.2022.103684.

[134] S. Dell’Orco *et al.*, “Online Biogenic Carbon Analysis Enables Refineries to Reduce Carbon Footprint during Coprocessing Biomass- and Petroleum-Derived Liquids,” *Anal. Chem.*, vol. 93, no. 10, pp. 4351–4360, Mar. 2021, doi: 10.1021/acs.analchem.0c04108.

[135] M. Schimmel, G. Toop, S. Alberici, and M. Koper, “Determining the renewability of co-processed fuels.” pp. 1–34, 2018, [Online]. Available: https://ec.europa.eu/energy/sites/ener/files/documents/co-processing_final_report_090418.pdf.

[136] Environmental Protection Agency (EPA), “Standards of Performance for Greenhouse Gas Emissions From New, Modified, and Reconstructed Stationary Sources: Electric Utility Generating Units.” Federal Register, Vol. 80, No. 205, RIN 2060–AQ91, pp. 64509–64660, 2015, [Online]. Available: https://www.federalregister.gov/documents/2015/10/23/2015-22837/standards-of-performance-for-greenhouse-gas-emissions-from-new-modified-and-reconstructed-stationary.

[137] J. G. Backes, J. Suer, N. Pauliks, S. Neugebauer, and M. Traverso, “Life Cycle Assessment of an Integrated Steel Mill Using Primary Manufacturing Data : Actual Environmental Profile,” pp. 1–18, 2021.

[138] J. Klement, J. Rootzén, F. Normann, and F. Johnsson, “Supply Chain Driven Commercialisation of Bio Energy Carbon Capture and Storage,” *Frontiers in Climate*, vol. 3. 2021, [Online]. Available: https://www.frontiersin.org/article/10.3389/fclim.2021.615578.

[139] J. Rootzén and F. Johnsson, “Paying the full price of steel – Perspectives on the cost of reducing carbon dioxide emissions from the steel industry,” *Energy Policy*, vol. 98, pp. 459–469, Nov. 2016, doi: 10.1016/j.enpol.2016.09.021.

[140] J. Rootzén and F. Johnsson, “Managing the costs of CO_2 abatement in the cement industry,” *Clim. Policy*, vol. 17, no. 6, pp. 781–800, Aug. 2017, doi: 10.1080/14693062.2016.1191007.

[141] S. Karlsson, F. Normann, M. Odenberger, and F. Johnsson, “Modeling the development of carbon capture and transportation infrastructure - a case study of the Swedish industry,” *to be Submitt.*, 2022.

[142] DOE, “Carbon Dioxide Capture from Existing Coal-Fired Power Plants - DOE/NETL-401/110907,” vol. 2008, no. December 2006, p. 268, 2007, doi: DOE/NETL-401/110907.

[143] DOE, “Cost and Performance of PC and IGCC Plants for a Range of Carbon Dioxide Capture - DOE/NETL-2011/1498,” pp. 1–500, 2011, doi: DOE/NETL-2011/1498.

[144] Å. Eliasson, E. Fahrman, M. Biermann, F. Normann, and S. Harvey, “Integration of Industrial CO_2 Capture with Industrial District Heating Networks: A Refinery Case Study,” 2021, [Online]. Available: https://research.chalmers.se/publication/526225.

[145] G. Abrami, “Energy targeting for heat recovery from carbon capture processes using hybrid absorption heat pumps.” Masters’ Thesis; Politecnico di Milano, 2022, [Online]. Available: https://www.politesi.polimi.it/bitstream/10589/187439/5/2022_04_Abrami_01.pdf.

[146] A. Reyes-Lúa *et al.*, “Techno-economic analysis of CO_2 capture and transport from a Swedish Refinery,” *to be Submitt.*, 2022.

[147] M. Biermann *et al.*, “Preem CCS - Synthesis of main project findings and insights.” Chalmers University of Technology, Gothenburg, 2022, [Online]. Available: https://research.chalmers.se/publication/528685.

[148] Chemietechnik and Hüthig GmbH, “PCD - Preisindex für Chemieanlagen in Deutschland 2015-

2021," 2022. https://www.chemietechnik.de/assets/images/7/01-1073036e.jpg (accessed Jul. 06, 2022).

[149] Eurostat, "Energy statistics - prices of natural gas and electricity," 2022. https://ec.europa.eu/eurostat/databrowser/explore/all/envir?lang=en&subtheme=nrg.nrg_price&display=list&sort=category&extractionId=NRG_PC_205.

[150] Eurostat, "Harmonised Indices of Consumer Prices (HICP)," 2022. https://ec.europa.eu/eurostat/databrowser/view/prc_hicp_aind/default/table?lang=en.

[151] IEA, "World Energy Outlook 2021," Paris, 2021. [Online]. Available: www.iea.org.

[152] Agora Industry, Wuppertal Institut, and Lund University, "Global Steel at a Crossroads. Why the global steel sector needs to invest in climate-neutral technologies in the 2020s.," 2021. [Online]. Available: https://www.agora-energiewende.de/en/publications/global-steel-at-a-crossroads/.

[153] MIDREX, "MXCOL - Direct Reduction Using Coal," 2019. https://www.midrex.com/technology/midrex-process/mxcol/ (accessed Jul. 29, 2022).

[154] European Environment Agency, "Greenhouse gas emission intensity of electricity generation in Europe," 2022. https://www.eea.europa.eu/ims/greenhouse-gas-emission-intensity-of-1 (accessed Jul. 26, 2022).

[155] A. Otto, M. Robinius, T. Grube, S. Schiebahn, A. Praktiknjo, and D. Stolten, "Power-to-Steel: Reducing CO_2 through the Integration of Renewable Energy and Hydrogen into the German Steel Industry," *Energies*, vol. 10, no. 4, p. 451, Apr. 2017, doi: 10.3390/en10040451.

[156] P. E. Duarte and J. Becerra, "Decrease of GHG emissions through the Carbon Free Emissions ENERGIRON DR Scheme in Integrated Mills," *HYL Technologies SA de CV, Mexico*, 2011. https://www.energiron.com/wp-content/uploads/2019/05/2011-Decrease-of-GHG-emissions-through-the-Carbon-Free-Emissions-ENERGIRON-DR-Scheme-in-Integrated-Mills.pdf (accessed Jul. 26, 2022).

[157] E. I. Nduagu *et al.*, "Comparative life cycle assessment of natural gas and coal-based directly reduced iron (DRI) production: A case study for India," *J. Clean. Prod.*, vol. 347, p. 131196, 2022, doi: https://doi.org/10.1016/j.jclepro.2022.131196.

[158] Eurofer, "A steel roadmap for a low carbon Europe 2050," Brussels, http://www.nocarbonnation.net/docs/roadmaps/2013-Steel_Roadmap.pdf, 2013.

[159] M. C. Romano *et al.*, "Comment on 'How green is blue hydrogen?,'" *Energy Sci. Eng.*, vol. 10, no. 7, pp. 1944–1954, Jul. 2022, doi: https://doi.org/10.1002/ese3.1126.

[160] C. Bauer, K. Treyer, C. Antonini, J. Bergerson, and M. Gazzani, "On the climate impacts of blue hydrogen production," pp. 1–9, 2021, [Online]. Available: https://chemrxiv.org/engage/api-gateway/chemrxiv/assets/orp/resource/item/6141926f27d906e30288cff1/original/on-the-climate-impacts-of-blue-hydrogen-production.pdf.

[161] F. Ueckerdt *et al.*, "On the cost competitiveness of blue and green hydrogen [preprint]," *Nat. Portf. J.*, 2022, doi: https://doi.org/10.21203/rs.3.rs-1436022/v1.

[162] IEAGHG, "Feasibility study on achieving deep decarbonization in worldwide fertilizer production," vol. 2022–05, 2022, [Online]. Available: https://ieaghg.org/ccs-resources/blog/new-ieaghg-report-feasibility-study-on-achieving-deep-decarbonization-inworldwide-fertilizer-production.

[163] Cementa and Heidelberg Cement Group, "Ett steg närmare en klimatpositiv cementfabrik i Sverige," 2022. https://www.cementa.se/sv/ett-steg-narmare-en-klimatpositiv-cementfabrik-i-sverige.

[164] Cementa AB, "Färdplan cement för ett klimatneutralt betongbyggande," 2018. https://www.cementa.se/sv/fardplancement.

[165] M. Nivard and M. Kreijkes, “The European Refining Sector: A diversity of markets?” Clingendael International Energy Programme (CIEP), 2017, [Online]. Available: https://www.clingendaelenergy.com/inc/upload/files/CIEP_paper_2017-02_web.pdf.

[166] Porthos CO_2 Transport and Storage C.V., “Porthos - Port of Rotterdam CO_2 Transport Hub and Offshore Storage,” 2022. https://www.porthosco2.nl/en/.

[167] Equinor, “Equinor sets ambition to reach net-zero emissions by 2050,” 2020. https://www.equinor.com/en/news/20201102-emissions.html (accessed Nov. 09, 2020).

[168] R. Oxburgh *et al.*, “Lowest Cost Decarbonisation for the UK: the Critical Role of CCS,” no. September, p. 70, 2016, [Online]. Available: http://www.sccs.org.uk/images/expertise/reports/oxford/oxburgh_report_the_critical_role_of_CCS.pdf.

[169] S. Jenkins, E. Mitchell-Larson, M. C. Ives, S. Haszeldine, and M. Allen, “Upstream decarbonization through a carbon takeback obligation: An affordable backstop climate policy,” *Joule*, vol. 5, no. 11, pp. 2777–2796, 2021, doi: https://doi.org/10.1016/j.joule.2021.10.012.

[170] T. M. O’Donnell, “Of loaded dice and heated arguments: Putting the Hansen?Michaels global warming debate in context,” *Soc. Epistemol.*, vol. 14, no. 2–3, pp. 109–127, Apr. 2000, doi: 10.1080/02691720050199199.

[171] R. D. Besel, “Accommodating Climate Change Science: James Hansen and the Rhetorical/Political Emergence of Global Warming,” *Sci. Context*, vol. 26, no. 1, pp. 137–152, 2013, doi: DOI: 10.1017/S0269889712000312.

[172] M. Allen and E. Mitchell-Larson, “TCCS-10 - Keynote: Achieving Net-Zero by decarbonising fossil fuels,” *2019*. https://www.youtube.com/watch?v=9SuAoU50uus&t=194s.

[173] Y. Zhang and C. C. Chen, “Modeling CO_2 absorption and desorption by aqueous monoethanolamine solution with Aspen rate-based model,” *Energy Procedia*, vol. 37, pp. 1584–1596, 2013, doi: 10.1016/j.egypro.2013.06.034.

[174] WBCSD and WRI, “The Greenhouse Gas Protocol - A Corporate Accounting and Reporting Standard,” 2012.

[175] Olje- og energidepartementet Norge, “Mulighetsstudier av fullskala CO_2-håndtering i Norge.” p. 55, 2016, [Online]. Available: https://www.regjeringen.no/globalassets/departementene/oed/pdf/mulighetsstudien.pdf.

[176] C. Barrington, “The iron ore challenge for direct reduction on road to carbon-neutral steelmaking,” 2022. https://www.midrex.com/tech-article/the-iron-ore-challenge-for-direct-reduction-on-road-to-carbon-neutral-steelmaking/ (accessed Jul. 26, 2022).

Paper A

International Journal of Greenhouse Gas Control 82 (2019) 192–203

Contents lists available at ScienceDirect

International Journal of Greenhouse Gas Control

journal homepage: www.elsevier.com/locate/ijggc

Integrating carbon capture into an industrial combined-heat-and-power plant: performance with hourly and seasonal load changes

Guillermo Martinez Castilla*, Maximilian Biermann, Rubén M. Montañés, Fredrik Normann, Filip Johnsson

Department of Space, Earth and Environment, Division of Energy Technology, Chalmers University of Technology, S-412 98, Gothenburg, Sweden

ARTICLE INFO

Keywords:
Flexibility
Process dynamics
CCS
Process modeling
Partial capture
Steel mill
MEA

ABSTRACT

The present work aims to map the variations in process gas and available excess heat of an integrated steel mill and to investigate the effects of these variations on the performance of a chemical absorption CO_2 plant. Two time-scales are considered for the variations: seasonal and hourly changes. Dynamic process simulations are used to investigate the dynamic interactions between the steel mill and the capture unit. This includes the effect that periodic variations in the reboiler heat duty have on the performance of the capture plant and the effect of implementing a control strategy. The mapping of the operation of the steel mill reveals numerous variations on an hourly basis that are important for the design and operation of the capture plant, including decreases in the blast furnace gas (BFG) flow to 0% on approximately 10 occasions per year and variations of ± 30 MW in the available heat more than 40 times per year. The simulations show that the capture unit responds very differently depending on the season, with a generally slower response during winter operation due to a lower level of circulation of the solvent. The capture unit shows also non-linearity in its response to changes in heat load - the deviation from the steady-state value is more pronounced when the heat is increased than when it is decreased. Thus, the simulation results indicate that implementing CO_2 capture with chemical absorption in an integrated steel mill requires flexible operation of the capture plant. Dynamic simulations over a two-week period with historical (hourly) boundaries demonstrate that the capture process can operate in the presence of the steel mill variations. Implementation of a decentralized control strategy increases the amount of captured CO_2 by 1.2%.

1. Introduction

Carbon dioxide (CO_2) emissions related to the extensive use of fossil fuels are the main cause of climate change (Raynaud and Stocker, 2013). The Paris Agreement aims to limit the increase in global temperature to well below 2 °C (UNFCCC, 2015). To meet this target, transformative changes in the processes and practices in energy and industrial systems will be required. Transformation of the energy-intensive basic industry, which is one of the most polluting sectors with 21% of the worldwide greenhouse gas (GHG) emissions (IPCC, 2014), will be an important contribution to reach the target.

This work considers the implementation of carbon capture and storage (CCS) in steel manufacturing process that follows the blast furnace route. Steel processing accounts for 10% of the CO_2 emissions from fossil fuel use in the world (OECD, 2004), corresponding to 5% of the total global GHG emissions. The blast furnace route accounts for more than 70% of global steel production according to the World Steel Association (WorldSteel, 2010) and emits on average 1.8 t of CO_2 per tonne of steel (Remus et al., 2013). In this process, the iron ore is reduced in the blast furnace. Coal and coke are used to form the reducing agent, which is mainly carbon monoxide (CO). Most of the emissions are formed as a result of the use of fossil fuels in the generation of the reducing agents and in the combustion processes that provide the energy required by the process (Hummel and Canapa, 2013).

The Steel Roadmap EU 2050 (Hummel and Canapa, 2013) suggests that implementation of the best available steel-making technologies and large energy savings will not be sufficient to mitigate the carbon footprint of steel manufacturing. This is partially due to the predicted increase in steel demand (Allwood, 2012). Therefore, new low-carbon techniques are required. ULCOS (Ultra-Low CO_2 Steel Making) (ULCOS, 2018) is an ambitious program aimed at achieving dramatic reductions in carbon dioxide emissions from steel production. The ULCOS program follows four routes, three of which are dependent upon carbon (coal) as a reducing agent and CCS technologies to achieve the emissions reductions. Steel mills inherently operate with a surplus of energy, as the required reducing potential in the blast furnace generates an off-gas

---

* Corresponding author.
E-mail address: castilla@chalmers.se (G. Martinez Castilla).

https://doi.org/10.1016/j.ijggc.2019.01.015
Received 3 October 2018; Received in revised form 14 January 2019; Accepted 15 January 2019

Nomenclature

BF	Blast furnace
BFG	Blast furnace gas
BOF	Basic oxygen furnace
BOFG	Basic oxygen furnace gas
COG	Coke oven gas
MEA	Monoethanolamine
PCC	Post-combustion capture
RC	Relative change, %
C_{abs}	Capture rate at the absorber, %
LL	Lean concentration at absorber inlet, mol/mol
Θ	Dead time, s
P_{CO2}	Production of CO_2, kg/s
$m_{CO_2,Produced}$	Amount of CO_2 produced over time, kg
P_{el}	Electrical power, MW
Q_{DH}	Heat used for district heating, MW
Q_f	Heat provided to the boiler, MW
Q_{OF}	Heat sent to other facilities, MW
Q_{SM}	Heat sent to the steel mill, MW
RL	Rich concentration at stripper inlet, mol/mol
t_s	10% Stabilization time, s
t_{sta}	Total stabilization time, s
TS	Temperature at stripper bottom, °C / K
y_0	Initial value
y_∞	Final value
Δy	Change in process variable value
η	Total efficiency, %

with a high heating value. This energy is often utilized in an integrated combined heat and power (CHP) plant, to provide the energy required for steel processing, send power to the grid, and deliver heat to local district heating networks (if present).

The surplus heat can also be utilized to power a carbon capture process. Absorption technologies have been at the forefront of carbon capture from heavy industries, given that these technologies are relatively mature and easily retrofitted to existing plants as an “end-of-pipe” solution and that they may be powered by low-value heat. The best-studied solvents are aqueous solutions of amines, usually monoethanolamine (MEA). This technology has been demonstrated at commercial scale for coal-fired power plants (NETL, 2019; Singh and Stéphenne, 2014) and more than 15 large-scale projects worldwide incorporate the full CCS chain (Global CCS, 2019). Application of chemical absorption to steel mills has also been studied, including its heat integration potential and techno-economic aspects (Tsupari et al., 2013; Antti Arasto et al., 2013). Arasto et al. (Tsupari et al., 2013), who assessed the possibilities for applying post-combustion capture to an integrated steel mill, concluded that it was possible to capture 50%–75% of the total site emissions by utilizing available excess heat. Moreover, various process and heat integration alternatives were evaluated. Gazzant et al. (Gazzani et al., 2015; Kärki et al. (2013)) have pointed out the importance of investigating heat integration opportunities when evaluating CCS options within integrated steel mills. A steel mill exhibits notable transient behavior that is related to its integrated CHP plant, as well as the large variations in available excess heat throughout the year. Flaring is a commonly used procedure to handle the excess blast furnace gas that the system cannot take care of, which also results in frequent fluctuations in the flare gas flow. Some studies, such as that published by Storck et al. (Storck, 2009) have investigated the consequences of the strategies of the niche markets in the steelmaking industry. The study of Storck (Storck, 2009) shows the need for flexible production processes that are capable of handling product variability, which confers operational flexibility. This might enhance the need for flexible operation of steel mills (Sundqvist et al., 2017). Thus, similar flexibility in operation may be required for an associated capture plant.

The design of CO_2 absorption processes that include control strategies for operation with varying load is important for successful technology development and implementation (IEAGHG, 2012; IEAGHG, 2016). The load of thermal power plants depends on daily and seasonal variations, and, with the high penetration of renewable energy sources, on weather conditions (Montañés et al., 2016). In the case of the steel mill-integrated CHP, the power plant must also consider the variations in steel mill operation. Several studies have assessed the transient performances of post-combustion capture (PCC) processes through pilot plant testing (Tait et al., 2016; Bui et al., 2016; Faber et al., 2011; Montañés et al., 2018), and dynamic process models have been developed to evaluate the transient performance of the system (Flø et al., 2016; Montañés et al., 2017a; Wu et al., 2018), control strategies (He et al., 2018; Panahi and Skogestad, 2012; Luu et al., 2015), and the operational strategies of carbon capture plants (Mechleri et al., 2017; Montañés et al., 2017b; Gardarsdóttir et al., 2017). Bui et al. (Bui et al., 2014) reviewed the studies published on dynamic models of CO_2 absorption processes. They proposed that future studies should focus on: validating the models with pilot plant data obtained during transient operation; and developing operational strategies for flexible operation. Recent works have focused on the validation of dynamic process models of the post-combustion CO_2 capture process that uses amines with transient pilot plant data (Montañés et al., 2017a; Van De Haar et al., 2017; Enaasen Flø et al., 2015; Chinen et al., 2016). Gardasdóttir et al. (Gardarsdóttir et al., 2015a) conducted dynamic process simulations of the PCC unit applied to a coal-fired power plant, using the model developed by Åkeson et al. (Åkesson et al., 2011), thereby deriving control strategies to optimize the transient behavior of the capture plant. Montañés et al. (Montañés et al., 2017c) validated a dynamic model with steady-state and transient large-scale pilot plant data from the amine plant at the Technology Centre Mongstad in Norway. That work included evaluation of the open-loop response of the plant for different combined cycle power plant loads, as well as four different control strategies in the PCC unit for fast load changes. Recent publications have integrated dynamic process models of the power plant and the PCC unit so as to understand the transient performance of the integrated system for coal-fired power plants (Gardarsdóttir et al., 2017; Wellner et al., 2016; Lawal et al., 2012) and natural gas-fired combined cycle power plants (Montañés et al., 2017b). Several papers have been published on the flexible operational requirements of CCS in power plants in future energy systems (Montañés et al., 2016; Lucquiaud et al., 2009; Domenichini et al., 2013; Heuberger et al., 2017; Mac Dowell and Staffell, 2016). Cohen et al. (Cohen et al., 2013) have also focused on the optimal CO_2 capture operation in future electricity grids, concluding that flexible operation is crucial to its deployment.

In summary, although the above-described studies have provided valuable information on the transient performance of CO_2 capture units, most studies have focused on PCC with application to the energy sector. Little work has been carried out on the variations in process heat in steel mills with implications for the performance of the capture plant. The aim of the present work is to identify and quantify variations in load conditions in a steel mill, so as to evaluate the effect of integration of a CO_2 absorption process. The study is based on operational data from the integrated steel mill placed in Luleå, Sweden and its associated CHP plant. It includes load changes on time scales that range from hours to seasons. The capture plant is designed based on the operational data analysis, considering seasonal variations in available excess heat for the capture unit. In addition, a dynamic model of the capture plant is developed to investigate the transient performance of the process, including the periodic oscillations in reboiler heat during different time periods and the open-loop transient performance of the capture process associated with the identified disturbances related to the steel mill variations. The analysis is carried out for three cases with different levels of heat available for CCS, i.e., each case represents a season of the year. Furthermore, the present work compares the CO_2 captured when considering a constant average amount of heat available for CCS and when considering the actual available heat that changes on an hourly basis over a period of two weeks.

2. Method

The present work investigates the implications of transients and varying load conditions in industrial processes through a case study of the SSAB´s steel mill in Luleå. The work is divided into two parts. The first part maps the actual transient events (varying load conditions) that are important for the implementation of CCS on the industrial site during one full year of operation with the present-day process design, i.e., without CCS. The second part examines, through dynamic process modeling, the implications of the identified load conditions for the operation of a future capture plant that is integrated into a steel mill. In this analysis, it is assumed that the heat consumption (for the steelmaking process, other facilities, and district heating demand) and power production are the same as in the case without CCS, and the excess heat for CCS is calculated by analyzing the load increase in the cold condenser. The dynamic model of the capture process was developed in the Dymola tool, through the use of the Gas Liquid Contactors (GLC library) (Modelon, 2018a) developed by Modelon AB (Modelon, 2018b). The two parts of the work are described in more detail below.

2.1. Plant data analysis

The Luleå steel mill plant, which follows the blast furnace route, has the capacity to produce 3000 kt of steel slabs per year, with a mean of 1880 kt/a being produced during the last 7 years (SSAB, 2016). The average carbon footprint is 1.7 t of CO_2 per tonne of steel produced. The plant is integrated with a combined heat and power (CHP) plant that utilizes the excess process gas to generate steam for the steel mill and some other facilities ($Q_{SM} + Q_{OF}$), district heating (Q_{DH}) for the nearby city, and electricity (P_{el}). The process gases that the CHP plant cannot combust (due to limitations related to plant capacity and disturbances) are sent for flaring. Eq. (1) expresses the total efficiency of the CHP plant, where Q_f is the heat input to the boiler, accounting for both process gases and oil (auxiliary fuel):

$$\eta = \frac{Q_{SM} + Q_{OF} + P_{el} + Q_{DH}}{Q_f} \times 100 \tag{1}$$

The steam boiler operates at full capacity throughout the year, with an average output of 290 MW. The levels of heat required by the steel mill and the nearby facilities are constant. The district heating ranges from 200 MW delivered in winter to 30 MW in summer. The electricity generation is 20% higher in summer than in winter owing to the use of the condensing turbine.

2.1.1. Boundaries between the capture plant and the steel mill

Fig. 1 shows a schematic of the capture plant integrated into the steel mill. The capture unit separates the CO_2 from the blast furnace gas (BFG) and utilizes excess heat from the gas flaring and the CHP plant according to the integration scheme proposed previously (Sundqvist et al., 2017). Capturing of CO_2 from the BFG is chosen because it increases the heating value of the gas sent to the CHP, represents the largest flow of CO_2 within the steel mill, and it has a relatively high partial pressure of CO_2. Thus, three connections (boundaries) between the steel mill and the capture plant should be considered: the BFG flow; the amount of gas that is sent to flaring; and the heat available in the CHP.

Gas flaring and the CHP are considered as heat sources. Steam of the appropriate quality (temperature and pressure) for the capture plant may be extracted from the steam cycle in times of lower demand for district heating. The excess heat that is available ranges from 0 MW to 125 MW. Flaring gases are recovered in a new steam boiler. The amount of heat available in the flare is, thus, estimated as being proportional to the volume of flow gases flared. This value ranges from 0 MW to 30 MW.

As the amount of available excess heat will be highly dependent upon the need for district heating, three cases with different steady-state values for the reboiler heat duty (i.e., the amount of excess heat) depending on season are defined. *Case A* represents summer operation with a steady-state reboiler duty of 155 MW, which represents the full capacity of the excess heat collection system. *Case B* represents operation during a winter month with a steady-state reboiler heat duty of

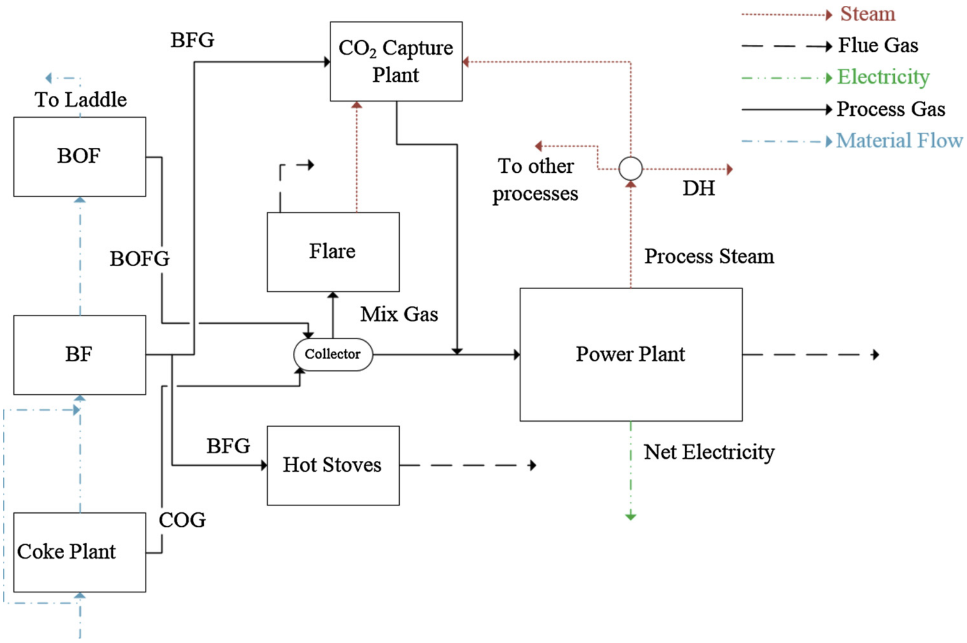

Fig. 1. Simplified process diagram of the capture plant integrated into the steel mill and CHP plant.

30 MW. *Case C* represents the intermediate operation (spring/autumn) with a steady-state reboiler duty of 110 MW.

2.1.2. *Analysis of variations*

An analysis of the hourly operational data from the steel mill regarding the BFG flow, gas flaring, and heat available in the CHP was performed for Year 2017. Disturbances were mapped with respect to: 1) magnitude, i.e., value above or below the steady-state value; 2) duration, i.e., number of consecutive hours that the variable remains under/above the threshold; and 3) frequency, which is number of times the variation occurred during the year.

2.2. *Modeling and simulations*

The modeling of the capture unit is divided into two parts. The first part is performed in steady state and aims to design the capture plant for the steady-state conditions. The second part is a dynamic model that utilizes the design from the steady-state simulations to investigate the operation and performance during transient events.

2.2.1. *Design of the capture plant*

The carbon capture unit integrated into the steel mill is a chemical absorption unit with 30 wt% aqueous MEA. The capture plant was designed for the maximum amount of available heat (155 MW). The design and sizing of the process were carried out in the Aspen Plus software. Fig. 2 shows a schematic of the process and Table 1 lists the relevant design parameters of the process. The configuration considered contains two columns: one absorber that includes a washing section on the upper part, and one stripper with a reboiler and overhead condenser. More efficient process configurations as e.g. proposed in Ref. (Amrollahi et al., 2011) were not considered in this work to simplify the dynamic simulations. The process model used has been presented elsewhere (Gardarsdóttir et al., 2015b; Biermann et al., 2018; Sundqvist et al., 2017). It follows a rate-based modeling approach using the correlations by Bravo et al. (1985) to predict mass transfer in the structured packing of both columns.

Within its design parameters, the plant treats 60.5 Nm^3/s of BFG, capturing a maximum of 90% of the CO_2 present in the stream. Mellapack 250Y was chosen as the structured packing for both columns. The diameters of the columns were calculated after defining a flooding limit of 85% for both the absorber and stripper. The absorber is pressurized owing to the pressure of the blast furnace gas (1.81 bar), which leads to a higher optimal rich loading than the conventional one for flue gases at close to atmospheric pressure, as experimentally demonstrated by Dreillard et al. (2017). The lean loading chosen for the design point was 0.32 mol/mol. A regulatory control layer was implemented in the model, following the methodology suggested by Skogestad (Aske and Skogestad, 2009), as also shown in Fig. 2. Regarding the tuning of the controllers, the simplified internal model control (SIMC) method for smooth PID controller tuning was followed, as developed by Skogestad and Grimhold (Skogestad and Grimholt, 2012).

Table 1
Design values of the absorber, washer, stripper and heat exchanger in the capture unit.

Absorber	
Theoretical Stages	30
Total Height	35.60 m
Packing Height	25.00 m
Diameter	8.42 m
Lean Loading	0.32 mol/mol
Rich Loading	0.54 mol/mol
Lean Solvent Temperature	40 °C
Pressure	1.81 bar
Washer	
Total Height	2.10 m
Packing Height	1.50 m
Diameter	8.42 m
Stripper	
Theoretical Stages	20
Total Height	21.40 m
Packing Height	15.00 m
Diameter	6.89 m
Lean Loading	0.32 mol/mol
Rich Loading	0.54 mol/mol
Lean Solvent Temperature	120 °C
Pressure	2.00 bar
Heat Exchanger	
Average U	1.50 kW/m^2K
L-R Temperature Approach	10 K
Heat Exchanger Area	8,281 m^2

Five process variables were defined in order to measure the performance of the process, which can also be seen in Fig. 2:

- CO_2 capture rate at absorber stack C_{abs};
- CO_2 product mass flow rate at the outlet of the condenser of the stripper P_{CO2};
- Solvent lean loading at the inlet of the absorber *LL;*
- Solvent rich loading at the inlet of the stripper *RL;* and
- Temperature at the stripper bottom *TS*.

The operating points for the different seasons (Cases A–C) were found following an approach similar to that for the so-called *u-curves* for pilot plant testing (Gjernes et al., 2017). The solvent flow rates and loadings that maximize the capture rate for the given heat at steady

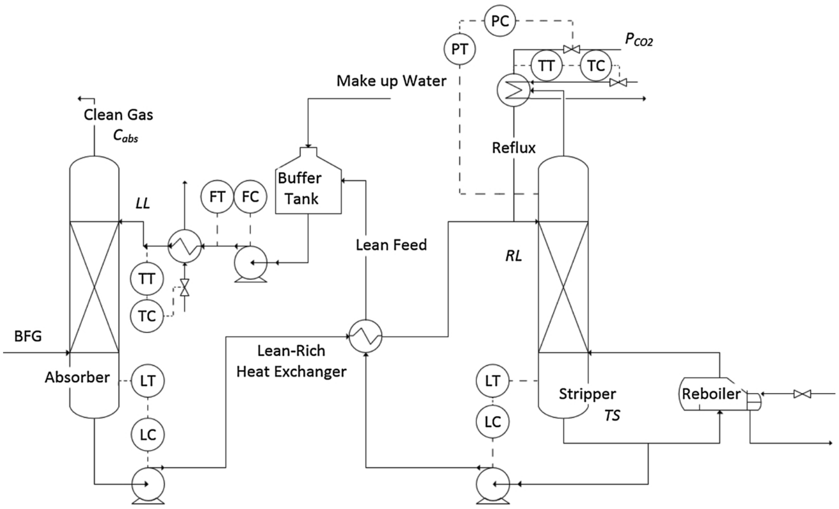

Fig. 2. Process diagram of the capture unit used to treat the blast furnace gas (BFG). The five main process variables analyzed in this work are shown in italic. The regulatory control loops are shown as dashed lines. The first letter indicates the controlled variable as follows: L, level; T, temperature; F, flow; and P: pressure. The second letter indicates the type of unit: T, transmission; C, controller.

state, i.e., minimize the specific reboiler duty, are given in Table 2.

2.2.2. The dynamic model

The dynamic model of the MEA CO_2 capture process was developed in the modeling language Modelica using the Dymola tool. The model is based on the unit blocks developed by Modelon AB in the GLC library (Modelon, 2018a), which has been presented previously (see (Montañés et al., 2017a; Gardarsdóttir et al., 2015a; Åkesson et al., 2011)) and is only briefly described below.

All the reactions were assumed to occur in the liquid phase and to be in equilibrium (Åkesson et al., 2011). The mass transfer was modeled following a rate-based approach, in which an enhancement factor was included to describe the impacts of chemical reactions on the mass transfer. Concentrations and pressure gradients were used to calculate the mass transfer for both the liquid and gas phase, respectively, with mass transfer coefficients taken from Onda et al. (1968). Phase equilibrium was assumed at the gas-liquid interface. The solubility of CO_2 in water was computed using Henry´s Law, with the Henry´s constant being taken from van Holst et al. (2009) and the activity coefficients from Böttinger (2005).

The two columns were modeled as several packed volumes with a sump at the bottom, which was assumed to be ideally mixed. A packing surface area of 256 m^2/m^3 was included, together with a void fraction of 0.987. Within each packed volume, both the liquid and gas flows were modeled as separate media with different thermodynamic properties: the ideal gas law applied in the gas phase to calculate densities and pressures, while a constant density was used for the liquid. The pressure in the columns was determined by the gas phase. Other assumptions considered in the model were the same as those described previously in (Montañés et al., 2017c; Åkesson et al., 2011): 1) MEA was considered nonvolatile and nondegradable, so no MEA make-up was needed; 2) the reboiler was modeled as an equilibrium flash stage; 3) mass and heat transfers were restricted to the packed section; 4) there was a negligible temperature difference between the liquid bulk and the interface to the gas phase; and 5) all the liquid from the packing bottom in the stripper was fed to the reboiler with a constant liquid level.

A static heat exchanger model was used for the lean-rich heat exchanger, which followed the ε-NTU approach. A solvent buffer tank was positioned before the absorber, to which a water make-up stream was added to compensate for the water losses. The design of the units was derived from the steady-state design.

The solvent inventory of the plant is crucial for the transient performance of the plant. The solvent hold-up in different units of the process was scaled-up from pilot plant data (Omell et al., 2017; Flø, 2015). Fig. 3 shows the circulation time of the solvent over the main volumes of the plant for each one of the cases studied, computed following the approach described previously in (Montañés et al., 2018). The total circulation time for the process is around 42 min for Case A, 2 h and 39 min for Case B, and 1 h and 30 min for Case C.

The dynamic models of the GLC library have been validated by Montañés et al. (2017c) Montañés et al. (2017a) through the collection of steady-state and transient data from the Technology Center Mongstad. In the present work, due to the lack of data from pilot plants integrated into steel mills, a verification of the dynamic model with the Aspen steady-state model was performed. For the design case, the absolute percentage errors were close to 1%, and were slightly higher (5%–7%) for the off-design cases.

2.2.3. Transient scenarios

Three types of transient scenarios for the boundary conditions considered were investigated: 1) a theoretical periodic oscillation; 2) an open-loop step response to step-changes identified in the plant data analysis; and 3) full two-week historical operational data.

2.2.4. Periodic oscillation in reboiler load

A sinusoidal boundary condition was applied to the reboiler heat duty, to investigate the effect of a periodic variation on the performance of the capture plant. This type of analysis has been conducted for other types of processes, such as combined gas and steam cycles (Shin, 2002). Based on the magnitudes of the disturbances relevant to the investigated application, a sinusoidal variation with an amplitude of ± 30 MW was applied to the average heat duty of 110 MW (Case C). The time of each period (the wavelength) was increased on a logarithmic scale from 10^{-1} to 10^6 seconds.

The evolution of the responses with the frequency of the disturbance was defined as the relative amplitude of the response for a certain period, A_i, normalized to the amplitude of the response after a long oscillation period, A_∞, according to Eq. (2). Here, x_i is the maximum value of the variable response, x_S is the steady value at 110 MW, and x_∞ is the maximum value of the response after a long oscillation period, i.e., when the amplitude of the response no longer changes with the period. Due to the non-linearity of the system, the amplitudes were calculated separately for the maximum and minimum values of the periodic responses. Refer to (Shin, 2002) for a more detailed visualization and explanation of the variables.

$$\frac{A_i}{A_\infty} = \frac{x_i - x_S}{x_\infty - x_S} \tag{2}$$

2.2.5. Open-loop step response simulations

The simulations consisted of step-changes in boundary conditions with magnitudes relevant to the investigated application. Two scenarios were defined based on the analysis of the plant operational data and variations thereof, which represent the events that need to be simulated in the dynamic model.

- *Scenario 1: Blast furnace gas variations.* Three main events were identified in the variations analysis: 10% drop, 20% drop, and 100% drop in the gas flow, relative to the nominal value. This scenario represents blast furnace operations that produce variations in the gas outflow.
- *Scenario 2: Available heat variations.* For both sources of heat considered, the identified events are within the same magnitude: ± 10 MW, ± 20 MW, and ± 30 MW. This scenario reflects variations in electricity generation or in district heating load, as well as operational events within the steel mill that lead to an increase or decrease in the level of flare gas.

The step-changes were applied while maintaining constant the remaining process variables and tracking the outputs in open-loop responses, i.e., with no control structure implemented aside from the regulatory control layer. The dynamic performance of the process was defined by the following parameters, following the methodology

Table 2
Operational conditions for Cases A, B and C.

Case	Capture Rate (%)	Solvent Flow Rate (kg/s)	Lean Loading (mol/mol)	Rich Loading (mol/mol)	BFG Mass Flow (kg/s)
A	90	940	0.32	0.54	140
B	24	250	0.41	0.60	140
C	67	450	0.24	0.55	140

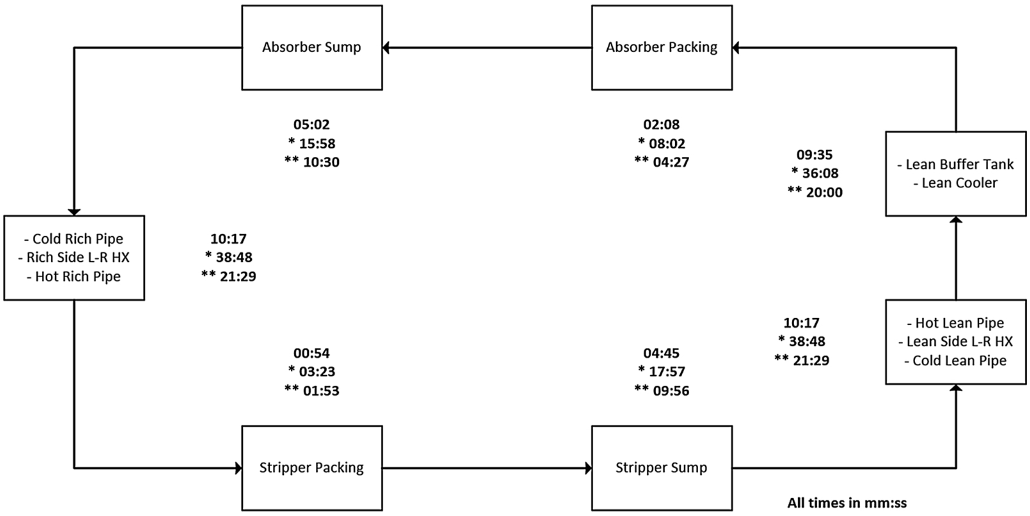

Fig. 3. Circulation times for all the volumes of the process. In each instance, the first number refers to the solvent flow rate in Case A – 940 kg/s; * refers to Case B – 250 kg/s; and ** refers to Case C – 450 kg/s.

described elsewhere (Montañés et al., 2017a; Flø et al., 2016).

- The dead time, Θ, represents the delay time between the change in boundary conditions and the response. The start of a response is defined as a change in the trajectory of the process variable from the initial steady state towards the final steady state.
- The 10% settling time, t_s, is the time from the start of the response until it settles within an error of ± 10% at the final steady-state, as expressed in Eq. (3).
- The total stabilization time, t_{sta}, is the sum of the dead time and the 10% settling time.
- The relative change of the response, RC, is the difference between the new and the initial steady states, as expressed by Eq. (4), where y_0 is the initial steady state and y_∞ is the new steady state.

$$y_\infty - 0.1\Delta y < y_\infty < y_\infty + 0.1\Delta y \tag{3}$$

$$RC(\%) = 100\cdot\frac{y_\infty - y_0}{y_0} \tag{4}$$

2.2.6. Boundary conditions from historical data

Boundary conditions were collected for a two-week period during the intermediate case (Case C, average available heat of 110 MW), to perform an analysis of the capture unit performance under actual running conditions. The operation of the capture plant was compared to a capture plant running at constant load (the average value for the investigated time period). The amount of CO_2 produced was computed by integrating the P_{CO2} trajectory, from the initial time t_0 to the final time t_f, as shown in Eq. (5).

$$m_{CO_2,Produced} = \int_{t_0}^{t_f} P_{CO2}(t)dt \tag{5}$$

Four cases were included in the comparison, following an approach similar to that utilized by Montañés et al. (2017a):

- Steady-state plant: utilizes a constant heat load corresponding to the average available heat.
- Ideal static plant: utilizes the actual boundary conditions, although it assumes that the plant has an instantaneous response to the disturbances, i.e., it attains the new steady-state at the same time as the boundary is changed. This case is useful for analyzing the effect of the inertia of the process. This case did not include any control loop in the solvent flow rate.
- Dynamic plant: utilizes the actual boundary conditions and the real response of the plant in open-loop, i.e., with no control strategy implemented.
- Dynamic controlled plant: utilizes the actual boundary conditions, and the real response of the plant in that it includes a decentralized control loop that controls the temperature in the stripper to a set value by controlling the lean amine solvent flow rate. Note that since the reboiler heat duty is a boundary condition and not modelled in the dynamic model, the only available degree of freedom in the advanced control layer is the solvent mass flow rate.

3. Results and discussion

3.1. Analysis of steel mill operational data

Fig. 4 shows the hourly values of the blast furnace gas flow, available excess heat, and heat in the flare gas throughout the year considered. The solid line represents the weekly average. The outlying period at the end of August represents a maintenance outage of the power plant, during which all the process gases are flared. The steel mill presents frequent variations on an hourly time scale.

The variations in the steel mill operation are quantified in Figs. 5 and 6. The performance of the steam cycle is highly dependent upon the need for district heating and the season of the year. During the winter period, all heat may be utilized for district heating and usually there is no heat left for CCS, whereas during the summer the average level of available heat for CCS is 110 MW. Therefore, as it can be seen in Fig. 5, the winter period only experiences events if the available heat is increased, while during the summer the available heat may vary upwards or downwards from the average value. The variations observed during summer are generally smaller and less frequent. This is expected since the district heating demand is more constant during the summer than during the winter. The variations in the flare gas and BFG flow (Fig. 6) are not dependent upon the season. In general, the fluctuations in the flare gas are relatively frequent and short-lived, being often maintained for just two hours. The blast furnace gas flow is stable compared to the other variables analyzed, although the gas flow dropped to zero thirteen times during the year considered.

3.2. Capture plant performance during transient operation

The performance of the capture plant during transient operation is presented in three parts. First, the results of the theoretical study with periodic boundary conditions for the reboiler heat duty are discussed. Second, the open-loop responses to step-changes corresponding to the magnitudes seen in the steel mill operation are presented. Third, the

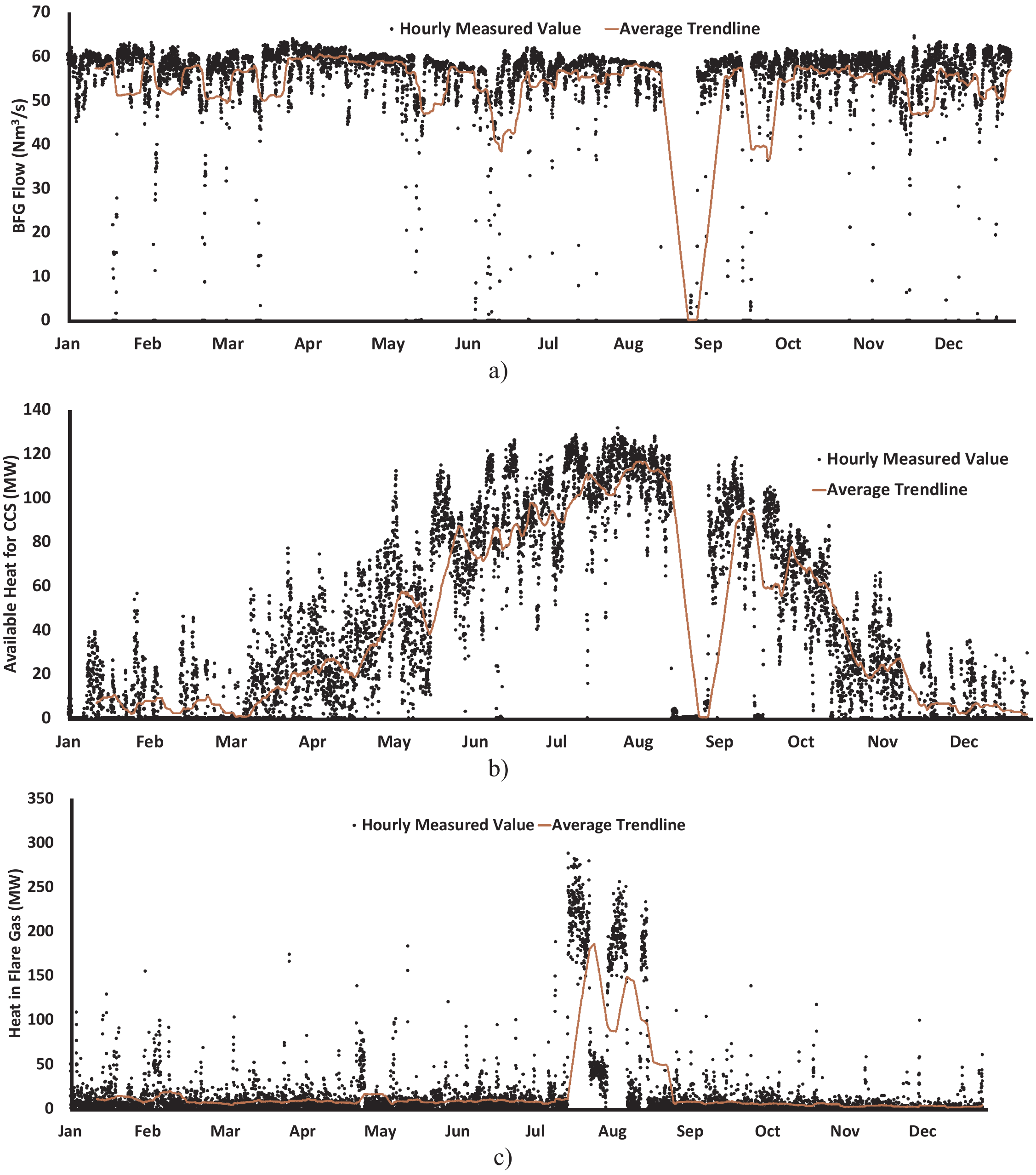

Fig. 4. Data analysis for the reference plant in 2017. a) Blast furnace gas (BFG) flow during 2017; b) available heat for CCS in the steam cycle; and c) available heat in the flare gas. The black dots are the hourly averages and the red solid lines represent the weekly averages. The drop seen in August corresponds to a maintenance outage.

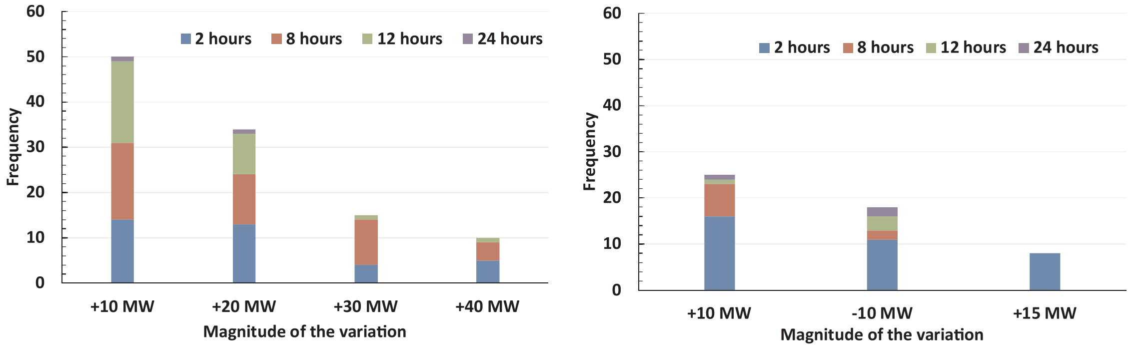

Fig. 5. Variations in average available heat from the steam cycle to be used for driving CCS in a) winter period (average = 0 MW) and b) summer period (average = 110 MW). The graphs show the duration and frequency (occurrence) of the variations for several magnitudes. For readability of columns refer to color code in electronic version.

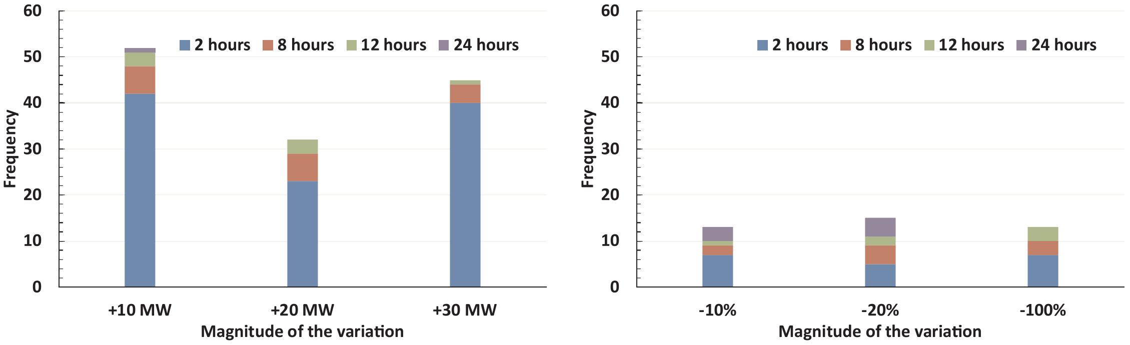

Fig. 6. Variations in available heat from a) the flare gas (average = 10 MW) and b) in the blast furnace gas (BFG) flow (average = 60 Nm^3/s). The graphs show the duration for which the variable is above or below certain values and the frequency (occurrence). For readability of columns refer to color code in electronic version.

capture plant performance with boundary conditions for a full two-week operational period of the steel mill is presented.

3.2.1. Periodic boundary conditions in reboiler load

Fig. 7a and 7b give the capture plant responses as CO_2 produced and absorbed to the periodic boundary conditions for reboiler heat duty for periods of 1000 and 10,000 s (i.e., around 15 min and 3 h), respectively. In both cases, the CO_2 produced in the stripper follows closely the heat load variations. This is caused by the instantaneous response of the stripper bottom temperature to the change in reboiler heat duty. The CO_2 absorbed in the absorber column shows a much slower response and lower amplitude of variation than the CO_2 produced in the stripper. This illustrates the damping effect of the absorber location and of the hold-up in the recycle loop between the stripper and absorber on the changes in reboiler heat duty. For the 1000 s-period, the amount of CO_2 absorbed barely changes within a cycle. However, with an increase in period, the absorber shows larger variations. This effect is illustrated in Fig. 7c, where differences are noted between the lean loading measured at the stripper outlet LL_{str} and at the absorber inlet LL_{abs}. Note that the dead time that affects the absorber is also shown, since the LL_{abs} values do not start to differ from the steady state until 1000 s after the disturbance is introduced.

Fig. 8 illustrates how the normalized response depends on the length of the period between cycles, according to Eq. (2). All the main process variables have different responses depending on the period of the reboiler heat load variation. Note that the maximum and minimum values of the periodic response are plotted separately, since the amplitudes of the responses are different when increasing and decreasing the load. This is due to the non-linearity of the process. P_{CO2} responds to the heat variations already for one-second cycles, while the CO_2 absorbed requires cycles of 1000 s to show a noticeable change. The maximum responses are steeper for both the CO_2 absorbed and produced. This means that when the heat in the reboiler is increased by a certain amount, the amount of CO_2 produced increases more than the drop in

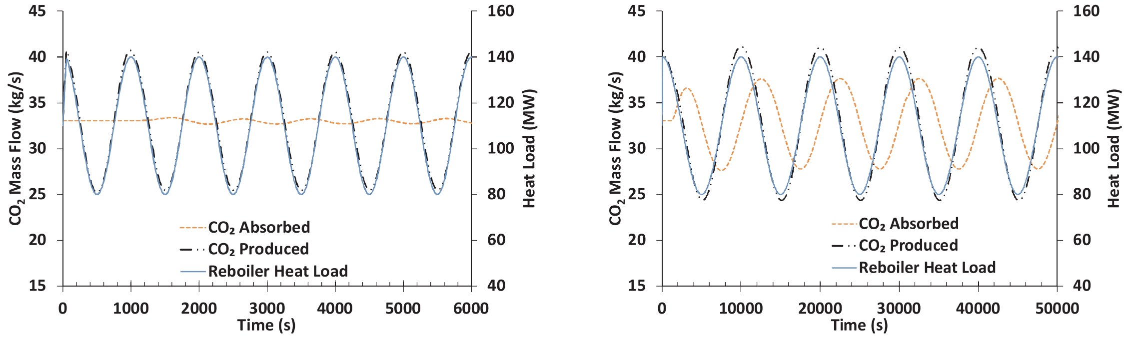

a) C_{abs} and P_{CO2} Response for τ_p = 1,000 s

b) C_{abs} and P_{CO2} Response for τ_p = 10,000 s

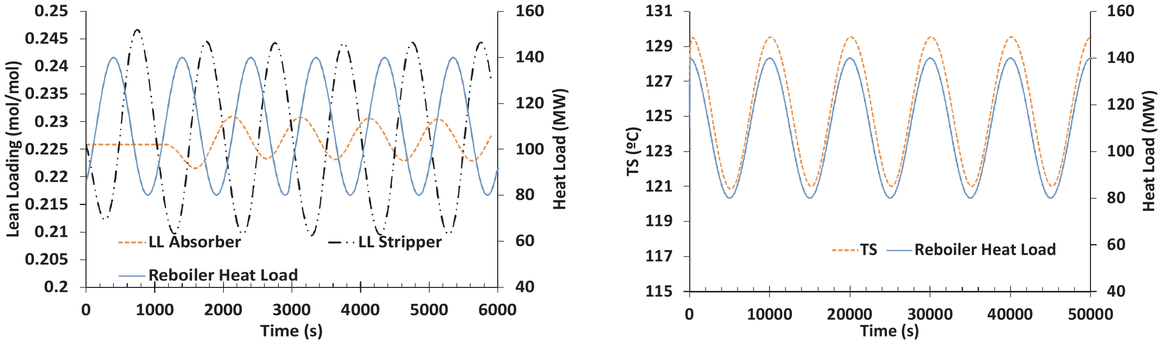

c) LL_{abs} and LL_{str} Response for τ_p = 1,000 s

d) TS Response for τ_p = 10,000 s

Fig. 7. Responses of the main process variables under periodic oscillation with reboiler load of ± 30 MW, which is plotted as a straight line. The variations are introduced in Case C, where the steady-state reboiler load is 110 MW. a) C_{abs} and P_{CO2} responses for a time period of 1000 s; b) C_{abs} and P_{CO2} responses for a time period of 10,000 s; c) LL_{abs} and LL_{str} responses for a time period of 1000 s: and d) TS response for a time period of 10,000 s. Note that the time scales in the panels are different.

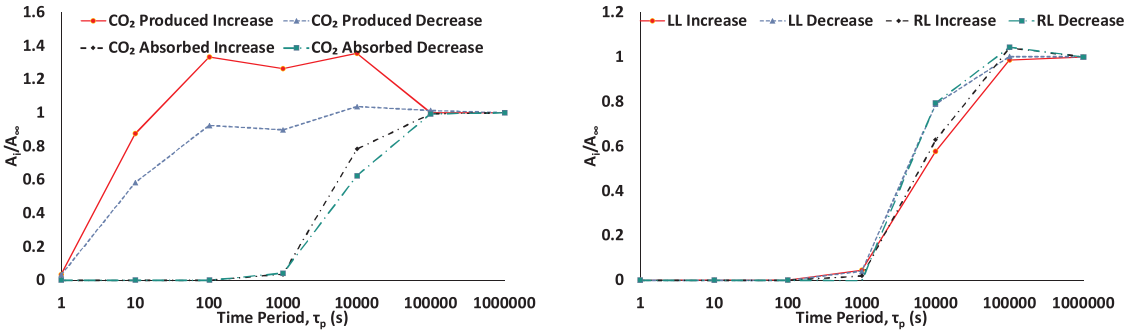

a) CO_2 Produced and CO_2 Absorbed b) Lean Loading and Rich Loading

Fig. 8. The relative amplitudes of the process responses depending on the cycle length of a periodic variation of the reboiler heat duty. The maximum (Max) and minimum (Min) values of the responses are plotted separately. a) CO_2 produced and absorbed. b) Lean and Rich loadings.

response experienced during the corresponding decrease in reboiler heat duty. Note that the increase in CO_2 produced exceeded one for several periods. This effect can also be observed in Fig. 8b, where the decrease in *LL* (caused by a heat load increment) is steeper than the increase (caused by a heat load drop), which eventually will affect the CO_2 absorbed in the absorber. For a cycle duration of around 10^5 seconds (around 28 h), the change is sufficiently slow for the process to respond with a quasi-static behavior.

3.2.2. Open-loop response to step-changes

The stabilization times of the main process variables responses to step-changes in BFG flow during the different seasons are shown in Fig. 9. The capture rate, C_{abs}, stabilizes considerably faster (after around 1 h) under summer conditions than under winter conditions (after 3–4 h), for the same disturbances. The slower response is attributed to the low solvent flow rate during winter, which increases the residence times in all the components. As expected, the production of CO_2 in the stripper, P_{CO2}, has a shorter stabilization time than C_{abs}, as the rich loading, *RL*, stabilizes faster than the lean loading, *LL*. The solvent hold-up in the active components and the position of the buffer tank at the inlet of the absorber are the reasons for this behavior.

After a 100% decrease (shut down) of the BFG flow, the stabilization times of all the responses are increased considerably, except for the amount of CO_2 absorbed (which substitutes for the capture rate due to computational considerations), which quickly drops to zero. The production of CO_2 continues for a few hours, even though there is no gas entering the absorber, as a large amount of CO_2 is stored in the solvent, i.e., the solvent loading is high under steady-state operation. The winter case again shows the slowest responses, due to the lower solvent flow rate and the higher solvent lean loading. The results suggest that it takes a 3-fold longer circulation time (see Fig. 3) for the plant to empty the stored CO_2 for the two extreme cases A and B. Fig. 10 shows the process response (during winter) after making the step-change followed by another step-change back to the normal gas flow after two and twelve hours, respectively. The timings of the steps are indicated with vertical dashed lines. The CO_2 production flow, the rich and the lean loading responses all include a significant dead time. After the second step-change when the gas flow is increased, the production reaches a steady state faster than the absorption, which is also seen for the rich and lean loadings. This difference is caused by the severe non-linearity of the process. Note that in the absence of gas entering the absorber, the steady state that both the lean and rich loadings would reach is the same, since the heat in the reboiler and solvent flow are kept constant. This situation has been studied by de Koeijer et al. (De Koeijer et al., 2014) in the amine plant at CO_2 Technology Center Mongstad, in the form of an equipment failure test. The results of that study show similar trends for the main process variables, where the CO_2 production flow remained above zero for several hours, presenting a faster ramp-up than down. However, some constraints must be taken into account when investigating these conditions, since this disturbance can also be seen as a short-term shutdown followed by a hot start-up. General constraints for this are identified in a previous paper (Marx-Schuba and Schmitz, 2017), with the temperature reboiler being limited to 125 °C and the solvent flow rate being above a certain value representing the main aspects to consider.

Leaving the reboiler and solvent recirculation unaltered is not the only strategy to consider in the event of the feed gas dropping to zero. A shutdown of the heat source or a complete shutdown of the plant are also viable options to save heat and plant operational costs. However, in the case studied, the heat is excess from the steel mill and the power plant. Therefore, keeping the stripper in operation while producing CO_2 stored in the solvent is the preferred over a total shutdown, not only from the production perspective, but also to keep the plant hot, considering the process constraints defined above. The ability of the compressor to handle flow variations should also be considered in this discussion. An analysis of the compressor operation is, however, outside the scope of the present work, and readers interested in compressor surge limits and efficiency at part load are directed to the study of (Walters et al. (2016)).

Fig. 11 shows the stabilization times of the process variables after step-changes in the reboiler heat duty for case C. The stabilization of the lean loading, *LL*, is faster than that of the rich loading, *RL*, since a change in reboiler duty affects primarily the lean part of the process. For the same reason, the produced CO_2, P_{CO2}, stabilizes faster than the absorbed CO_2, C_{abs}. Note that the temperature of the stripper, *TS*, shows the fastest response. Note also that the solvent temperature in the stripper bottom may become sufficiently high to cause thermal degradation of the solvent. The non-linearity of the process is evident also

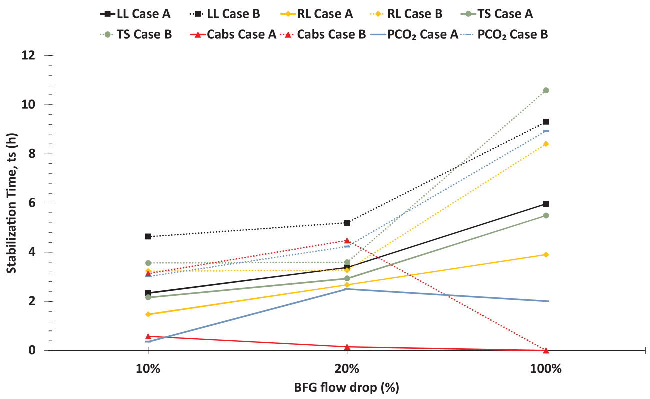

Fig. 9. Stabilization times (hours) for step-changes in the blast furnace gas flow. Solid lines represent Case A (summer) and dashed lines represent Case B (winter). LL, Lean Loading; RL, Rich Loading; TS, temperature in the stripper bottom; C_{abs}, CO_2 capture rate in the absorber; and P_{CO2}, CO_2 produced in the stripper.

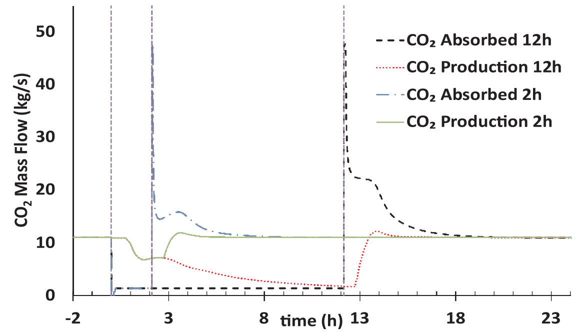

a) CO_2 absorbed and produced

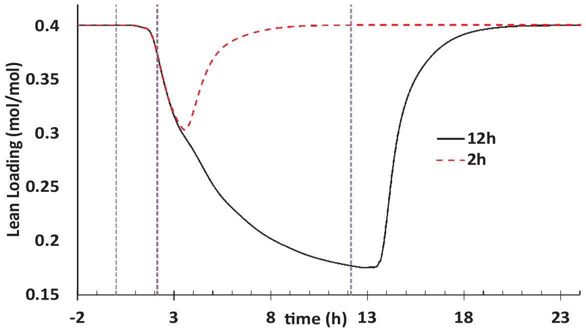

b) Lean Loading

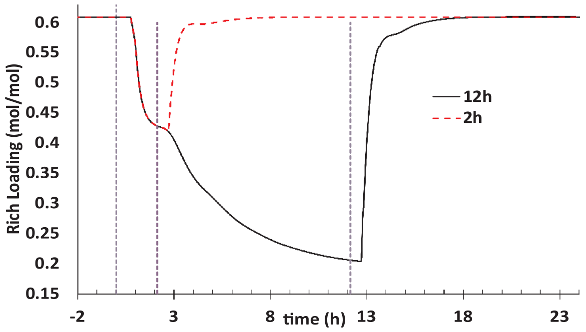

c) Rich Loading

Fig. 10. Transient responses of: a) CO_2 absorbed and produced; b) Lean Loading; and c) Rich Loading after a 100% drop in the blast furnace gas flow for 2 and 12 h, respectively. The initial steady-state condition corresponds to Case B with 30 MW in the reboiler. The step-change is introduced at t = 0, indicated with a vertical dashed purple line.

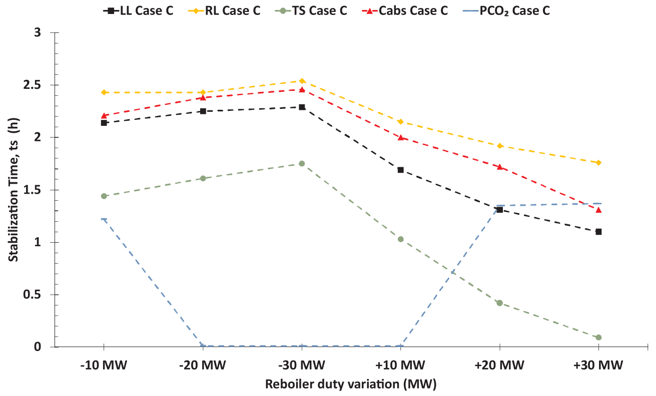

Fig. 11. Stabilization times (hour) of the main process variables for different steps in reboiler heat load for Case C. LL, Lean Loading; RL, Rich Loading; TS, temperature in the stripper bottom; C_{abs}, CO_2 capture rate in the absorber; and P_{CO2}, CO_2 produced in the stripper.

in Fig. 11: the response to an increase in reboiler heat is always faster than the response to a decrease of the same magnitude. It is also noteworthy that the responses are faster for smaller changes if the heat is decreasing, while the opposite occurs if the heat is increasing – the variables reach the steady state faster for larger changes. Fig. 12 illustrates the responses for each of the variables when a step-change of ± 30 MW is introduced.

3.2.3. *Comparing steady-state and dynamic operations*

Fig. 13 shows the boundary conditions of the reboiler heat and BFG flow trajectory over the two-week period that is studied in detail. Fig. 14 shows the response in the form of produced CO_2, P_{CO2}. The capture plant frequently deviates from the steady-state average value (indicated by a dotted line in Fig. 14). This illustrates the importance of considering disturbances. The drops in CO_2 production observed on Days 1 and 11 correspond to the periods of zero BFG flow. The variations in reboiler heat duty cause disturbances with magnitudes of ± 10 kg/s (approximately 20% deviation from the average value).

The amount of CO_2 produced over the two-week period was 40.9 ktonne or 42.4 ktonne assuming the steady-state average or the actual heat and BFG flow as boundary conditions with control strategy implemented, respectively. The higher amount (2.4%) of CO_2 captured with the dynamic controlled system is explained by the non-linearity of the system, as discussed in the periodic oscillation analysis (see Section 3.2.1). This feature can also be seen when calculating the CO_2 captured under the assumption of an ideal-static plant (41.1 ktonne). The results show that the CO_2 capture unit is efficient in dealing with the process variations from the steel mill, and that efforts to smoothen the variations are not required from the CO_2 absorption perspective. If the capture plant is not equipped with a process control strategy, the amount of CO_2 captured with the actual boundary conditions is decreased by 1.2% to 41.9 ktonne.

4. Conclusions

This work maps the variations in process gas and available excess heat of an integrated steel mill, and investigates the effects of these variations on the performance of a plant for chemical absorption of CO_2 using MEA. The implications on a seasonal and hourly basis are investigated using a Swedish steel mill as a case study. Furthermore, this work investigates the implications of these load variations on the implementation of an excess-heat-powered CO_2 absorption process for carbon capture and storage using a dynamic process model. Simulations were run with periodic, as well as with actual boundary conditions for reboiler heat duty and process gas flow.

The results show large variations in the conditions, based on a seasonal as well as on an hourly basis, that are important to consider in the design and operation of the capture plant. In an energy system with considerable levels of district heating, the optimal capture rate for a certain amount of available excess heat will differ significantly between winter and summer operations. Regarding variations on an hourly time scale, the capture plant has considerable buffering capacity in terms of solvent hold-up, and measures to even out these variations should not be necessary. The amount of CO_2 captured in the absorber responds relatively slowly (from 1 to 3 h depending on the solvent circulation rate and the magnitude of the disturbance) to changes in reboiler heat duty. The general trend shows that during winter operation the capture plant responds slower than during the summer. The capture unit shows clear non-linearity in its responses to changes in heat load - the deviation from the steady-state value is greater when the heat is increased than when it is decreased.

The simulation of the capture plant operation during a two-week period with actual (historical) boundary conditions shows that it is possible to operate a CO_2 absorption process in the presence of the variations caused by the steel mill. Integration requires flexible operation of the capture process, and CO_2 production is favored by a

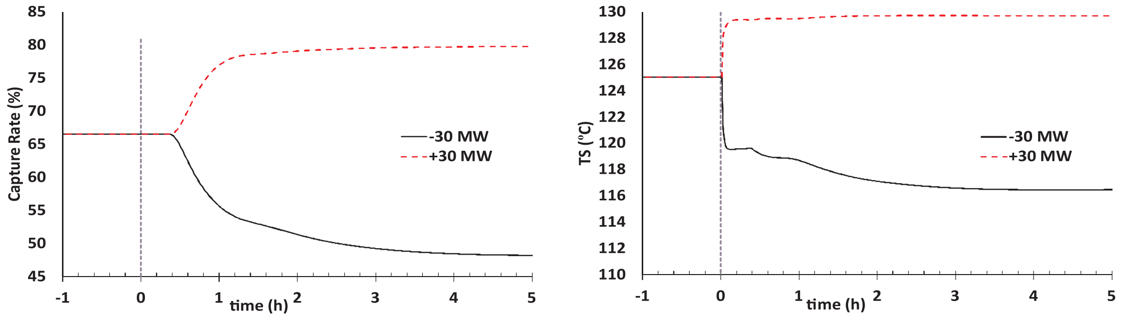

a) C_{abs} b) TS

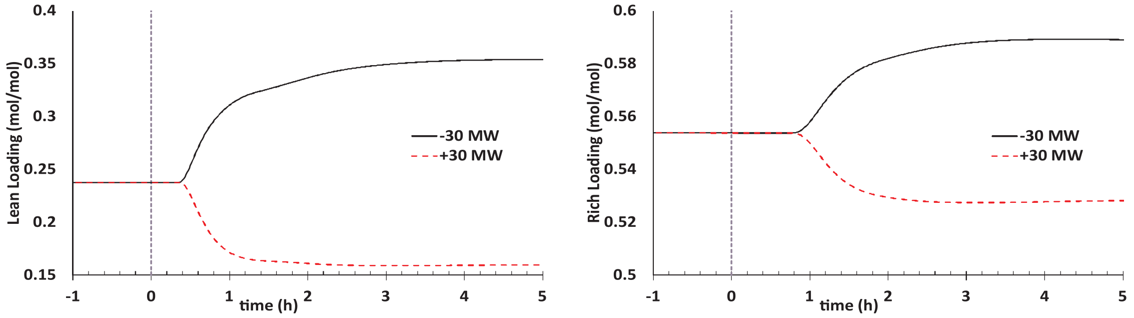

c) LL d) RL

Fig. 12. Transient responses of the main process variables for ± 30 MW-steps. The initial steady-state condition corresponds to Case C with 110 MW in the reboiler. The steps are introduced at t = 0, indicted with a vertical dashed purple line. a) CO_2 absorbed; b) temperature at stripper bottom; c) Lean Loading; and d) Rich Loading.

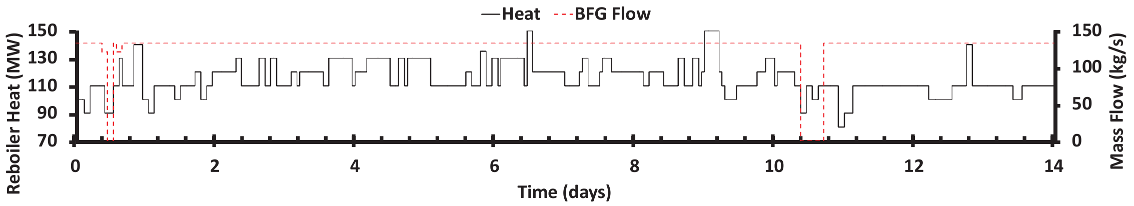

Fig. 13. Variations in available heat for CCS and blast furnace gas (BFG) flow occurring in the two-week period considered, after being discretized.

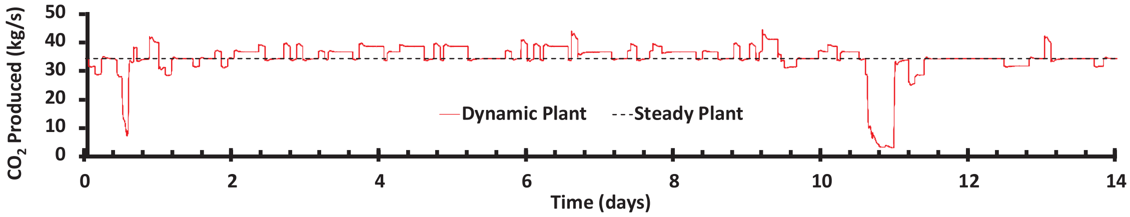

Fig. 14. Transient responses in CO_2 production during the two-week period simulated. The dashed line represents capture under the assumption of average steady-state heat.

decentralized control strategy, showing a 1.2% increase relative to the non-controlled case.

Acknowledgment

This work is financed by the CO2stCap project.

References

Åkesson, J., et al., 2011. Models of a post-combustion absorption unit for simulation, optimization and non-linear model predictive control schemes. 8th Modelica Conference 64–74.

Allwood, J., 2012. Sustainable Materials – With Both Eyes Open.

Amrollahi, Z., Ertesvåg, I.S., Bolland, O., 2011. Optimized process configurations of post-combustion CO_2 capture for natural-gas-fired power plant — exergy analysis. Int. J. Greenh. Gas Control 5, 1393–1405.

Antti Arasto, L.S., Tsupari, Eemeli, Käarki, Janne, Pisilä, Erkki, 2013. Post-combustion capture of CO_2 at an integrated steel mill- Part I: technical concept analysis. Int. J. Greenh. Gas Control 16, 271–277.

Aske, E.M.B., Skogestad, S., 2009. Consistent inventory control. Ind. Eng. Chem. Res. 48 (24), 10892–10902.

Biermann, M., Normann, F., Johnsson, F., Skagestad, R., 2018. Partial carbon-capture by absorption cycle for reduced specific capture cost. Ind. Eng. Chem. Res. 57, 15411–15422.

Böttinger, W., 2005. NMR-spektroskopische Untersuchung der Reaktivabsorption von Kohlendioxid in wässrigen Aminlösungen. University of Stuttgart, Stuttgart, Germany.

Bravo, J.L., Rocha, J.A., Fair, J.R., 1985. Mass transfer in gauze packings. Hydrocarb. Process 64 (1), 91–95.

Bui, M., Gunawan, I., Verheyen, V., Feron, P., Meuleman, E., Adeloju, S., 2014. Dynamic modelling and optimisation of flexible operation in post-combustion CO_2 capture plants-a review. Comput. Chem. Eng. 61, 245–265.

Bui, M., Gunawan, I., Verheyen, V., Feron, P., Meuleman, E., 2016. Flexible operation of CSIRO's post-combustion CO_2 capture pilot plant at the AGL Loy Yang power station. Int. J. Greenh. Gas Control 48, 188–203.

Chinen, A.S., Morgan, J.C., Omell, B.P., Bhattacharyya, D., Miller, D.C., 2016. Dynamic data reconciliation and model validation of a MEA-based CO_2 capture system using pilot plant data. IFAC-PapersOnLine 49 (7), 639–644.

Cohen, S.M., Rochelle, G.T., Webber, M.E., 2013. Optimal CO_2 capture operation in an advanced electric grid. Energy Procedia 37, 2585–2594.

De Koeijer, G.M., Aasen, K.I., Steinseth Hamborg, E., 2014. Scale-up and transient operation of CO_2 capture plants at CO_2 technology centre mongstad. Abu Dhabi Int. Pet. Exhib. Conf.

Domenichini, R., Mancuso, L., Ferrari, N., Davison, J., 2013. Operating flexibility of power plants with carbon capture and storage (CCS). Energy Procedia 37, 2727–2737.

Dreillard, M., Broutin, P., Briot, P., Huard, T., Lettat, A., 2017. Application of the DMXTM CO_2 capture process in steel industry. Energy Procedia 114 (November), 2573–2589.

Enaasen Flø, N., Knuutila, H., Kvamsdal, H.M., Hillestad, M., 2015. Dynamic model validation of the post-combustion CO_2 absorption process. Int. J. Greenh. Gas Control 41, 127–141.

Faber, R., Köpcke, M., Biede, O., Knudsen, J.N., Andersen, J., 2011. Open-loop step responses for the MEA post-combustion capture process: experimental results from the Esbjerg pilot plant. Energy Procedia 4, 1427–1434.

Flø, N.E., 2015. Nina Enaasen Flø Post-Combustion Absorption-Based CO_2 Capture: Modeling, Validation and Analysis of Process Dynamics.

Flø, N.E., Kvamsdal, H.M., Hillestad, M., Mejdell, T., 2016. Dominating dynamics of the post-combustion CO_2 absorption process. Comput. Chem. Eng. 86, 171–183.

Gardarsdóttir, S.Ó., Normann, F., Andersson, K., Prölss, K., Emilsdóttir, S., Johnsson, F., 2015a. Post-combustion CO_2 capture applied to a state-of-the-art coal-fired power plant-The influence of dynamic process conditions. Int. J. Greenh. Gas Control 33, 51–62.

Gardarsdóttir, S.Ó., Normann, F., Andersson, K., Johnsson, F., 2015b. Postcombustion CO_2 capture using monoethanolamine and ammonia solvents: The influence of CO_2 concentration on technical performance. Ind. Eng. Chem. Res. 54 (2), 681–690.

Gardarsdóttir, S., Montañés, R.M., Normann, F., Nord, L.O., Johnsson, F., 2017. Effects of CO_2-absorption control strategies on the dynamic performance of a supercritical pulverized-coal-fired power plant. Ind. Eng. Chem. Res. 56 (15), 4415–4430.

Gazzani, M., Romano, M.C., Manzolini, G., 2015. CO_2 capture in integrated steelworks by commercial-ready technologies and SEWGS process. Int. J. Greenh. Gas Control 41, 249–267.

Gjernes, E., et al., 2017. Results from 30 wt% MEA Performance Testing at the CO_2 Technology Centre Mongstad. Energy Procedia 114, 1146–1157.

Global CCS "Global CCS." [Online]. Available: https://www.globalccsinstitute.com/projects/large-scale-ccs-projects. (Accessed 25 May 2018).

He, X., Wang, Y., Bhattacharyya, D., Lima, F.V., Turton, R., 2018. Dynamic modeling and advanced control of post-combustion CO_2 capture plants. Chem. Eng. Res. Des. 131, 430–439.

Heuberger, C.F., Staffell, I., Shah, N., MacDowell, N., 2017. What is the Value of CCS in the Future Energy System? Energy Procedia 114 (November), 7564–7572.

Hummel, H., Canapa, R., 2013. Steel Roadmap EU 2050.

IEAGHG, 2012. Operating Flexibility of Power Plants with CCS.

IEAGHG, 2016. Evaluation of Process Control Strategies for Normal, Flexible and Upset Operation Conditions of CO_2 Post-combustion Capture Processes.

IPCC, 2014. Climate Change 2014: Mitigation of Climate Change. Cambridge University Press.

Kärki, J., Tsupari, E., Arasto, A., 2013. CCS feasibility improvement in industrial and municipal applications by heat utilization. Energy Procedia 37, 2611–2621.

Lawal, A., Wang, M., Stephenson, P., Obi, O., 2012. Demonstrating full-scale post-combustion CO_2 capture for coal-fired power plants through dynamic modelling and simulation. Fuel 101, 115–128.

Lucquiaud, M., Chalmers, H., Gibbins, J., 2009. Capture-ready supercritical coal-fired power plants and flexible post-combustion CO_2 capture. Energy Procedia 1 (1), 1411–1418.

Luu, M.T., Abdul Manaf, N., Abbas, A., 2015. Dynamic modelling and control strategies for flexible operation of amine-based post-combustion CO_2 capture systems. Int. J. Greenh. Gas Control 39, 377–389.

Mac Dowell, N., Staffell, I., 2016. The role of flexible CCS in the UK's future energy system. Int. J. Greenh. Gas Control 48, 327–344.

Marx-Schubach, T., Schmitz, G., 2017. Optimizing the Start-up Process of Post-combustion Capture Plants by Varying the Solvent Flow Rate. pp. 121–130.

Mechleri, E., Fennell, P.S., Mac Dowell, N., 2017. Flexible operation strategies for coal- and gas-CCS power stations under the UK and USA markets. Energy Procedia 114, 6543–6551.

Modelon, A.B., 2018a. Capture with Amine Solutions.

Modelon, A.B., 2018b. Modelon Home. [Online]. Available:. (Accessed February 2018). https://www.modelon.com/.

Montañés, R.M., Korpås, M., Nord, L.O., Jaehnert, S., 2016. Identifying operational requirements for flexible CCS power plant in future energy systems. Energy Procedia 86 (1876), 22–31.

Montañés, R., Flø, N., Nord, L., 2017a. Dynamic process model validation and control of the amine plant at CO_2 technology centre mongstad. Energies 10 (10), 1527.

Montañés, R.M., Gardarsdóttir, S., Normann, F., Johnsson, F., Nord, L.O., 2017b. Demonstrating load-change transient performance of a commercial-scale natural gas combined cycle power plant with post-combustion CO_2 capture. Int. J. Greenh. Gas Control 63 (May), 158–174.

Montañés, R.M., Flø, N.E., Dutta, R., Nord, L.O., Bolland, O., 2017c. Dynamic process model development and validation with transient plant data collected from an MEA test campaign at the CO_2 technology center mongstad. Energy Procedia 114 (1876), 1538–1550.

Montañés, R.M., Flø, N.E., Nord, L.O., 2018. Experimental results of transient testing at the amine plant at Technology Centre Mongstad: Open-loop responses and performance of decentralized control structures for load changes. Int. J. Greenh. Gas Control 73 (January), 42–59.

NETL, "Petra Nova Parish Holdings. W.A. Parish Post-combustion CO2 Capture and Sequestration Project.".

OECD, 2004. Prospects for CO_2 Capture and Storage. OECD Publishing.

Omell, B., Chinen, A.S., Morgan, J.C., Bhattacharyya, D., David, C., Energy, N., 2017. Rigorous Model Development of a MEA-based CO_2 Capture System and Validation with Pilot Plant Data Across Multiple Scales. TCCS-9.

Onda, K., Takeuchi, H., Okumoto, Y., 1968. Mass transfer coefficients between gas and liquid phases in packed columns. J. Chem. Eng. Japan 1 (1), 56–62.

Panahi, M., Skogestad, S., 2012. Economically efficient operation of CO_2 capturing process. Part II. Design of control layer. Chem. Eng. Process. Process Intensif. 52, 112–124.

Raynaud, D., Stocker, T.F., 2013. IPCC 2013: CLIMATE CHANGE 2013 - The Physical Science Basis, Contribution of Working Group I to the Fifth Assessment Report of the Intergovernmental Panel on Climate Change. Cambirdge University Press.

Remus, R., Roudier, S., Monsonet, Ma.Aguado, Sancho, L.D., 2013. Best Available Techniques (BAT) Reference Document for Iron and Steel Production. vol. BREF-IS, Luxembourg.

Shin, J., 2002. Analysis of the dynamic characteristics of a combined-cycle power plant. Energy 27 (12), 1085–1098.

Singh, A., Stéphenne, K., 2014. Shell Cansolv CO_2 capture technology: Achievement from first commercial plant. Energy Procedia 63, 1678–1685.

Skogestad, S., Grimholt, C., 2012. The SIMC method for smooth PID controller tuning. Adv. Ind. Control 147–175 9781447124245.

SSAB, 2016. Ssab Annual Report 2016 Toward Industry-Leading Profitability Contents.

Storck, J., 2009. Strategic and Operational Capabilities in Steel Production. KTH.

Sundqvist, M., Biermann, M., Normann, F., Larsson, M., Nilsson, L., 2017. Evaluation of low and high level integration options for carbon capture at an integrated iron and steel mill. Int. J. Greenh. Gas Control 77 (July), 27–36.

Tait, P., Buschle, B., Ausner, I., Valluri, P., Wehrli, M., Lucquiaud, M., 2016. A pilot-scale study of dynamic response scenarios for the flexible operation of post-combustion CO_2 capture. Int. J. Greenh. Gas Control 48, 216–233.

Tsupari, E., Kärki, J., Arasto, A., Pisilä, E., 2013. Post-combustion capture of CO_2 at an integrated steel mill - Part II: economic feasibility. Int. J. Greenh. Gas Control 16, 278–286.

ULCOS, 2018. Ulcos. [Online]. Available:. [Accessed: April-2018]. http://ulcos.org/en/index.php.

UNFCCC, 2015. Paris agreement. Conf. Parties Its Twenty-First Sess., no 32.

Van De Haar, A., Trapp, C., Wellner, K., De Kler, R., Schmitz, G., Colonna, P., 2017. Dynamics of Postcombustion CO_2 Capture Plants: Modeling, Validation, and Case Study. Ind. Eng. Chem. Res. 56 (7), 1810–1822.

van Holst, J., Versteeg, G.F., Brilman, D.W.F., Hogendoorn, J.A., 2009. Kinetic study of CO_2 with various amino acid salts in aqueous solution. Chem. Eng. Sci. 64 (1), 59–68.

Walters, M.S., Edgar, T.F., Rochelle, G.T., 2016. Regulatory Control of Amine Scrubbing for CO_2 Capture from Power Plants. Ind. Eng. Chem. Res. 55 (16), 4646–4657.

Wellner, K., Marx-Schubach, T., Schmitz, G., 2016. Dynamic Behavior of Coal-Fired Power Plants with Post-combustion CO_2 Capture. Ind. Eng. Chem. Res. 55 (46), 12038–12045.

WorldSteel, 2010. Steel Statistical Yearbook 2010. Beijing. .

Wu, X., Shen, J., Li, Y., Wang, M., Lawal, A., Lee, K.Y., 2018. Nonlinear dynamic analysis and control design of a solvent-based post-combustion CO_2 capture process. Comput. Chem. Eng. 115 (July), 397–406.

Paper B

International Journal of Greenhouse Gas Control 118 (2022) 103689

Contents lists available at ScienceDirect

International Journal of Greenhouse Gas Control

journal homepage: www.elsevier.com/locate/ijggc

Efficient heat integration of industrial CO_2 capture and district heating supply

Åsa Eliasson, Elin Fahrman, Maximilian Biermann, Fredrik Normann [*], Simon Harvey

Department of Space, Earth and Environment, Division of Energy Technology, Chalmers University of Technology, Gothenburg S41298, Sweden

ARTICLE INFO

Keywords:
Carbon capture
District heating
Excess heat
Specific cost
Seasonal variations
Process industry

ABSTRACT

Excess heat from industrial processes can be used for carbon capture and storage (CCS) as well as providing heat to a district heating network, leading to increased energy efficiency and reduction of on-site and/or off-site CO_2 emissions. In this work, both options are assessed with respect to economic performance and potential reduction of CO_2 emissions. The work includes a generic study based on five heat load curves for each of which three CO_2 capture plant configurations were evaluated. The economic assessment indicates that the specific cost of capture ranges from 47-134 €/t CO_2 depending on heat profile and capture plant configuration. Having excess heat available during a long period of the year, or having a high peak amount of heat, were shown to lead to low specific capture costs. The paper also includes results of a case study in which the methodology was applied to actual seasonal variations of excess heat for an integrated steel mill located in northern Sweden. Specific capture costs were estimated to 27-44 €/t CO_2, and a 36% reduction of direct plant emissions can be achieved if the CO_2 capture plant is prioritized for usage of the available excess heat.

1. Introduction

The industry sector accounts for a significant fraction of global CO_2 emissions. One measure to reduce CO_2 emissions is to recover available residual heat, often denoted “excess heat”. Excess heat may be used internally in the process to decrease primary energy usage, or externally, for e.g. district heating, thereby decreasing energy usage elsewhere. In Sweden, the expansion of district heating networks over the past decades has led to substantially decreased CO_2 emissions from the heating sector (Werner, 2017). Part of this reduction stems from the utilization of industrial excess heat, since the emissions related to such heat have typically been allocated to the main products of the industrial plant, thereby the use of industrial excess heat for district heating is normally considered to be emissions-free – although there are extensive ongoing discussions about whether industrial excess should be categorised as CO_2-free or CO_2-neutral, as summarized in a recent paper by Pelda et al. (2020). As a result, many studies have pointed out that further expansion of district heating networks would be a cost-effective option to reduce emissions in the EU energy system (e.g. Connolly et al., 2014; Manz et al., 2021). Möller et al. (2019) estimate that up to 71% of the urban heating demand can be met by district heating in 14 analyzed EU member states. Of this, up to 78% could be supplied by excess heat. However, other studies have pointed out that utilizing excess heat for district heating can have different levels of impact on the net change in emissions from the heating sector, depending on the heat supply option that is replaced, the applied system boundaries, and the assumptions about future energy market scenarios (Broberg et al., 2014; Ivner and Broberg Viklund, 2015; Olsson et al., 2015; Pettersson et al., 2020).

Carbon capture and storage (CCS) is an emerging technology that can utilize considerable amounts of industrial excess heat. CCS has been acknowledged as a technology that will be important in limiting global warming, both by enabling emissions reduction through retrofitting of existing plants in the near-term and, in the long-term, by contributing to reduction of hard-to-abate-process emissions as well as enabling negative emissions by capturing biogenic emissions (IEA, 2020; Rogelj, 2018). Although large-scale deployment of CCS has so far been slow due to lack of incentives (e.g. policy support), many new CCS projects have been announced in recent years. The reason for the new-found interest in CCS is that it is now perceived as an enabling technology to reach net-zero corporate and national emission targets, compliant with the Paris agreement (IEA, 2020). Chemical absorption using an amine solvent is widely considered to be the most mature CO_2 capture technology that is suitable for retrofitting of industrial plants. Aqueous monoethanolamine (MEA) was long considered as the benchmark solvent for amine-based capture (Oh et al., 2016). More recently,

---

[*] Corresponding author.
E-mail address: fredrik.normann@chalmers.se (F. Normann).

https://doi.org/10.1016/j.ijggc.2022.103689
Received 7 July 2021; Received in revised form 15 February 2022; Accepted 2 May 2022

Nomenclature

AMP	2 amino 2 methyl 1 propanol
BFG	blast furnace gas
CAPEX	capital expenditures
CCS	carbon capture and storage
CEPCI	chemical engineering plant cost index
CHP	combined heat and power
DH	district heating
EDF	enhanced detailed factor
EIC	equipment installed cost
IEA	international energy agency
MEA	monoethanolamine
MH	maximum amount of available excess heat
OPEX	operational expenditures
PZ	piperazine
SL	seasonal length
TDC	total direct cost
TIC	total installed cost

2-amino-2-methyl-1-propanol (AMP) promoted with piperazine (PZ) has been the subject of increased interest (Feron et al., 2020). CO_2 capture requires both high capital expenditures (CAPEX), as well as large amounts of heat for regeneration of the solvent and thus high operating expenditures (OPEX) (Garðarsdóttir et al., 2018). Previous studies have therefore focused on reducing cost to facilitate the implementation of CCS. Garðarsdóttir et al. (2018) investigated the influence of flowrate and concentration of the CO_2 source on CAPEX for CO_2 capture. They concluded that both parameters have a high influence on the specific investment cost (cost per unit amount of captured CO_2), with increased flowrate or CO_2 concentration of the emission source resulting in a decrease in specific CAPEX. On the other hand, Biermann et al. (2018) found that depending on site conditions, the specific cost of capture may be decreased if partial capture (capturing <90% of the CO_2) is applied instead of full capture (defined as capturing 90% of the CO_2 from the source), despite the disadvantage of smaller scale, due to reduced specific heat supply cost and decreased heat demand. Recovery of available excess heat from the industrial plant to drive the CCS capture unit is clearly an attractive option for increasing energy efficiency and reducing the specific cost, hence making the operation of a CO_2 capture plant more economically feasible (Andersson et al., 2016; Biermann et al., 2019; Biermann et al., 2021; Sundqvist et al., 2018). In a recent study by Johnsson et al. (2020), the costs required to install and operate amine-based post-combustion CO_2 capture were mapped for all 28 manufacturing plants in Sweden with annual emissions of 500 kt CO_2 or more, of both fossil and of biogenic origin, and included a petrochemical site, refineries, iron and steel plants, cement plants and pulp and paper mills. The work considered differences in the investment required as well as differences in potential for using excess heat to cover the steam demand of the capture process, and concluded that full CO_2 capture applied to the 28 industrial plants would capture emissions corresponding to 50% of Swedish total CO_2 emissions (from all sectors) at a cost ranging from around 40 €/t CO_2 to 110 €/t CO_2, depending on emission source.

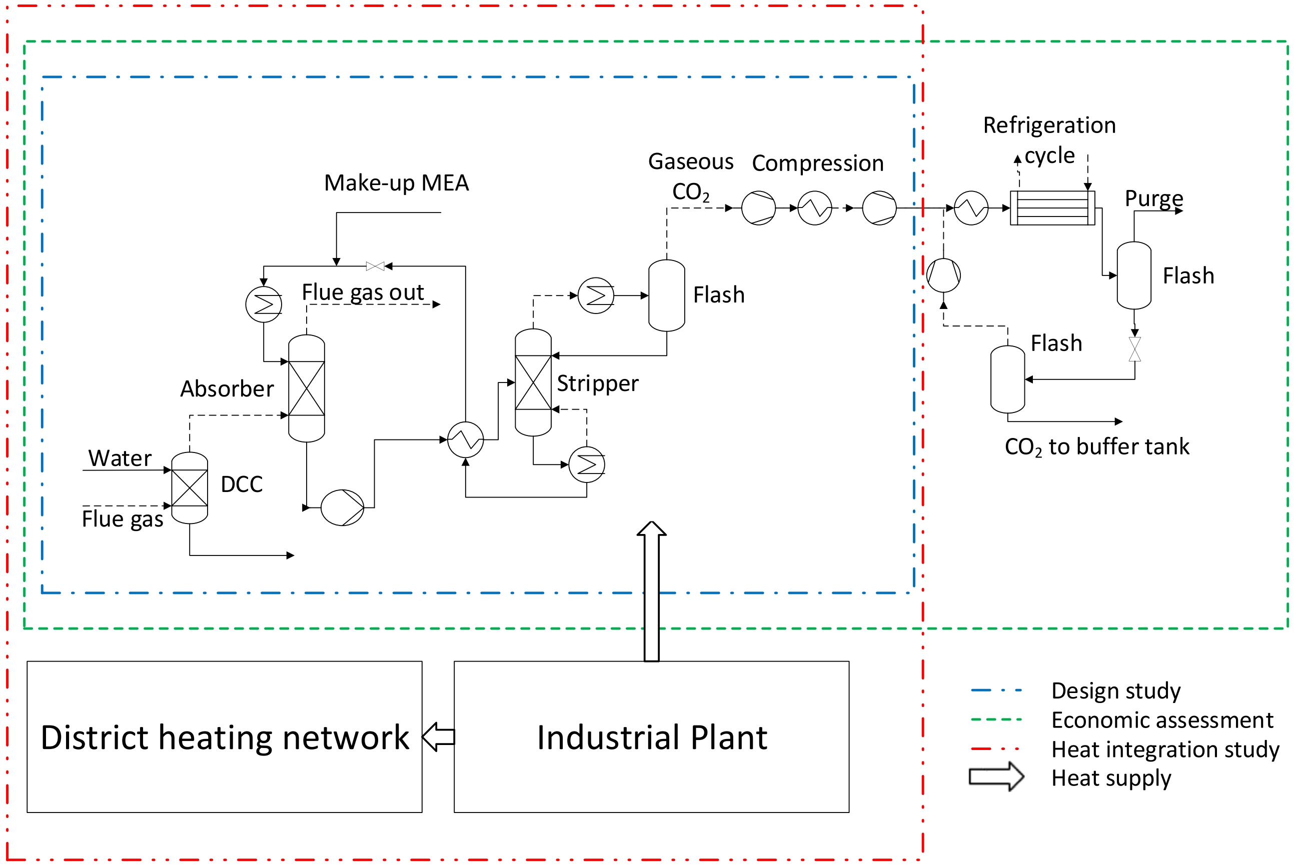

Fig. 1. An overview of the methodology and the studied system. The red border indicates the scope of the heat integration study, the blue border shows the boundaries of the design study, while the green border indicates the scope of the economic assessment. The arrows indicate heat supply from one system to another. DCC = Direct Contact Cooler; MEA = Monoethanolamine.

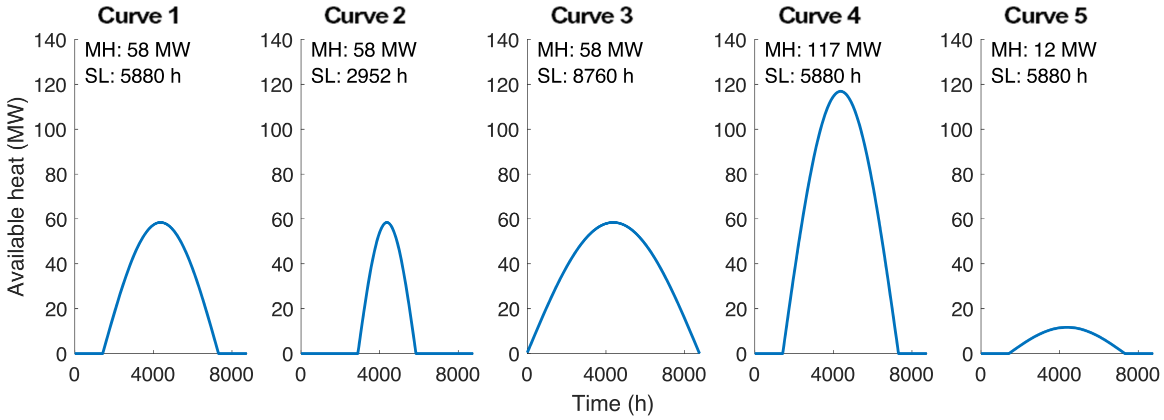

Fig. 2. Theoretical heat load curves evaluated in the generic study, defined by their seasonal length (SL, hours/year) and maximum amount of available heat (MH, MW).

Although most studies of opportunities to reduce industrial CO_2 emissions focus on single technology options, it is important to consider the effect of implementing different CO_2 mitigation options in relation to or in combination with each other. Jönsson and Algehed (2010) investigated the emissions reduction potential and economic performance of implementing district heating and CCS (among other options) at a kraft pulp mill. Eriksson et al. (2018) compared the economic feasibility of increased energy efficiency at a chemical complex site with heat recovery for external utilization. The interplay between CCS and district heating as well as the potential heat integration between them have been investigated in some studies, mostly in relation to implementation of CCS in the power generation sector. Bartela et al. (2014), for example, found that the cost of implementation of CCS at a super-critical coal-fired combined heat and power (CHP) plant could be significantly reduced if residual heat is recovered from the capture plant and delivered to a district heating network. Huang et al. (2017) examined the performance of a natural gas combined cycle-CHP plant configured to deliver heat to a district heating network as well as supplying heat to a CCS plant. It was assumed that the district heating supply should be prioritized, and alternative options for heat supply for CCS were investigated so as to achieve a 90% CO_2 capture rate all year round, i.e., despite the fluctuating district heating demand. It was concluded that the most technically and economically feasible option was supplementary firing in the heat recovery steam generators, which led to lower CO_2 emissions per unit product as compared to the other heat supply options, as well as relatively constant levels of CO_2 emissions per unit of product despite the fluctuating district heating supply.

This work compares the economic performance of possible strategies for using industrial excess heat for supplying heat to a CCS unit and a district heating network. The options investigated include strategies for design and operation of the CO_2 capture plant and their impact on how the excess heat is divided between the CCS unit and the district heating network. It is assumed that the industrial plant runs at constant capacity throughout the year, thus, the total amount of excess heat that can be delivered to the two heat sinks is constant. Heat pumps could be used to boost heat supply to the carbon capture unit by recovering low-grade excess heat discharged from the industrial plant, as suggested by Andersson et al. (2016). It could also be possible to recover low-grade residual heat from the carbon capture unit itself, as discussed in, e.g., Andersson (2020) and Hammar (2022). This was, however, beyond the scope of this study and should be investigated in future work.

When discussing the utilization of excess heat, it is also important to adopt a proper definition of the term. Olsson et al. (2015) define excess heat as “Excess energy that cannot be utilized internally and where the alternative is that the heat is released into the surroundings”. Bendig et al. (2013) discuss the important distinction between avoidable and unavoidable excess heat. Pettersson et al. (2020) propose adopting a pragmatic techno-economic perspective whereby avoidable excess heat refers to heat that could be reused internally within the process through heat recovery measures that meet the plant owner’s investment performance criteria. The latter definition is adopted in this work and the term “available excess heat” refers to the excess heat that is available for utilization in the CO_2 capture plant under given conditions.

2. Method

Fig. 1 provides an overview of the studied system and the system boundaries considered for different parts of the analysis. To evaluate the potential of different strategies for heat delivery to a CCS unit and a district heating network, two studies were conducted: a generic study that illustrates the effects of the main system characteristics, and a case study that uses real plant data. The generic study determines how the magnitude of excess heat over time affects the suitable choice of design and operation of the capture plant. To estimate the size and performance of the CO_2 capture equipment, a design study was carried out, which included simulations of the capture plant and the compression sequence using Aspen Plus software (v11). Furthermore, an economic assessment was performed, including a sensitivity analysis with respect to key parameters, to compare the economic performance of the heat recovery options. In the case study, the methodology was applied using input data based on historical seasonal variations of excess heat from a steel mill and its integrated off-gas fired CHP plant, and a comparison between prioritizing the district heating network or the CO_2 capture plant as recipient of the excess heat was conducted.

2.1. Setup of the generic study

Five theoretical heat load curves (Fig. 2) were considered in the generic study. The heat displayed in these curves represents the excess heat available at the industrial site for CCS after delivery of heat to the district heating network. Since the district heating demand is low during summer, the peak value is the maximum amount of heat available from the industrial plant. The curves were generated using Eq. (1), in which the two main parameters are the maximum amount of available heat, MH (MW), and the length of the season during which excess heat is available for CCS, SL (hours).

$$y = MH\cos\left(\frac{\pi}{SL}(x - 4380)\right) \tag{1}$$

The seasonal length of the theoretical heat load curves, shown in Fig. 2, was defined as either short season (Curve 2; excess heat available May-August, 2952 h), medium-long season (Curves 1, 4, and 5; heat available March-October, 5880 h) or long season (Curve 3; heat available all year, 8760 h). The peak of the heat load curves, i.e., the

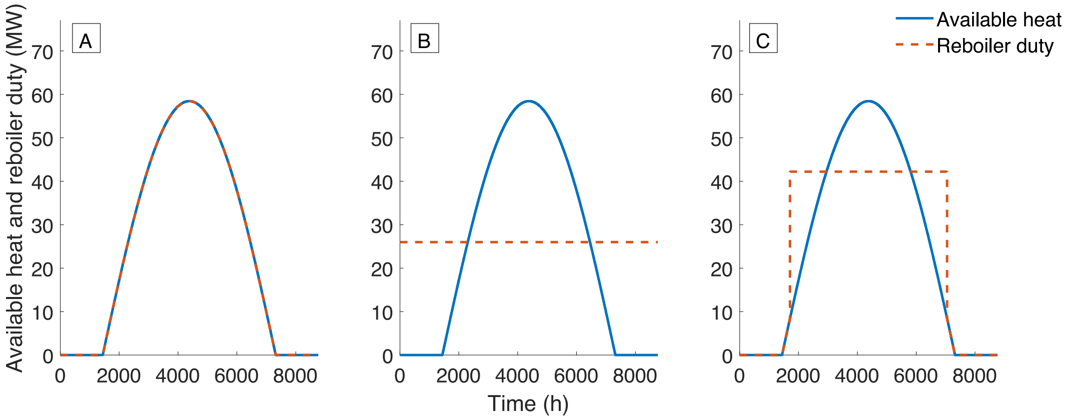

Fig. 3. Illustration of Configurations A, B and C for heat load curve 1.

Table 1
Flue gas specification used in the generic study (adapted from Onarheim et al. (2017)) and the case study (adapted from Biermann et al. (2019)), respectively.

Component/ property	Unit	Generic study	Case study (BFG)
CO_2	mol%	13.0	24.6
H_2O	mol%	17.0	2.2
N_2	mol%	67.7	49.6
O_2	mol%	2.3	0
CO	mol%	0	20.4
H_2	mol%	0	3.2
T	°C	184	29
P	kPa	101.3	181.3
Flow	kNm^3/h	50-497	352.4

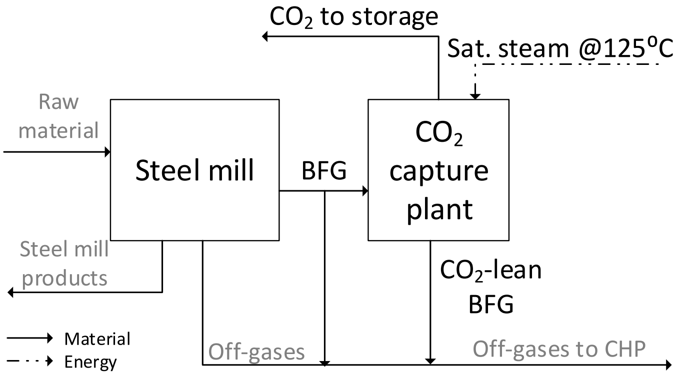

Fig. 4. Overview of the integration between the steel mill, the CO2 capture plant and the CHP plant considered in the case study. The material and energy flows of interest for the study are marked in black, others are grey. BFG = Blast Furnace Gas.

maximum amount of available heat, was defined on the basis of the heat input (MW) to the capture plant reboiler required to achieve a design capture rate of 100, 500 or 1000 kton CO_2/year (12, 58 and 117 MW), corresponding to capture rates of 11, 57 and 114 t CO_2/h respectively.

For each of the 5 excess heat load curves, three CCS plant configurations (i.e. plant size combined with plant operating strategy) were defined as follows and illustrated in Fig. 3:

(1) Configuration A: carbon capture capacity determined by the peak value of available heat, and operated at varying capture rate throughout the year, depending on the availability of excess heat as determined by the heat load curve.
(2) Configuration B: the carbon capture plant operates at constant capture load throughout the year, and is sized to achieve the same annual capture rate as Configuration A.
(3) Configuration C: designed for hybrid operation, i.e. constant capture rate during some parts of the year and reduced capture rate during other parts of the year (following the heat load curve). The capture plant size was set as the average of the plants sizes of Configurations A and B, and the length of the constant capacity operation was adjusted to achieve the same yearly capture rate as in A and B.

Operation for Configurations B and C results in a heat deficit during some parts of the year, which was assumed to be covered by heat generated by combustion of biomass (with assumed CO_2 emissions of 0 g CO_2/MJ_{fuel} and a fuel-to-heat efficiency of 90%). The energy penalty of these configurations was estimated by dividing the primary energy supply (heat supply by combustion of additional fuel) to the total heat input to the capture plant. The degree of utilization of each capture plant was estimated according to Eq. (2). The configurations were compared based on the trade-off between energy penalty and degree of utilization. Assuming a carbon neutral make-up fuel illustrates the best-case scenario, where the carbon dioxide mitigation potential of the capture plant is not affected by its energy demand.

$$Degree\ of\ utilization\ (\%) = \left(\frac{Actual\ capture\ rate\ (kton/a)}{Design\ capture\ rate\ (kton/a)} \times 100\right) \quad (2)$$

The assumed characteristics of the flue gas in the generic study are specified in Table 1. The flue gas composition was determined such that the two following criteria were fulfilled:

(1) CO_2 concentration somewhere in the middle of the normal range of CO_2 content in industrial flue gases, i.e. 5-30 vol%.
(2) Representative values for concentration of other common species such as H_2O and O_2.

The composition, as well as the temperature and pressure, were therefore based on values for the flue gas from a pulp mill recovery boiler, adopted from Onarheim et al. (2017), which fulfills the two criteria described above. The flue gas flow rate was varied to correspond to 100, 500 or 1000 kton/a of captured CO_2 for design point operation, assuming a capture rate of 90%.

2.2. Case study: SSAB integrated steel mill in Luleå

The case study is an integrated steel mill located in Luleå in northern Sweden owned by SSAB with direct plant emissions of about 3.4 $MtCO_2$/a. The most important emitter is the blast furnace, where iron ore is reduced to pig iron using coke or coal, and blast furnace gas (BFG),

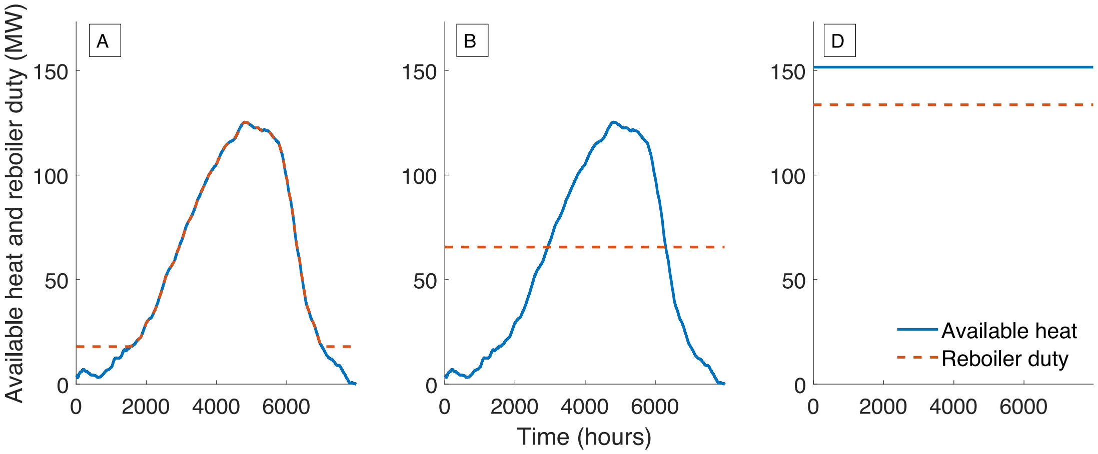

Fig. 5. Available heat and reboiler duty for configurations A, B and D respectively in the case study. Heat load curves were based on the work by Martinez Castilla et al. (2019).

Table 2
Characteristics of the capture plant configurations evaluated in the case study. DH = district heating.

Configuration	A	B	D
Capture plant size criteria	Corresponding to peak amount of available heat	To achieve equal CO_2 avoidance as Conf. A	Corresponding to peak amount of available heat
Design capture rate	144 t/hr	76 t/hr	154 t/hr
Operation	Varying	Constant	Constant
Reboiler duty	Max 125 MW	66 MW	134 MW
DH supply	Unchanged	Unchanged	Decreased
CO_2 avoided	< CO_2 captured	< CO_2 captured	Equal to CO_2 captured

containing considerable amounts of both carbon dioxide and carbon monoxide, is produced as a by-product. In the integrated CHP plant, off-gases (mainly BFG) from the steel mill are combusted to generate process steam, electricity, and district heating.

2.2.1. *Studied system*

Fig. 4 shows the integration between the steel mill, the CHP plant and the CO_2 capture plant considered in this work. The CO_2 capture plant is located downstream from the steel mill but upstream from the CHP plant. Carbon dioxide is assumed to be captured from the blast furnace gas, since previous studies (see e.g. Biermann et al. (2019)) have pointed out the benefits of capturing carbon dioxide from the blast furnace gas directly instead of applying capture to the flue gas stream after the boiler in the CHP plant, thus, partial capture of the site emissions is applied. The blast furnace gas characteristics are listed in Table 1. Please note that the CO_2 concentration and total pressure are higher than in the generic study; high CO_2 concentration and total pressure both have a positive effect on CO_2 separation energy required. Depending on the availability of heat, either all of the blast furnace gas, or only part of it, is lead through the capture plant, otherwise it is fed directly to the CHP plant together with the rest of the steel mill off-gases. After CO_2 has been captured, the CO_2-lean blast furnace gas is also sent to the CHP to be combusted. In the CHP plant, it is assumed that steam can be extracted at suitable conditions for heat supply to the CCS plant (125°C, saturated).

2.2.2. *Definition of heat load curves and configurations*

The heat load curve of available heat was determined based on data from Martinez Castilla et al. (2019). All heat delivered to the district heating network was considered as excess heat, and the maximum amount of available heat was calculated from the district heat peak delivery (about 160 MW). In the CHP plant, heat is transferred to the district heating network through two condensers in series, where steam (at 81°C and 95°C, respectively) from the steam turbine is condensed to supply heat to the district heating water. Since the steam utilized for district heating is at lower pressures than the pressure suitable for CCS supply, the amount of available heat was corrected to the pressure required for CCS, resulting in a maximum of about 150 MW of excess heat available for CCS.

Fig. 5 shows the heat load curve and reboiler duty for the configurations evaluated in the case study. The seasonal length was assumed to be equal to the steel mill operating hours (7972 h/a) (Garðarsdóttir et al., 2018). The characteristics of the case study configurations are described hereinafter and summarized in Table 2. Since the district heating demand was around 25 MW during the summer, the peak amount of available heat for Configurations A and B was set to 125 MW (instead of 150 MW available without DH generation). In addition to Configurations A and B, an additional configuration was defined (Configuration D) in which it was assumed that the district heating network only receives excess heat if the CCS demand has been satisfied. Configuration C was not evaluated in the case study. Furthermore, for Configuration A, the capture plant was assumed to operate at a minimum-heat level during periods of little to no available excess heat, since in practice, it may be desirable to avoid shutting down operation of the capture plant (Martinez Castilla et al., 2019). To compensate for the heat deficit in Configurations A and B, combustion of additional natural gas was assumed with an efficiency of 90% (fuel-to-heat) and a CO_2 emission factor of 50 gCO_2/MJ_{fuel} (Song et al., 2004). A fossil fuel was chosen to illustrate the effect of non-carbon neutrality, since it is common that industrial plants use fossil make-up fuels. The capture plant of Configuration B was sized to achieve the same CO_2 avoidance as the capture plant of Configuration A, i.e. the amount of captured CO_2 minus the emissions originating from the additional combustion of fossil fuels. For Configuration D, 134 MW of heat was utilized at a constant load all year, since that amount of heat corresponded to capturing 90% of the CO_2 in the blast furnace gas. Thus, the heat required for maximum capacity of CCS is lower than the maximum amount of available excess heat, enabling a small district heating supply to be maintained for Configuration D as well. However, the effect of the capture plant integration on the CHP outputs were not taken into consideration when evaluating the CO_2 avoided (i.e., CO_2 avoided was equal to CO_2 captured in Configuration D). Although Configuration D imposes a large change in the potential to supply district heating from the steel mill, the loss in district heating supply was not accounted for in the analysis. Furthermore, extracting steam at a higher pressure (see Equation (3)) implies a loss of electric power output from the CHP plant, which can also lead to

Table 3
Simulation specifications, common for all simulations.

Capture plant	Unit	
Absorber packing height	m	20
Stripper packing height	m	15
Lean/rich heat exchanger hot inlet/cold outlet ΔT	°C	10
Stripper overhead pressure	bar(a)	2
Compression sequence		
Discharge pressure compressor 1/2	bar(a)	6.3/20
Intercooling exit temperature	°C	25

Table 4
Simulation specifications applied in the generic study and the case study, respectively. Lean loading and reboiler temperature were optimized to achieve the lowest specific heat input.

Property	Unit	Generic study	Case study
Lean loading	mol CO_2/mol MEA	29	30
Reboiler temperature	°C	121.4	120.9
Lean solvent supply temperature	°C	40	29

Table 5
Assumptions for the economic assessment.

CAPEX		
Cost year	2016	
First- or N:th-of-a-kind	N:th of a kind	
Greenfield or Brownfield	Brownfield	
Location factor	1	
Annualized factor	10.8067	
Plant lifetime	years	25 (including 2 years construction)
Discount rate	%	7.5
Currency conversion[1]	NOK/€	9.7
OPEX		
Fixed OPEX	% of TIC	6
Variable OPEX		
Electricity price[2]	€/MWh	40
Biomass cost[3]	€/MWh_{steam}	20
Natural gas cost[4]	€/MWh_{steam}	18
Cooling water	€/m^3	0.02
MEA	€/m^3	2000
NaOH[3]	€/t	270
Steam[5]	€/t	1

[1] Used in the capture plant CAPEX assessment (2.4.1) since the method by Ali et al. (2019) was developed for NOK.

[2] Average electricity price. The seasonal variations of electricity prices were accounted for as described in 2.4.3.

[3] Used in the economic assessment of the generic study.

[4] Tax-free import price, no distribution cost included. Used in the economic assessment of the case study.

[5] Used in the economic assessment of the case study.

higher emissions depending on alternative grid power plant technology used to compensate for this. If new district heating and/or electricity generation would imply additional carbon emissions, the CO_2 avoided would be smaller than the CO_2 captured also for Configuration D.

2.3. CO_2 capture modeling

The modeling of the CO_2 capture plant, including compression stages up to 20 bar(a) for liquefaction (see boundaries in Fig. 1) was performed using Aspen PLUS v11 simulation software. The capture plant is an absorption-desorption cycle with 30 wt% of MEA as solvent, and the set-up includes rich-solvent splitting (RSS) and absorber intercooling (ICA), based on the work by Garðarsdóttir et al. (2015) and Biermann et al. (2018). The absorber intercooler was only included in the case study, since the addition of ICA has mainly proven important for flue gases with high CO_2 concentrations (Biermann et al., 2018). The direct contact cooler (DCC) was only included in the generic study, since the purpose of the unit is the reduce the water content in the flue gas, as well as to provide cooling prior to the absorber, and the flue gas used in the case study already had low water content and temperature (cf. Table 1).

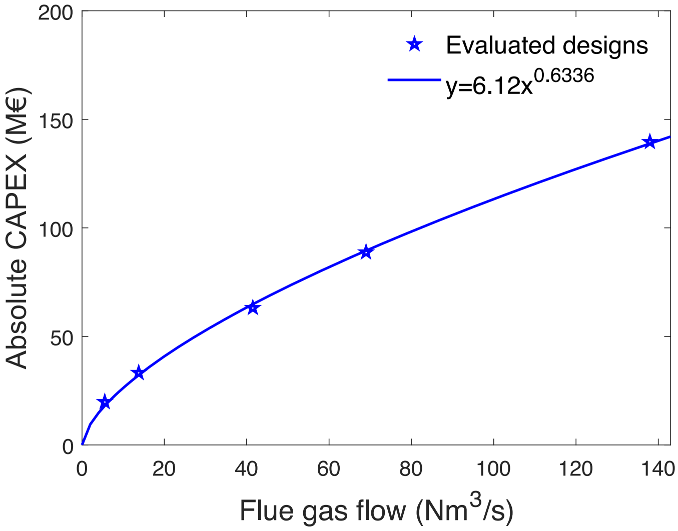

Fig. 6. CAPEX (M€) as a function of flue gas flow (Nm3/s). The CAPEX was evaluated for five designs (indicated by the star symbols), to which a power function was fitted to set up the cost function.

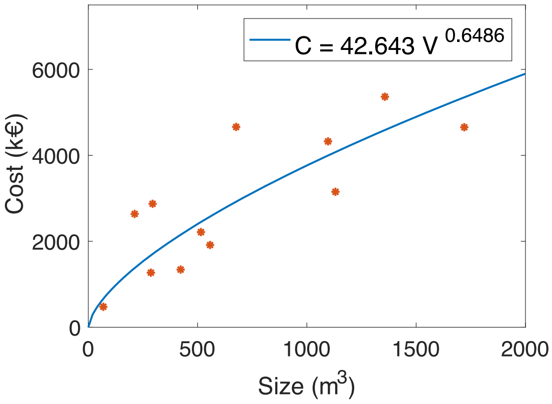

Fig. 7. Cost function for columns, including internals, material: welded SS316. The red dots represent column costs estimated in previous work (Biermann et al., 2019; Gardarsdottir et al., 2019; van der Spek et al., 2017). The blue line shows the power function fitted to the data points. The sizing parameter (V) for columns is the volume in m3.

The CO_2 compression was modeled using the Peng-Robinson with Boston-Mathias extrapolation as vapor property method (Mazzoccoli et al., 2012). The pressure was set to obtain a transport pressure of 7 bar (a) after the liquefaction plant (Deng et al., 2019). Other relevant design specifications of the CO_2 capture and liquefaction plant are listed in Tables 3 and 4, with the latter specifying conditions that generated the lowest specific reboiler duty (i.e. heat input per amount of captured CO_2) for the generic study and the case study respectively. The capture plant was designed for a 90% separation rate in the absorber. This target was achieved by adjusting the lean solvent flow, and the column diameters as well as the main dimensions of other equipment were calculated based on design point simulations. Off-design simulations were also carried out, in which the performance of the capture plant was

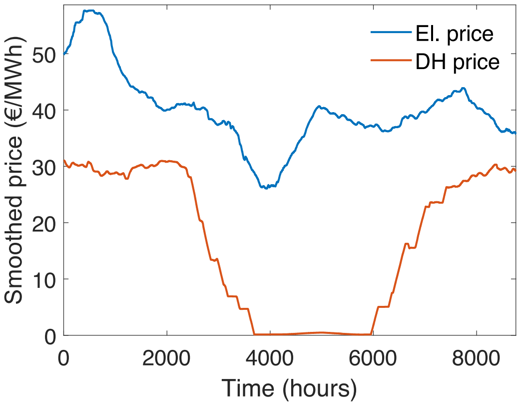

Fig. 8. Seasonally varying electricity prices (blue) and district heating prices (red).

estimated for absorber separation rates of <90%, corresponding to varying heat input to the reboiler.

2.4. Economic assessment

Key assumptions for the economic assessment are listed in Table 5. The CAPEX estimation for the capture plant is described in 2.4.1, and for the compression sequence and liquefaction plant in 2.4.2. In the generic study, the total CAPEX (capture plant, compression sequence and liquefaction plant) was set as a function of the flue gas flow, according to Fig. 6, by estimating the cost of five designs (indicated by star symbols), to which a power function was fitted.

2.4.1. Capture plant

For the capture plant, the cost of the equipment was estimated using sizing parameters. A detailed flow sheet and an equipment list over all included equipment pieces for two evaluated designs can be found in Appendix A. The equipment cost was calculated by equipment-specific cost estimation power functions, which were set up based on cost estimations in previous work (Biermann et al., 2019; Gardarsdottir et al., 2019; van der Spek et al., 2017). For example, the power function used to estimate the cost of columns is displayed in Fig. 7, while the cost functions for other equipment can be found in Appendix B. The equipment installed cost (EIC) was estimated using the enhanced detailed factor (EDF) method as described by Ali et al. (2019). In the EDF method, different factors for direct costs, engineering costs, administration costs, commissioning and contingency are applied based on the absolute value of the equipment cost. The total installed cost (TIC) of the capture plant were obtained by summation of the EIC of individual equipment. The cooling, heating and power duties, as well as the consumption of chemicals (MEA, NaOH) included in the evaluation of operational expenditures (OPEX) were based on the simulations.

2.4.2. Liquefaction plant

For the liquefaction plant, the total direct cost (TDC) was estimated as a single unit by scaling the costs derived by Deng et al. (2019) to the CO_2 flow in this work. The TIC was then obtained by multiplying the TDC with factors for process and project contingency, indirect cost and owner cost in accordance with the method described in Deng et al. (2019). The TIC for the liquefaction plant is equal to the total CAPEX since one single unit is assumed. The compressor duties, and the duties of the intermediate cooling, were obtained from the simulations. The duties for other equipment in the liquefaction plant was estimated based on the work by Deng et al. (2019) by scaling their results to the compression duties and duties of intermediate cooling from the simulations carried out in this work.

2.4.3. Operational expenditures

Assumptions for fixed and variable OPEX, independent of season, are given in Table 5. Seasonally varying electricity prices and district heating prices are given in Fig. 8. The electricity prices are the moving average over 720 h (one week) of spot prices in Sweden (average of SE1-4) in 2019 (NordPool, 2019). The district heating prices are moving averages over 720 h of marginal heat generation cost for the city of Gothenburg, as modelled according to Romanchenko et al. (2020). The seasonally varying electricity price was applied when evaluating the total cost of electricity for the CO_2 capture and liquefaction plant in both the generic study and the case study. The potential loss of revenue due to reduced electric power output from the CHP was however not taken into account as an expense allocated to the capture plant in the case study. The district heating price is important as district heating is the alternative use of the heat used for CCS, and was taken into account in the economic assessment of Configuration D in the case study (cf. Fig. 5), since that configuration imposed a large change to potential to supply district heat. In the generic study, the steam cost was assumed to be zero if only available heat was used, and equal to the fuel cost, (i.e. biomass price divided by fuel-to-heat efficiency), if primary energy was supplied. In the case study, the cost of steam applied when available heat was used was 1 €/t steam, based on the work by Biermann et al. (2019). If primary energy was used, the steam cost was equal to the cost of natural gas (natural gas price divided by fuel-to-heat efficiency).

Table 6
Key performance indicators for Configurations A, B and C (cf. Fig. 3) evaluated in the generic study.

Heat load curve	Heat capacity (MW)	Seasonal length (h)	Configuration	Captured CO_2 (kton/a)	Degree of utilization (%)	Energy penalty (%)
1	58	5880	A/B/C	222	45/100/62	0/43/17
2	58	2952	A/B/C	112	22/100/37	0/67/26
3	58	8760	A/B/C	331	66/100/80	0/22/10
4	117	5880	A/B/C	445	45/100/62	0/43/17
5	12	5880	A/B/C	44	45/100/62	0/43/17

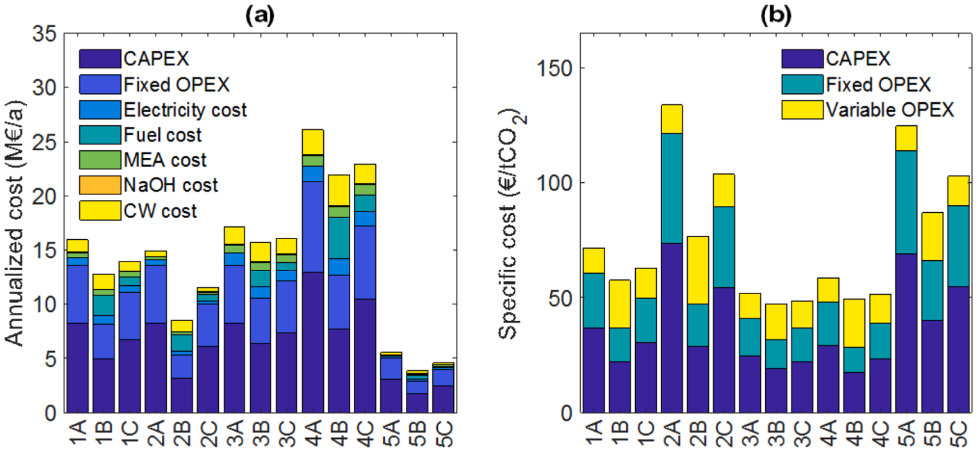

Fig. 9. Economic assessment of the generic study. (a) Annualized cost (CW = cooling water). (b) Specific cost of each configuration.

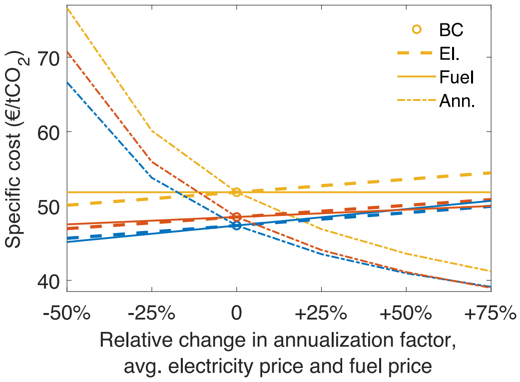

Fig. 10. Sensitivity analysis of the economic assessment of configurations related to curve 3. Investigated parameters are average electricity price (El.), fuel price (Fuel) and annualized factor (Ann.). Configuration A results in yellow, configuration B results in blue and configuration C results in red. The starting point (base case, BC) for each configuration is indicated by the circles.

3. Results

3.1. Generic study

Table 6 shows an overview of key performance indicators for the different configurations depending on the characteristics of the heat availability. Since heat load curves 1, 4 and 5 have the same seasonal length, the degree of utilization and energy penalty is also equal between the corresponding configurations. Comparing curves of different seasonal lengths, it is clear that the seasonal length has an important impact on the degree of utilization obtained for the different configurations, since e.g. a shorter season leads to a smaller capture rate than a longer season. The seasonal length also affects the energy penalty since a longer season implies less need for additional energy supply.

3.1.1. Annualized cost

Fig. 9(a) displays the annualized cost for all evaluated configurations in the generic study. Configuration B has the lowest cost for all investigated heat load curves, which shows that regardless of the excess heat availability, it is more expensive to have a low utilization of the capture plant than of the energy supply system. The effect of the season duration is seen by comparing the results for heat load curves 1- 3. A short season with low district heating demand (heat load curve 2) results in larger differences between the plant sizes, and thus their costs, between configurations, since the degree of utilization of Configurations A and C are lowest for heat load curve 2. Conversely, a long season (heat load curve 3) reduces the differences in utilization between configurations. The effect of economy of scale can be clearly seen by comparing heat load curves 1, 4 and 5, which have the same seasonal length.

3.1.2. Specific cost

Fig. 9(b) shows the specific cost for the configurations evaluated in the generic study. The degree of utilization is clearly reflected in the specific CAPEX: for configuration A, the specific CAPEX is a larger contributor to the total specific cost than for B and C configurations. Note that Fixed OPEX is a factor of the TIC and, thus, responds to the

Table 7
Key performance indicators for the configurations investigated in the case study. The energy penalty for configuration A arises from combustion of natural gas during periods of little or no available excess heat, to avoid having to shut down the capture plant.

Heat load curve	Configuration	Captured CO_2 (kton/a)	Avoided CO_2 (kton/a)	Avoided CO_2 (% of site emissions)	Degree of utilization (%)	Energy penalty (%)
SSAB	A/B	567/603	562	17	49/100	5/39
SSAB	D	1228	1228	36	100	0

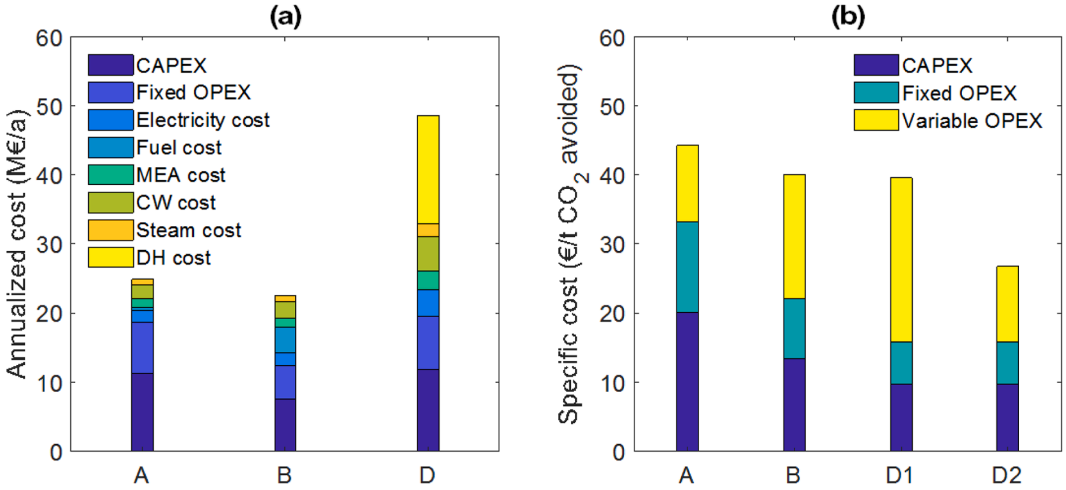

Fig. 11. Economic assessment for the case study configurations. (a) Annualized cost (CW = cooling water, DH = district heating). (b) Specific cost. Configurations A and B have different capture rates but equal CO2 avoidance.

same factors as CAPEX. Short season (heat load curve 2) and small peak of available heat (heat load curve 5) both lead to increased specific costs. In addition, for heat load curves 2 and 5, the specific cost is more sensitive to the choice of configuration compared to other curves. Having either a long season (heat load curve 3) or a high peak of available heat (heat load curve 4) results in similar specific costs, with a long season being slightly less expensive as well as less sensitive to the choice of configuration (i.e. specific costs are more similar among configurations).

3.1.3. *Sensitivity analysis*

Fig. 10 shows the sensitivity analysis conducted for Configurations A, B and C for heat load curve 3. The sensitivity is shown for heat load curve 3 as the corresponding configurations had a relatively similar performance for this profile. The sensitivity analysis indicates that configuration A is the most expensive for all cases, although favored by reduced CAPEX and increased fuel price. To achieve break-even costs, Configurations B and C require a 50% increase in annualized factor or around a 35% increase in fuel price.

3.2. *Case study: SSAB integrated steel mill in Luleå*

Table 7 shows the key performance indicators for the configurations investigated in the case study. The performance is similar to the corresponding configurations of heat load curve 4 in the generic study, since both curves have high peak amounts of available heat. Furthermore, even though the seasonal length for the SSAB curve is 7972 h, for a considerable part of the season, the amount of available heat is very low and thus, in reality, the season becomes comparable to the intermediate season length in the generic study. This is reflected by the similarities in degree of utilization of Configuration A, and in energy penalty for Configuration B.

3.2.1. *Annualized cost*

The annualized costs for the configurations evaluated in the case study are displayed in Fig. 11(a). The annualized costs of Configurations A and B are similar to the ones for heat load curve 4 in the generic study, which is reasonable since both have large peak amounts of available heat. Configurations A and D have almost the same size, which leads to similar values for CAPEX and fixed OPEX. In Configuration D, however, the degree of utilization is higher and thus also the variable OPEX, especially considering that the loss in district heating revenue is accounted for as an expense allocated to the capture plant. For Configuration A, the lower degree of utilization results in CAPEX and fixed OPEX that represents almost 80% of the total annualized cost, while the corresponding share for Configuration B is around 50%.

3.2.2. *Specific cost*

Fig. 11(b) shows the specific costs for the configurations evaluated in the case study. As in the generic study, Configuration B has a lower specific cost than Configuration A. The specific cost of Configuration D is displayed in two ways; D1 in which the loss of district heating revenue is taken into account, and D2 in which it is not accounted for, with the purpose of clearly illustrating the impact of the district heating revenue on the economic assessment of the capture plant. Configuration D2 shows the lowest specific cost of all configurations. When the loss of district heating revenue is taken into account (D1), the difference between configurations is not as pronounced.

4. Discussion

4.1. *Site specific implications*

Site specific conditions will have an impact on the cost and feasibility of implementing CO_2 capture. The economic assessment carried out in the generic study (cf. Fig. 9) showed that both scale (i.e. how large the point source of CO_2 is, reflected in the peak of available heat in this work) and season length are important site-specific parameters to consider when evaluating the potential for integration of CCS and district heating. Adopting a seasonally varying operation might be feasible for a large-scale point source with long season, i.e. high availability of heat. This option might be considered if it is desired to retain the district heating supply initially, while having the opportunity to scale-up CCS operation if carbon prices rise. In that sense, implementing a capture plant with low degree of utilization has an advantage, since scale-up of operation of a capture plant with high degree of utilization is not possible without investment in additional CO_2 capture facilities. However, for a smaller point source, or a short season, it is clear that applying a low degree of capture plant utilization is by far the costliest option, thus in that case, such configuration should be avoided. The cost for transport and storage of CO_2 have not been considered in this work. However, these costs would pose a challenge for plants with low capture rate since they are also favored by economy of scale (Roussanaly et al., 2021).

Furthermore, even though a value for the CO_2 intensity of natural gas was considered in the design and economic assessment in the case study, make-up fuels used at industrial plants might have even higher CO_2 intensities (e.g. if oil or coal is used). If higher CO_2 intensities are considered, an increase in both CAPEX and OPEX for a plant with high degree of utilization would be required in order to achieve the same CO_2 avoidance as a capture plant that is operated following the seasonal variations in available heat, which may cause a shift in which the most favorable option is in terms of specific cost. Additionally, to generate steam from combustion of biomass to supply heat to the CO_2 capture plant could require large amounts of scarce resources (Biermann et al., 2019; Karlsson et al., 2021). Hence, it is important to consider the type of energy supply available for CO_2 capture, both with respect to the CO_2 avoidance potential and with respect to the competition of resources, which again supports the conclusion of the advantage of utilizing any available excess heat.

4.2. Utilization

The results from both the generic study and the case study showed that a low plant utilization (Configuration A) is not economically competitive compared to supplying additional primary energy when needed (Configuration B, i.e. low utilization of the available excess heat in the plant energy system), cf. Figs. 9 and 11. Although, the sensitivity analysis (cf. Fig. 10) showed that if the price of fuel for primary energy supply increases significantly (~80-100%), it would become competitive to decrease the utilization of the capture plant. It should be noted, however, that the sensitivity analysis was carried out for the configurations of heat load curve 3, i.e. the curve with the least differences in specific cost among configurations, and the overall highest degree of capture plant utilization. Hence, it is not evident that similar results would be obtained for the other heat load curves, with lower degrees of capture plant utilization.

Furthermore, additional energy supply was considered a utility, i.e. costs associated with additional heat supply capacity were not considered. This assumption implies an excess capacity in the current industrial energy system, which is not necessarily the case. A low utilization of the available excess heat may, thus, result in an increase in the cost of energy not reflected in the present work. Biermann et al. (2021) identified possibilities to utilize both excess heat and excess capacity for CO_2 capture at a refinery and emphasized the importance of considering the potential in the existing plant energy system for cost-efficient implementation of CO_2 capture. Another aspect to consider is that, in the case study, a maximum of 36% of direct plant emissions were captured. Under the assumption that all fossil CO_2 emissions must be eliminated, the energy system at the industrial plant might have to be extended with new infrastructure regardless of the current amount of available excess heat.

4.3. Definition of excess heat

If carbon neutrality is seen as a necessity for industry, the capture plant should reasonably be considered as an internal part of the industrial plant to offset fossil emissions. Hence, since the term excess heat refers to heat that cannot be utilized for internal heat integration, it would be more appropriate to consider that all heat that could be used for CCS is not excess heat. Hence, in contrast to how the term excess heat has been used in other studies related to heat supply to a CCS unit (e.g. Andersson et al. (2016); Biermann et al. (2019)), the term would then refer to heat that cannot be utilized for CCS due to insufficient temperature levels, and/or heat that can be recovered from the capture plant for external heat supply. By adopting such definition, the potential to supply district heating from industrial plants would be highly affected. However, a previous study by the authors has shown that the potential to recover heat from the capture plant for district heating purposes can be significant (~25% of the amount of heat supplied to the CCS unit) (Eliasson et al., 2021). Another consequence of re-defining excess heat is that the energy penalty that was allocated to the capture plant in this study would instead be allocated to the district heating network, which would make constant operation of the capture plant even more favorable compared to the alternatives. However, since there may still be a lack of incentives for implementing CCS, to not be able to supply district heating would cause economic losses for the industrial plant, and potentially increased emissions elsewhere depending on the technology used to replace the heat. When considering the economic impact of lost district heating supply in the case study, implementing CCS with retained district heating supply was seen to have comparable specific capture cost to the configuration where CCS was prioritized (cf. Fig. 11(b)). Thus, it is feasible to apply a capture plant with seasonally varying operation, i.e., low degree of utilization, and retain the district heating supply. The advantage of such an investment is the potential to scale-up operation, since all CO_2 emissions will have to be avoided in order to reach the target of net-zero emissions.

5. Conclusion

In this work, process simulations and an economic assessment of an amine-based CO_2 capture plant were conducted to investigate the interplay between usage of available excess process heat to provide heat for CO_2 capture at the plant site and supplying heat to a district heating network. Different heat load curves, representing seasonal variations of excess heat availability for CO_2 capture, were considered to investigate the relation between utilization of the capture plant and the heat supply system. The results showed that:

(1) The size of the CO_2 point source and the length of the period during which excess heat is available are important parameters for achieving cost-efficient co-integration of industrial carbon capture and district heating supply.
(2) A low degree of utilization of the capture plant has a more pronounced impact on the total annual cost than a low degree of utilization of the available excess heat. A significant increase in fuel prices (at least by 100%) is needed for seasonally varying operation of the capture plant to become economically competitive compared to the alternative of supplying primary energy, even when capture plant utilization is relatively high.
(3) Accounting for the loss of revenue from district heating supply when evaluating the cost of capture plant integration has a significant impact on the specific capture cost and can make seasonally varying operation comparable in cost to the alternative where CCS is prioritized for usage of excess heat (44 €/t CO_2 avoided for the former, 40 €/t CO_2 avoided for the latter). If maintaining the amount of district heating supplied is not prioritized, specific capture costs of 29 €/t CO_2 avoided can be achieved.

Declaration of Competing Interest

The authors declare that they have no known competing financial interests or personal relationships that could have appeared to influence the work reported in this paper

Acknowledgement

This work was conducted within the framework of the Preem CCS project with funding provided by Preem AB, SINTEF Energi AS, Aker Carbon Capture, Equinor, the Norwegian CLIMIT Programme and the Swedish Energy Agency.

Appendix A

Fig. 12 shows a detailed flow sheet of the CO_2 capture plant, including all equipment pieces for whom which individual costs were

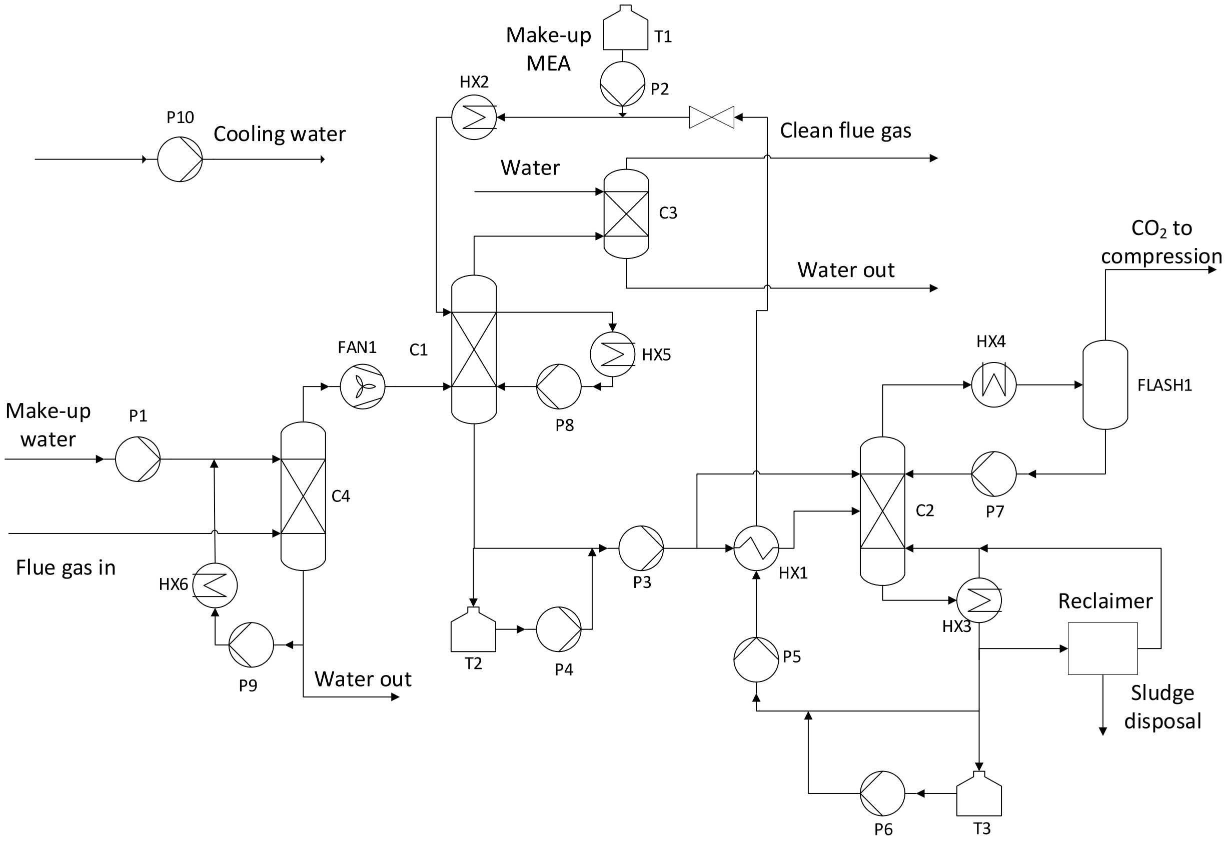

Fig. 12. Detailed flow sheet of the CO2 capture plant in this study.

Table 8
Equipment list describing the different pieces of equipment included in this work. Included designs are the one of Configuration A of heat load curve 4 in the generic study, and Configuration D in the case study. d = diameter, h = total height, KO = knock-out.

Equipment	ID	Type	Case study		Generic study	
			Size	EIC	Size	EIC
Columns			m^3	k€	m^3	k€
Absorber	C1	Packed column	1382 (d 7.9, h 28.5)	12218	2343 (d 10.2, h 28.5)	17202
Stripper	C2	Packed column	724 (d 6.6, h 21.4)	8032	630 (d 6.12, h 21.4)	7335
Washer	C3	Packed column	82 (d 7.9, h 1.7)	2601	378 (d 10.2, h 4.6)	6357
Direct contact cooler	C4	Packed column	-	-	765 (d 9.4, h 16.2)	8325
Heat exchangers			m^2		m^2	
Lean/ rich heat exchanger	HX1	Shell and tube	15107	9969	9799	8094
Lean solvent cooler	HX2	Shell and tube	2640	2680	2011	2089
Stripper reboiler	HX3	Reboiler	48444	32729	47035	31912
Stripper condenser	HX4	Shell and tube	1624	1718	1703	1794
Absorber intercooler	HX5	Shell and tube	4500	3973	-	-
DCC reflux cooler	HX6	Shell and tube	-	-	5886	5078
Pumps			kW		kW	
Water make-up	P1	Centrifugal	0.007	13	6	218
MEA make-up	P2	Centrifugal	0.001	3	0.03	30
Rich pump	P3	Centrifugal	48	619	71	781
Rich make-up	P4	Centrifugal	24	409	20	456
Lean pump	P5	Centrifugal	306	1301	251	1155
Lean make-up	P6	Centrifugal	31	470	25	417
Stripper reflux pump	P7	Centrifugal	3	146	3.4	158
Absorber intercooler pump	P8	Centrifugal	99.6	814	-	-
DCC reflux pump	P9	Centrifugal	-	-	97.1	802
Cooling water pump	P10	Centrifugal	976	2613	910	2507
Tanks			m^3			
MEA make-up	T1		10	292	60	743
Rich solvent make-up	T2		10	292	10	292
Lean solvent make-up	T3		10	292	10	292
Other						
Reclaimer			29 kg HSS/hr	2884	24 kg HSS/hr	2524
Condenser KO drum	FLASH1		65 m^3 (d 3.6, h 6.4)	784	46 m^3 (d 3.1, h 6.0)	621
Flue gas fan[1]	FAN1		349 kW	954	774	1353
Pre and post filter	-		-	76	-	76
Active carbon filter	-		-	217	-	217
MEA first fill[1]	-		532 m^3	1063	446 m^3	892

[1] Material: Carbon steel

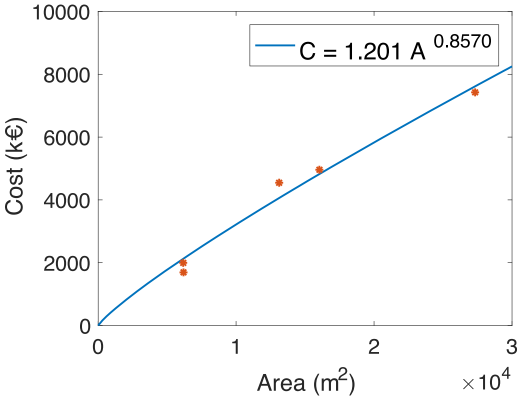

Fig. 13. Reboiler cost function, material: welded SS316. The sizing parameter (A) for the reboiler is the total heat exchanger area (m2).

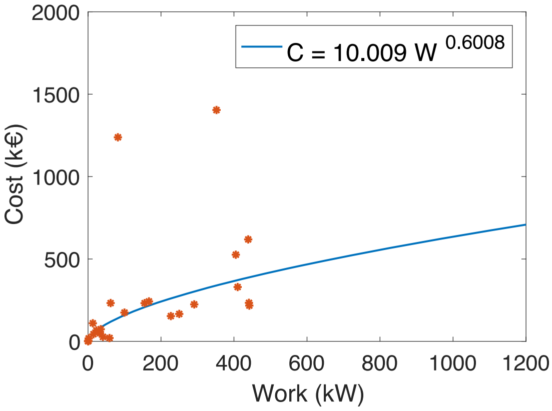

Fig. 14. Pump cost function, material: machined SS316. The sizing parameter (W) for pumps is the required work (kW).

estimated according to 2.4.1. Table 8 shows equipment lists for the capture plant of Configuration A of heat load curve 4 in the generic study, and the capture plant of Configuration D in the case study. Packing in columns is Sulzer Mellapak 250Y, and total height of columns is 1.425 times the packing height. The material is stainless steel for all equipment unless other is specified. Table 8 also includes the cost of MEA first-fill in the capture plant, which was estimated under the assumption of a MEA residence time of 40 min (Montañés et al., 2018).

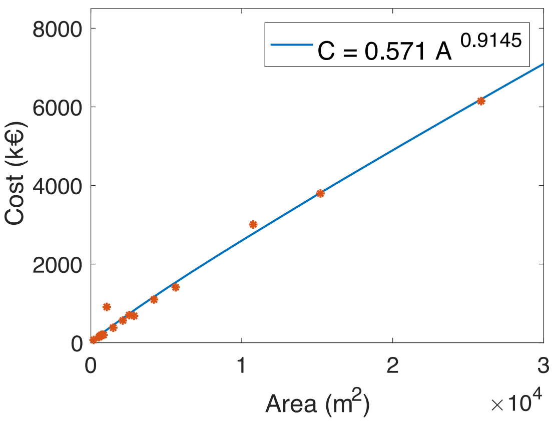

Fig. 15. Cost function for heat exchangers (other than reboiler), material: welded SS316. The sizing parameter (A) for the heat exchangers is the total heat exchanger area (m2).

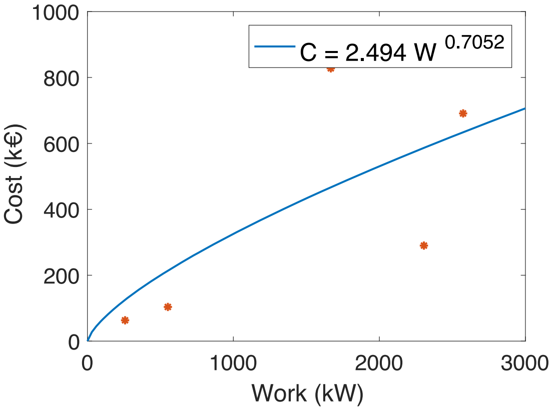

Fig. 16. Flue gas fan cost function, material: carbon steel. The sizing parameter (W) for the flue gas fan is the required work (kW).

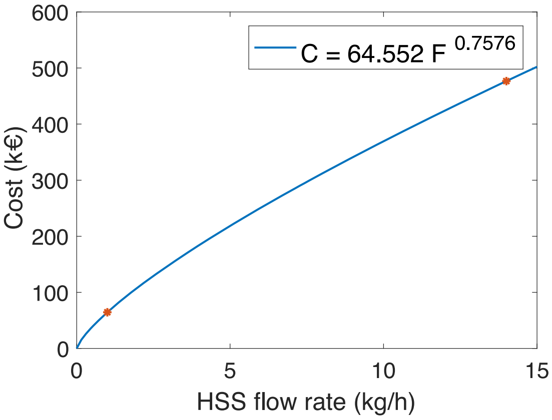

Fig. 17. Cost function reclaimer, material: welded SS316. The sizing parameter (F) for the reclaimer is the HSS flow rate (kg/h).

Appendix B

Figs. 7 and 13–17 shows the cost functions used for estimating the cost of the different equipment pieces in the capture plant, with equipment cost displayed on the y-axis and the sizing parameter displayed on the x-axis. The data points (red dots in the figures) from which the power functions are fitted to were gathered from equipment cost data from Biermann et al. (2019); Gardarsdottir et al. (2019); van der Spek et al. (2017), which were converted to a common cost year (2015) using the chemical engineering plant cost index (CEPCI). To estimate the TIC, the equipment costs of all individual equipment were estimated from the power functions using the sizing parameters as input. The equipment costs then needed to be converted to the desired cost year (2016 in this work). The EIC’s were obtained by multiplying the equipment costs with individual factors in accordance with the EDF method as described by Ali et al. (2019), whereby the TIC was obtained by summation of the EIC’s. Note that these cost functions give an order-of-magnitude estimate and are inferior to detailed case-by-case assessments using e.g. Aspen Process Economic Analyzer, however they serve the purpose of such high-level studies as this one.

References

Ali, H., Eldrup, N.H., Normann, F., Skagestad, R., Øi, L.E., 2019. Cost estimation of CO_2 absorption plants for CO_2 mitigation – method and assumptions. Int. J. Greenh. Gas Control 88, 10–23. https://doi.org/10.1016/j.ijggc.2019.05.028.

Andersson, J., 2020. An Investigation of Carbon Capture Technologies for Sävenäs Waste-To-Energy Plant. Department of Civil, Environmental and Natural Resources Engineering, Luleå University of Technology, Luleå, Sweden. MSc thesis report.

Andersson, V., Franck, P.Å., Berntsson, T., 2016. Techno-economic analysis of excess heat driven post-combustion CCS at an oil refinery. Int. J. Greenh. Gas Control 45, 130–138. https://doi.org/10.1016/j.ijggc.2015.12.019.

Bartela, L., Skorek-Osikowska, A., Kotowicz, J., 2014. Economic analysis of a supercritical coal-fired CHP plant integrated with an absorption carbon capture installation. Energy 64, 513–523. https://doi.org/10.1016/j.energy.2013.11.048.

Bendig, M., Maréchal, F., Favrat, D., 2013. Defining "Waste Heat" for industrial processes. Appl. Therm. Eng. 61 (1), 134–142. https://doi.org/10.1016/j.applthermaleng.2013.03.020.

Biermann, M., Ali, H., Sundqvist, M., Larsson, M., Normann, F., Johnsson, F., 2019. Excess heat-driven carbon capture at an integrated steel mill-considerations for capture cost optimization. Int. *J. Greenh. Gas Control* 91, 102833. https://doi.org/10.1016/j.ijggc.2019.102833.

Biermann, M., Langner, C., Eliasson, Å., Normann, F., Harvey, S., Johnsson, F., 2021. Partial capture from refineries through utilization of existing site energy systems. In: Proceedings of the 15th Greenhouse Gas Control Technologies Conference. https://doi.org/10.2139/ssrn.3820101.

Biermann, M., Normann, F., Johnsson, F., Skagestad, R., 2018. Partial carbon capture by absorption cycle for reduced specific capture cost. Ind. Eng. Chem. Res. 57 (45), 15411–15422. https://doi.org/10.1021/acs.iecr.8b02074.

Broberg Viklund, S., Johansson, M.T., 2014. Technologies for utilization of industrial excess heat: Potentials for energy recovery and CO2 emission reduction. Energy Convers. Manag. 77, 369–379. https://doi.org/10.1016/j.enconman.2013.09.052.

Connolly, D., Lund, H., Mathiesen, B.V., Werner, S., Möller, B., Persson, U., Boermans, T., Trier, D., Østergaard, P.A., Nielsen, S., 2014. Heat Roadmap Europe: Combining district heating with heat savings to decarbonise the EU energy system. Energy Policy 65, 475–489. https://doi.org/10.1016/j.enpol.2013.10.035.

Deng, H., Roussanaly, S., Skaugen, G., 2019. Techno-economic analyses of CO_2 liquefaction: Impact of product pressure and impurities. Int. J. Refrig. 103, 301–315. https://doi.org/10.1016/j.ijrefrig.2019.04.011.

Eliasson, Å., Fahrman, E., Biermann, M., Normann, F., Harvey, S., 2021. Integration of industrial CO_2 capture with district heating networks: a refinery case study. In: Proceedings of the TCCS-11 - Trondheim Conference on CO_2 Capture, Transport and Storage, pp. 197–201. Trondheim, Norway - June 22-232021.

Eriksson, L., Morandin, M., Harvey, S., 2018. A feasibility study of improved heat recovery and excess heat export at a Swedish chemical complex site. Int. J. Energy Res. 42 (4), 1580–1593. https://doi.org/10.1002/er.3950.

Feron, P.H.M., Cousins, A., Jiang, K., Zhai, R., Garcia, M., 2020. An update of the benchmark post-combustion CO_2-capture technology. Fuel 273, 117776. https://doi.org/10.1016/j.fuel.2020.117776.

Gardarsdottir, S.O., De Lena, E., Romano, M., Roussanaly, S., Voldsund, M., Pérez-Calvo, J.F., Berstad, D., Fu, C., Anantharaman, R., Sutter, D., Gazzani, M., Mazzotti, M., Cinti, G., 2019. Comparison of technologies for CO_2 capture from cement production-part 2: cost analysis. Energies 12 (3), 542. https://www.mdpi.com/1996-1073/12/3/542.

Gardarsdóttir, S.Ó., Normann, F., Andersson, K., Johnsson, F., 2015. Postcombustion CO_2 capture using monoethanolamine and ammonia solvents: the influence of CO_2 concentration on technical performance. Ind. Eng. Chem. Res. 54 (2), 681–690. https://doi.org/10.1021/ie503852m.

Garðarsdóttir, S.Ó., Normann, F., Skagestad, R., Johnsson, F., 2018. Investment costs and CO_2 reduction potential of carbon capture from industrial plants-a Swedish case study. Int. J. Greenh. Gas Control 76, 111–124. https://doi.org/10.1016/j.ijggc.2018.06.022.

Hammar, C., 2022. Heat integration between CO2 Capture and Liquefaction and a CHP Plant: Impact on Electricity and District Heating Delivery at Renova's CHP Plant in Sävenäs. Division of Energy Technology, Chalmers University of Technology, Göteborg, Sweden. MSc thesis project report.

Huang, Z., Li, J., Jing, C., An, H., Tong, Y., Xie, B., Zhao, Y., Li, C., 2017. Thermal integration of postcombustion CO_2 capture in existing natural gas combined cycle combined heat and power plant. J. Energy Eng. 143 (5), 04017025 https://doi.org/10.1061/(ASCE)EY.1943-7897.0000455.

IEA. (2020). *CCUS in clean energy transitions*. https://www.iea.org/reports/ccus-in-clean-energy-transitions.

Ivner, J., Broberg Viklund, S., 2015. Effect of the use of industrial excess heat in district heating on greenhouse gas emissions: a systems perspective. Resour. Conserv. Recycl. 100, 81–87. https://doi.org/10.1016/j.resconrec.2015.04.010.

Johnsson, F., Normann, F., Svensson, E., 2020. Marginal abatement cost curve of industrial CO_2 capture and storage – a Swedish case study. Front. Energy Res. 8, 175. https://doi.org/10.3389/fenrg.2020.00175.

Jönsson, J., Algehed, J., 2010. Pathways to a sustainable European kraft pulp industry: Trade-offs between economy and CO_2 emissions for different technologies and system solutions. Appl. Therm. Eng. 30 (16), 2315–2325. https://doi.org/10.1016/j.applthermaleng.2010.01.025.

Karlsson, S., Eriksson, A., Normann, F., Johnsson, F., 2021. CCS in the pulp and paper industry – implications on regional biomass supply. In: Proceedings of the 15th Greenhouse Gas Control Technologies Conference. https://doi.org/10.2139/ssrn.3820355.

Manz, P., Kermeli, K, Persson, U., Neuwirth, M., Fleiter, T., Crijns-Graus, W., 2021. Decarbonizing district heating in EU-27 + UK: how much excess heat is available from industrial sites? Sustainability 13 (3), 1439. https://doi.org/10.3390/su13031439.

Martinez Castilla, G., Biermann, M., Montañés, R.M., Normann, F., Johnsson, F., 2019. Integrating carbon capture into an industrial combined-heat-and-power plant: performance with hourly and seasonal load changes. Int. J. Greenh. Gas Control 82, 192–203. https://doi.org/10.1016/j.ijggc.2019.01.015.

Mazzoccoli, M., Bosio, B., Arato, E., 2012. Analysis and comparison of equations-of-state with p-?-T experimental data for CO_2 and CO_2-mixture pipeline transport. Energy Procedia 23, 274–283. https://doi.org/10.1016/j.egypro.2012.06.052.

Montañés, R.M., Flø, N.E., Nord, L.O., 2018. Experimental results of transient testing at the amine plant at technology centre mongstad: open-loop responses and performance of decentralized control structures for load changes. Int. J. Greenh. Gas Control 73, 42–59. https://doi.org/10.1016/j.ijggc.2018.04.001.

Möller, B., Wiechers, E., Persson, U., Grundahl, L., Søgaard Lund, R., Mathiesen, B.V., 2019. Heat roadmap europe: towards EU-Wide, local heat supply strategies. Energy 177, 554–564. https://doi.org/10.1016/j.energy.2019.04.098.

NordPool. (2019). *Historical market data: elspot prices 2019 hourly EUR*. https://www.nordpoolgroup.com/historical-market-data/.

Oh, S.Y., Binns, M., Cho, H., Kim, J.K., 2016. Energy minimization of MEA-based CO_2 capture process. Appl. Energy 169, 353–362. https://doi.org/10.1016/j.apenergy.2016.02.046.

Olsson, L., Wetterlund, E., Söderström, M., 2015. Assessing the climate impact of district heating systems with combined heat and power production and industrial excess heat. Resour. Conserv. Recycl. 96, 31–39. https://doi.org/10.1016/j.resconrec.2015.01.006.

Onarheim, K., Santos, S., Kangas, P., Hankalin, V., 2017. Performance and costs of CCS in the pulp and paper industry part 1: performance of amine-based post-combustion CO_2 capture. Int. J. Greenh. Gas Control 59, 58–73. https://doi.org/10.1016/j.ijggc.2017.02.008.

Pelda, J., Stelter, F., Holler, S., 2020. Potential of integrating industrial waste heat and solar thermal energy into district heating networks in Germany. Energy 203, 117812. https://doi.org/10.1016/j.energy.2020.117812.

Pettersson, K., Axelsson, E., Eriksson, L., Svensson, E., Berntsson, T., Harvey, S., 2020. Holistic methodological framework for assessing the benefits of delivering industrial excess heat to a district heating network. Int. J. Energy Res. 44 (4), 2634–2651. https://doi.org/10.1002/er.5005.

Rogelj, J., D. Shindell, K. Jiang, S. Fifita, P. Foster, V. Ginzburg, C. Handa, H. Kheshgi, S. Kobayashi, E. Kriegler, L. Mundaca, R. Séférian, M. V. Vilariño. (2018). Mitigation Pathways Compatible with 1.5°C in the Context of Sustainable Development. In Global Warming of 1.5°C. An IPCC Special Report on the impacts of global warming of 1.5°C above pre-industrial levels and related global greenhouse gas emission pathways, in the context of strengthening the global response to the threat of climate change, sustainable development, and efforts to eradicate poverty. [Masson-Delmotte, VP. Zhai, H.O. Pörtner, D. Roberts, J. Skea, P.R. Shukla, A. Pirani, W. Moufouma-Okia, C. Péan, R. Pidcock, S. Connors, J.B.R. Matthews, Y. Chen, X. Zhou, M.I. Gomis, E. Lonnoy, T. Maycock, M. Tignor, T. Waterfield (eds.)].

Romanchenko, D., Nyholm, E., Odenberger, M., Johnsson, F., 2020. Balancing investments in building energy conservation measures with investments in district heating-a Swedish case study. Energy Build. 226, 110353 https://doi.org/10.1016/j.enbuild.2020.110353.

Roussanaly, S., Berghout, N., Fout, T., Garcia, M., Gardarsdottir, S., Nazir, S.M., Ramirez, A., Rubin, E.S., 2021. Towards improved cost evaluation of carbon capture and storage from industry. Int. J. Greenh. Gas Control 106, 103263. https://doi.org/10.1016/j.ijggc.2021.103263.

Song, C., Pan, W., Srimat, S.T., Zheng, J., Li, Y., Wang, Y.H., Xu, B.Q., Zhu, Q.M., 2004. Tri-reforming of methane over Ni catalysts for CO_2 conversion to syngas with desired H_2/CO ratios using flue gas of power plants without CO_2 separation. In: Park, S.E., Chang, J.S., Lee, K.W. (Eds.), Tri-reforming of methane over Ni catalysts for CO_2 conversion to syngas with desired H_2/CO ratios using flue gas of power plants without CO_2 separation. Stud. Surf. Sci. Catal 153, 315–322. https://doi.org/10.1016/S0167-2991(04)80270-2.

Sundqvist, M., Biermann, M., Normann, F., Larsson, M., Nilsson, L., 2018. Evaluation of low and high level integration options for carbon capture at an integrated iron and steel mill. Int. J. Greenh. Gas Control 77, 27–36. https://doi.org/10.1016/j.ijggc.2018.07.008.

van der Spek, M., Sanchez Fernandez, E., Eldrup, N.H., Skagestad, R., Ramirez, A., Faaij, A., 2017. Unravelling uncertainty and variability in early stage techno-economic assessments of carbon capture technologies. Int. J. Greenh. Gas Control 56, 221–236. https://doi.org/10.1016/j.ijggc.2016.11.021.

Werner, S., 2017. District heating and cooling in Sweden. Energy 126, 419–429. https://doi.org/10.1016/j.energy.2017.03.052.